

# Numerical modelling of tidal circulation and studies on salinity distribution in Mandovi and Zuari estuaries

**Thesis**

*submitted to*

**Goa University**

*for the Degree of*

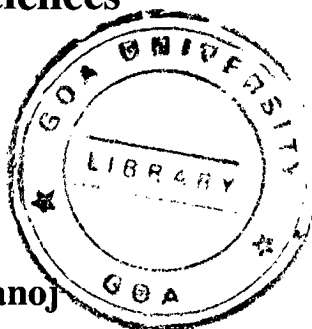
**Doctor of Philosophy**

*in*

**Marine Sciences**

by

**N. T. Manoj**



578.77

MAN/NUM

T-440

National Institute of Oceanography

Dona Paula, Goa 403 004

November 2008

440

# Statement

As required under the University ordinance 0.19.8.(vi), I state that this thesis entitled *Numerical modelling of tidal circulation and studies on salinity distribution in Mandovi and Zuari estuaries* is my original contribution and it has not been submitted on any previous occasion.

The literature related to the problem investigated has been cited. Due acknowledgements have been made wherever facilities and suggestions have been availed of.



N. T. Manoj

*National Institute of Oceanography, Goa*

*November 2008*

# Certificate

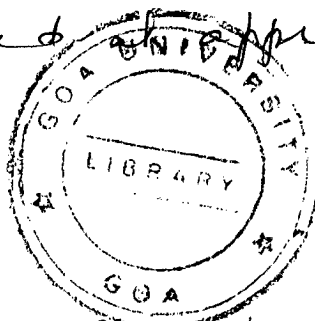
This is to certify that the thesis entitled *Numerical modelling of tidal circulation and studies on salinity distribution in Mandovi and Zuari estuaries*, submitted by N. T. Manoj to Goa University for the degree of Doctor of Philosophy, is based on his original studies carried out under my supervision. The thesis or any part thereof has not been previously submitted for any other degree or diploma in any university or institution.


  
A. S. UNNIKRISHNAN

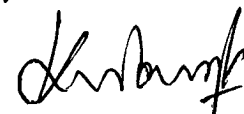
*National Institute of Oceanography, Goa*

*November 2008*

All corrections indicated by the referees have been incorporated at appropriate places in the thesis



  
A. S. Unnikrishnan  
04/09/09

  
04 09 09  
D. N. P. Kurian

# Vita

**Name** Manoj N. T

**Born** 30 March 1976, Naduvath, Kerala

## **Education**

**M.Sc.** Oceanography  
School of Marine Sciences  
Cochin University of Science and Technology, India  
August 2003

## **Work**

Senior Research Fellow (CSIR-UGC) 2005–2008  
Junior Research Fellow (CSIR-UGC) 2003–2005  
Physical Oceanography Division, National  
Institute of Oceanography  
Goa

## **Address for communication**

**Mailing address** Physical Oceanography Division,  
National Institute of Oceanography,  
Dona Paula, Goa 403 004, India.

**By e-mail** manojnt27@gmail.com,  
nmanoj@nio.org

---

## Publications

- **N. T. Manoj**, A. S. Unnikrishnan, and D. Sundar. Tidal asymmetry in the Mandovi and Zuari estuaries, the west coast of India. *Journal of Coastal Research.*, DOI:10.2112/08-1056.1.
- **N. T. Manoj** and A. S. Unnikrishnan. Tidal circulation and salinity distribution in the Mandovi and Zuari estuaries - A case study. *Journal of Waterway, Port, Coastal and Ocean Engineering, ASCE (In press)*.
- A. S. Unnikrishnan and **N. T. Manoj**. Numerical models. In S. R. Shetye, M. Dileep Kumar, and D. Shankar, editors, *The Mandovi and Zuari Estuaries.*, pages 39–47. National Institute of Oceanography, India, 2007.

# Acknowledgements

First and foremost I would like to thank my research supervisor Dr. A. S. Unnikrishnan, Scientist, National Institute of Oceanography, Goa. He taught me, the physics of ocean and numerical modelling techniques to solve the problems in oceanography with great dedication and sincerity. I thank all his efforts which in turn has helped my understanding of ocean, particularly coastal oceanography and estuarine dynamics more productive than ever before. I am thankful for all his contributions, which helped me to make this thesis practically possible in the present form.

I express my sincere thanks to my co-supervisor Dr. Aftab Can, Senior lecturer, Department of Marine Sciences, Goa University for his valuable advice, encouragement and continuous support during the course of my Ph.D. work.

I am thankful to Prof G. N. Nayak, the Head, Department of Marine Sciences, Goa University for his encouragement and support during my Ph.D. pursuit.

I am grateful to Dr. S. Prasanna Kumar, Scientist, N.I.O, for his help, support and continuous monitoring of the progress of my thesis work.

I am very much thankful to Dr. S. S. C. Sheno, Scientist and Project leader, for his valuable advice, help and support during my Ph.D. pursuit in the institute.

I express my sincere thanks to Dr. S. R. Shetye, the Director, N.I.O, for his support, encouragement and valuable guidance whenever needed for my Ph.D. work.

I would like to thank Dr. D. Shankar, Scientist, N.I.O, for his support, encouragement and an elder brotherly approach during the course of my Ph.D. work.

I am thankful to Dr. M. R. Ramesh Kumar and Dr. V. V. Gopalakrishna, Scientists, N.I.O, for their encouragement and support during my Ph.D. pursuit.

I am very much thankful to Mr. Michael, Mr. Sundar, Dr. Aparna and Mr. Mani Murali, Ms. Neetu, Mr. Suresh, Mr. Sathe, Mr. Almeida and Mr. Simon for their advice, help and support during my Ph.D. pursuit.

Special thanks go to my friends Rabindra, Alsafaani, Nisha, Sindhu, Ricky, Ajay, Nilesh, Dattaram, Jayent and Wilson.

I express my sincere thanks to my lab-mates Suprit, Syam, Nagesh, Thejna, Abhisek, Nanddeep, Amol, Ashok, Krupesh, Vijith, Nitin, Sarvesh and Mahalingam.

I would like to thank my friends in the institute Divya, Feby, Anindita, Sabu, Sabuji, Maya, Ramya, Vineesh, Laju, Honey, Rajani, Vidhya, Vijay, Bajish, Saji, Ikku, Praveen, Anu, Gavas, Anand, Vishwas, Lorreta, Santana and Gurudas for their support and help during my stay in N.I.O.

I express my sincere thanks to Sagar Sukti crew members especially Antony and Millind for their valuable support and help they extended to me during the field surveys onboard Sagar Sukti.

I thank India Meteorological Department and Centre Water Commission for providing the rainfall data and river discharge data required for my Ph.D. work.

I thank the project team of Mandovi and Zuari monsoon experiment for providing me salinity data of the Mandovi.

The Junior Research Fellowship and Senior Research Fellowship from University Grants Commission, Government of India is gratefully acknowledged.

I thank Council of Scientific and Industrial research (CSIR), Government of India, for the facilities availed to carry out my thesis work at N.I.O.

I acknowledge the funding made available to me from Supra Institutional Projects of N.I.O to conduct research cruises in the Mandovi estuary for my thesis work.

The model simulations of present work were carried out on SGI ALTIX 350 Cluster

installed in the Hydrodynamics Laboratory.

This thesis was typed using  $\text{\LaTeX}2_{\epsilon}$ <sup>1</sup>. The “style file”, `guthesis.sty` is the Goa University style written by Dr. D. Shankar. FERRET, GMT, and Latex were used extensively in this thesis.

I had got a good chance to interact with a lot of people in N.I.O and in other institutes. It is impossible to mention all their names. I would like to thank all of them who directly or indirectly helped me during the course of my Ph.D. work.

Finally, I wish to express my sincere thanks to all my family members for their constant encouragement and support.



N. T. MANOJ

*National Institute of Oceanography, Goa*

*November 2008*

---

<sup>1</sup> $\text{\LaTeX}2_{\epsilon}$  is an extension of  $\text{\LaTeX}$ , a collection of macros for  $\text{\TeX}$ .  $\text{\TeX}$  is a trademark of the American Mathematical Society.



# Synopsis

The estuaries on the west coast of India are unique in their physical and bio-geochemical features and the Mandovi and Zuari estuaries are two of these estuaries. Monsoon is a typical feature of this region. The south westerly winds blowing from the Indian Ocean bring heavy rainfall into the Indian subcontinent during June to September and these estuaries receive heavy river discharge during this period. Hence they are often called as “monsoonal estuaries”. Rainfall and subsequent discharge flushes out salinity very fast from these estuaries into the sea during southwest monsoon. Salinity in these estuaries undergoes intraseasonal variations during this period. Tidal dynamics, salinity distribution, flushing time etc. in an estuary are to be studied in detail for navigation, fishing, dredging and recreation purposes and also to determine the effects of oil spills, disposal of sewage and other potentially harmful wastes.

For the present study, the Mandovi and Zuari estuaries were chosen. These estuaries represent the other estuarine systems on the west coast of India in terms of tidal characteristics, channel convergence, heavy fresh water discharge etc. In addition, the Mandovi and Zuari estuaries play a vital role on the regional economy as these channels are exclusively used for the transportation of iron and manganese ores from their upstream regions to the nearest Port, Mormugao, which is one of the major ports along the west coast of India. The Mandovi and Zuari estuaries are connected by a narrow canal called Cumbarjua at their upstream regions. A number of tributaries also join the Mandovi and Zuari estuaries. Previous studies on tides and salinity in the Mandovi and Zuari estuaries

were limited to observations [Thomas et al., 1975; Varma et al., 1975; DeSousa, 1977; DeSousa et al., 1981; Qasim and Sengupta, 1981; Shetye et al., 1995; DeSousa, 1999b]. Shetye and Murty [1987] used a one dimensional numerical model for the simulation of salinity in the Zuari estuary. Unnikrishnan et al. [1997] used a one dimensional network model for the simulation of tidal decay during southwest monsoon at the upstream regions in the Mandovi and Zuari estuaries. Tide is major driving force in an estuary and tidal asymmetry can change the duration of flood and ebb in an estuary. Though many studies [Unnikrishnan et al., 1999a; Shetye, 1999; Unnikrishnan and Luick, 2003; Sundar and Shetye, 2005] were conducted to understand the variation of major diurnal and semidiurnal constituents in the gulfs and estuaries on the west coast of India, no detailed study was undertaken to know the variations of overtides ( $M_4$ ,  $M_6$ ) and compound tides ( $MSf$ ,  $MK_3$ ,  $MN_4$ ,  $MS_4$ ) inside an estuary. The overtides and compound tides have major role on tidal asymmetry inside the estuaries. Tidal asymmetry has important effects on both the geological evolution of shallow estuaries and the navigability of estuarine channels [Aubrey and Speer, 1985; Speer and Aubrey, 1985]. The aim of the present thesis is to simulate tides and salinity distribution in the Mandovi and Zuari estuaries using a hybrid network numerical model. The main objectives are (i) to study the tidal characteristics such as the longitudinal variation of tidal amplitudes during dry and wet seasons, freshwater influence on tides and the tidal asymmetry caused by overtides and compound tides (ii) to study the longitudinal variation of salinity distribution and freshwater influence on salinity distribution and (iii) to study the intraseasonal variations of salinity in the Mandovi estuary during southwest monsoon with the help of salinity measurements made in the estuary.

Chapter 1 of the thesis presents an introduction to the study area, the previous studies by earlier researchers and the objectives of the present study. Chapter 2 deals with the data and methodology. A hybrid network numerical model was developed to simulate tidal elevation, tidal currents and salinity distribution in the Mandovi and Zuari estuaries.

The hybrid network model consisting of a vertically averaged 2D model for the downstream regions in the Mandovi and Zuari estuaries and an area averaged 1D model for the upstream regions in the Mandovi, Zuari and for the Cumbarjua canal are described. The finite difference numerical scheme was used for solving partial differential equations of motion, continuity and advection-diffusion equation of salinity. The bathymetry data of the Mandovi, Zuari and Cumbarjua channels were obtained by digitizing the bathymetry maps (1968-1969) of minor ports survey organization, Ministry of Shipping and Transport, Government of India. The monthly mean averaged discharge data (1993) at Ganjem, an upstream station in the Mandovi estuary were used for prescribing river discharge at the upstream end boundaries of the model domain. The continuous measurements of tides and salinity in April and August, 1993 were used for the validation of the model and tidal measurements in March–April, 2003 were used to study the tidal asymmetry in these estuaries. Salinity measurements made along the longitudinal sections in the Mandovi during the selected days of 2005–2007 were analysed to study the intraseasonal variations of salinity during southwest monsoon.

Chapter 3 describes the simulation of tides, freshwater influence on tides, tidal currents and harmonic analysis of observed and simulated tides. The simulation of tidal currents were carried out using the numerical model described in Chapter 2. To simulate the tidal constituents and to study tidal asymmetry in the Mandovi and Zuari estuaries, the 35-days measurements of sea level were used for the harmonic analysis, and this one-month data was sufficient to resolve major diurnal and semidiurnal constituents, overtides and compound tides. Thereafter, the harmonic analysis of both observed and simulated tides was done. To find the difference between observation and model simulation, the complex difference module was calculated. The complex difference module gives synthetic information of the difference in both amplitude and phase of the observation and simulation. It was found that the model simulated tides successfully during dry and wet seasons in the Mandovi and Zuari estuaries. The results from the study show that fairly

strong tidal currents in the absence of river discharge mix the water column vertically in the Mandovi and Zuari estuaries during dry season. During wet season, the velocity associated with river discharge prevents upstream propagation of tides. The rapid increase of the first and second harmonics of  $M_2$  and compound tides inside these estuaries show the non-linear response of the Mandovi and Zuari estuarine systems to the tidal forcing. The  $M_4/M_2$  amplitude ratio indicates that the tide is subjected to more asymmetry in the Zuari than that in the Mandovi. The increase of the first harmonic of  $M_2$  and decrease of relative surface phase ( $2M_2 - M_4$ ) inside the Mandovi and Zuari estuaries show that these estuaries are flood dominant.

Chapter 4 deals with the salinity distribution in these estuaries. The simulation of the longitudinal variation of salinity during dry and wet seasons, freshwater effect on the salinity distribution and the intraseasonal variations of salinity during wet season are described in this Chapter. The analysis of salinity measured during the selected days of 2005–2007 in the Mandovi estuary shows the intraseasonal variation of salinity during southwest monsoon. The residual circulation and flushing time in the Mandovi and Zuari estuaries were also determined.

The results described above are summarized in Chapter 5.

# Contents

<b>Statement</b>	<b>iii</b>
<b>Certificate</b>	<b>iv</b>
<b>Vita</b>	<b>v</b>
<b>Acknowledgements</b>	<b>vii</b>
<b>Synopsis</b>	<b>x</b>
<b>List of Tables</b>	<b>xviii</b>
<b>List of Figures</b>	<b>xix</b>
<b>1 Introduction</b>	<b>1</b>
1.1 Definition . . . . .	1
1.1.1 Classification of estuaries . . . . .	1
1.1.2 Physical processes in an estuary . . . . .	2
1.2 The study area . . . . .	3
1.2.1 Objectives . . . . .	10
1.2.2 Chapter 2 . . . . .	11
1.2.3 Chapter 3 . . . . .	12
1.2.4 Chapter 4 . . . . .	13

---

1.2.5	Chapter 5 . . . . .	13
<b>2</b>	<b>Data and Methodology</b>	<b>14</b>
2.1	Introduction . . . . .	14
2.2	Data sets . . . . .	14
2.2.1	Bathymetry data . . . . .	15
2.2.2	Tides and salinity measurements during April and August 1993 . . . . .	15
2.2.3	Measurements of tides during March–April 2003 . . . . .	15
2.2.4	Salinity measurements in the Mandovi during 2005–2007 . . . . .	15
2.2.5	River discharge data . . . . .	16
2.2.6	Rainfall data . . . . .	16
2.3	Numerical model . . . . .	16
2.3.1	Numerical model for simulations of tides and salinity in the Man- dovi and Zuari estuaries . . . . .	21
2.3.2	2D model equations . . . . .	22
2.3.3	Equations in 1D model . . . . .	23
2.3.4	Finite difference scheme . . . . .	23
2.3.5	Coupling of numerical models . . . . .	29
2.3.6	Coupling between 2D and 1D models . . . . .	29
2.3.7	Coupling between two 1D models . . . . .	29
2.3.8	Freshwater influx inclusion in the model . . . . .	32
2.3.9	Stability criterion of the numerical scheme . . . . .	32
2.3.10	Initial and Boundary conditions . . . . .	33
<b>3</b>	<b>Simulations of tides in the Mandovi and Zuari estuaries</b>	<b>34</b>
3.1	Introduction . . . . .	34
3.1.1	Numerical model . . . . .	34
3.1.2	Initial and boundary conditions . . . . .	35

---

3.1.3	The coefficients used in the model . . . . .	35
3.2	Results . . . . .	35
3.2.1	Simulations of tides in the Mandovi estuary . . . . .	36
3.2.2	Simulations of tides in the Zuari estuary and Cumbarjua canal . . . . .	36
3.2.3	Simulations of tidal currents . . . . .	37
3.3	Tidal asymmetry . . . . .	46
3.3.1	Simulation of tides measured during March–April 2003 . . . . .	46
3.3.2	Harmonic analysis of tides . . . . .	47
3.3.3	Complex difference module . . . . .	47
3.3.4	Major diurnal and semidiurnal constituents . . . . .	53
3.3.5	Overtides and compound tides . . . . .	54
3.3.6	$M_4/M_2$ amplitude ratio and relative surface phase ( $2M_2 - M_4$ ) . . . . .	56
3.4	Discussion . . . . .	59
3.4.1	Longitudinal variation in tidal amplitudes . . . . .	59
3.4.2	Tidal currents and mixing of water column . . . . .	60
3.4.3	Nonlinearity in tidal propagation in the Mandovi and Zuari estuaries . . . . .	60
3.4.4	Increase in amplitudes and phases of major constituents . . . . .	61
3.4.5	Increase in amplitude and phase of overtides and compound tides . . . . .	62
3.5	Conclusion . . . . .	64
<b>4</b>	<b>Salinity distribution in the Mandovi and Zuari estuaries</b> . . . . .	<b>65</b>
4.1	Introduction . . . . .	65
4.1.1	Numerical model . . . . .	66
4.1.2	Initial and Boundary conditions . . . . .	66
4.1.3	Diffusion coefficient . . . . .	67
4.2	Results . . . . .	67
4.2.1	Salinity distribution during dry season . . . . .	67
4.2.2	Salinity distribution during wet season . . . . .	68

---

4.2.3	Simulation of longitudinal distribution of salinity for varying river discharges . . . . .	73
4.3	Residual currents . . . . .	73
4.4	Intraseasonal variations of salinity . . . . .	74
4.5	Flushing time in the Mandovi and Zuari estuaries . . . . .	79
4.5.1	Freshwater fraction method . . . . .	79
4.6	Discussion . . . . .	86
4.7	Conclusions . . . . .	90
<b>5</b>	<b>Summary and Conclusions</b>	<b>91</b>
5.1	Tidal propagation . . . . .	92
5.2	Salinity distribution . . . . .	93
5.3	Future studies . . . . .	94
<b>A</b>	<b>Notation</b>	<b>96</b>
	<b>Bibliography</b>	<b>98</b>



# List of Tables

3.1	Amplitudes (Amp), Phases (Pha) and Complex difference module (Diff) of tidal constituents in the Mandovi estuary. The number in bracket shown for each station name is the distance ( <i>km</i> ) from the mouth of the estuary. .	51
3.2	Amplitudes (Amp), Phases (Pha) and Complex difference module (Diff) of tidal constituents in the Zuari estuary. The number in bracket shown for each station name is the distance ( <i>km</i> ) from the mouth of the estuary. .	52
3.3	Amplitudes (Amp), Phases (Pha) and Complex difference module (Diff) of tidal constituents in the Cumbarjua canal. The number in bracket shown for each station name is the distance ( <i>km</i> ) from the mouth of the estuary. . . . .	53
3.4	$M_4/M_2$ amplitude ratio and relative surface phase ( $2M_2 - M_4$ ) in the Mandovi estuary . . . . .	56
3.5	$M_4/M_2$ amplitude ratio and relative surface phase ( $2M_2 - M_4$ ) in the Zuari estuary . . . . .	56
4.1	Table shows the computed flushing time for varying river discharges in the Mandovi and Zuari estuaries . . . . .	87

# List of Figures

1.1	Map of the west coast of India . . . . .	4
1.2	Map of the Mandovi and Zuari estuaries . . . . .	5
1.3	Observations of rainfall during 1999–2001 at Valpoi in the Mandovi estuary. The months on the x-axis starts from January, 1999. The rainfall data were obtained from India Meteorological Department. . . . .	7
1.4	Observations of rainfall during 1999–2001 at Sanguem in the Zuari estuary. The months on the x-axis starts from January, 1999. The rainfall data were obtained from India Meteorological Department. . . . .	8
1.5	River discharge for Ganjem in the Mandovi estuary. The months on the x-axis starts from January 1993. The river discharge data were obtained from Central Water Commission, Government of India. . . . .	8
2.1	Model domain of the Mandovi and Zuari estuaries. . . . .	24
2.2	Schematic diagram showing the coupling between 2D and 1D models and two 1D models. . . . .	25
3.1	Observed (dotted line) and simulated (solid line) tides at different stations in the Mandovi estuary in April 1993. The panels a, b and c represent Mormugao, Volvoi and Ganjem respectively. 72 <i>hours</i> shown on the x-axis correspond to 0.0 <i>hours</i> (IST) on 07/04/1993. . . . .	37

- 3.2 Observed (dotted line) and simulated (solid line) tides at different stations in the Mandovi estuary in August 1993. The panels a, b and c represent Mormugao, Volvoi and Ganjem respectively. 72 *hours* shown on the x-axis correspond to 0.0 *hours* (IST) on 19/08/1993. . . . . 38
- 3.3 Observed (dotted line) and simulated (solid line) tides at different stations in the Zuari estuary and Cumbarjua canal in April 1993. The panels a, b and c represent Mormugao, Banastarim and Sanguem respectively. 72 *hours* shown on the x-axis correspond to 0.0 *hours* (IST) on 07/04/1993. 38
- 3.4 Observed (dotted line) and simulated (solid line) tides at different stations in the Zuari estuary and Cumbarjua canal in August 1993. The panels a, b and c represent Mormugao, Banastarim and Sanguem respectively. 72 *hours* shown on the x-axis correspond to 0.0 *hours* (IST) on 19/08/1993. 39
- 3.5 Tidal currents during the spring tide in the Mandovi and Zuari estuaries. The currents shown are only for the 2D domain of the 1D and 2D model domain. The sea surface elevation predicted for April 1993 at Mormugao was used for prescribing boundary condition at the open boundary. The timings shown are with respect to the occurrence of high tide at Mormugao. 40
- 3.6 (Continued) Tidal currents during the spring tide in the Mandovi and Zuari estuaries. The currents shown are only for the 2D domain of the 1D and 2D model domain. The sea surface elevation predicted for April 1993 at Mormugao was used for prescribing boundary condition at the open boundary. The timings shown are with respect to the occurrence of high tide at Mormugao. . . . . 41

- 
- 3.7 (Continued) Tidal currents during the spring tide in the Mandovi and Zuari estuaries. The currents shown are only for the 2D domain of the 1D and 2D model domain. The sea surface elevation predicted for April 1993 at Mormugao was used for prescribing boundary condition at the open boundary. The timings shown are with respect to the occurrence of high tide at Mormugao. . . . . 42
- 3.8 Tidal currents during the neap tide in the Mandovi and Zuari estuaries. The currents shown are only for the 2D domain of the 1D and 2D model domain. The sea surface elevation predicted for April 1993 at Mormugao was used for prescribing boundary condition at the open boundary. The timings shown are with respect to the occurrence of high tide at Mormugao. 43
- 3.9 (Continued) Tidal currents during the neap tide in the Mandovi and Zuari estuaries. The currents shown are only for the 2D domain of the 1D and 2D model domain. The sea surface elevation predicted for April 1993 at Mormugao was used for prescribing boundary condition at the open boundary. The timings shown are with respect to the occurrence of high tide at Mormugao. . . . . 44
- 3.10 (Continued) Tidal currents during the neap tide in the Mandovi and Zuari estuaries. The currents shown are only for the 2D domain of the 1D and 2D model domain. The sea surface elevation predicted for April 1993 at Mormugao was used for prescribing boundary condition at the open boundary. The timings shown are with respect to the occurrence of high tide at Mormugao. . . . . 45
- 3.11 Observed (dotted line) and simulated (solid line) tides in the Mandovi estuary during 10 March–13 April 2003. 144 *hours* on the x-axis correspond to 0.0 *hours* (IST) on 10 March 2003. . . . . 48

- 3.12 Observed (dotted line) and simulated (solid line) tides in the Zuari estuary during 10 March–13 April 2003. 144 *hours* on the x-axis correspond to 0.0 *hours* (IST) on 10 March 2003. . . . . 49
- 3.13 Observed (dotted line) and simulated (solid line) tides in the Cumbarjua canal during 10 March–13 April 2003. 144 *hours* on the x-axis correspond to 0.0 *hours* (IST) on 10 March 2003. . . . . 49
- 3.14 Variation in amplitude (*cm*) and phase (*degree*) of observed (dotted line) and simulated (solid line) five major tidal diurnal and semidiurnal constituents in the Mandovi and Zuari estuaries. . . . . 55
- 3.15 Variation in amplitude (*cm*) and phase (*degree*) of observed (dotted line) and simulated (solid line) overtides in the Mandovi and Zuari estuaries. . . . . 57
- 3.16 Variation in amplitude (*cm*) and phase (*degree*) of observed (dotted line) and simulated (solid line) compound tides in the Mandovi and Zuari estuaries. . . . . 58
- 4.1 The longitudinal distribution of salinity at different stations in the Mandovi estuary during dry (April 1993) season. The panels a, b, c, d and e represent Mormugao, Saramanas, Volvoi, Sonamarg and Ganjem respectively. The 144 *hours* on the x-axis correspond to 0.0 *hours* (IST) on 07/04/1993. Dotted and solid lines are observed and model respectively. . . . . 69
- 4.2 The longitudinal distribution of salinity at different stations in the Mandovi estuary during wet (August 1993) season. The panels a, b, c, d and e represent Mormugao, Saramanas, Volvoi, Sonamarg and Ganjem respectively. The 216 *hours* on the x-axis correspond to 0.0 *hours* (IST) on 19/08/1993. Dotted and solid lines are observed and model respectively. . . . . 70

- 4.3 The longitudinal distribution of salinity at different stations in the Zuari estuary and Cumbarjua canal during dry (April 1993) season. The panels a, b, c, d and e represent Mormugao, Cortalim, Banastarim, Sanvordem and Sanguem. The 144 *hours* on the x-axis correspond to 0.0 *hours* (IST) on 07/04/1993. Dotted and solid lines are observed and model respectively. 71
- 4.4 The longitudinal distribution of salinity at different stations in the Zuari estuary and Cumbarjua canal during wet (August 1993) season. The panels a, b, c, d and e represent Mormugao, Cortalim, Banastarim, Sanvordem and Sanguem. The 216 *hours* on the x-axis correspond to 0.0 *hours* (IST) on 19/08/1993. Dotted and solid lines are observed and model respectively. . . . . 72
- 4.5 Simulations of tidally averaged salinity over  $M_2$  tidal period for varying river discharges in the Mandovi estuary. . . . . 74
- 4.6 Simulations of residual currents over  $M_2$  tidal period in the Mandovi and Zuari estuaries. The panels a, b, c and d represent the model runs for varying river discharges of 0, 10, 100, 400  $m^3s^{-1}$  respectively. . . . . 75
- 4.7 Vertical distribution of salinity measured on 23 August 2005 in the Mandovi estuary. The time (*hours*) at which the observations were made are indicated in cyan colour. . . . . 77
- 4.8 Vertical distribution of salinity measured on 13 September 2005 in the Mandovi estuary. The time (*hours*) at which the observations were made are indicated in cyan colour. . . . . 78
- 4.9 Time series measurements of salinity made at Old Goa, located at a distance of 15 *km* from the mouth in the Mandovi estuary on 19 September 2006. The time (*hours*) at which the observations were made are indicated in the bracket. . . . . 79

- 
- 4.10 Vertical distribution of salinity measured on 30 March 2007 in the Mandovi estuary. The time (*hours*) at which the observations were made are indicated in cyan colour. . . . . 80
- 4.11 Vertical distribution of salinity measured on 25 May 2007 in the Mandovi estuary. The time (*hours*) at which the observations were made are indicated in cyan colour. . . . . 81
- 4.12 Vertical distribution of salinity measured on 1 June 2007 in the Mandovi estuary. The time (*hours*) at which the observations were made are indicated in cyan colour. . . . . 82
- 4.13 Vertical distribution of salinity measured on 27 July 2007 in the Mandovi estuary. The time (*hours*) at which the observations were made are indicated in cyan colour. . . . . 83
- 4.14 Vertical distribution of salinity measured on 7 September 2007 in the Mandovi estuary. The time (*hours*) at which the observations were made are indicated in cyan colour. . . . . 84
- 4.15 Figure shows rainfall at Panaji (near the mouth of Mandovi) during the time of salinity measurements in the Mandovi estuary. Rainfall is plotted for about 5 days before and after the date (shown in each panel) of salinity measurements. The green and red curves indicate rainfall during wet and dry seasons respectively. The 32<sup>nd</sup> day on the panels d and f are for 1<sup>st</sup> April and June respectively. . . . . 85
- 4.16 The computed flushing time for varying river discharges in the Mandovi and Zuari estuaries. . . . . 87

# Chapter 1

## Introduction

### 1.1 Definition

Estuaries are semi enclosed bodies of water where freshwater from the river mix with saline water from the sea. The widely used definition of an estuary states that an estuary “is a semi enclosed body of water which has a free connection with sea and within which seawater is measurably diluted with freshwater derived from land drainage” [Cameron and Pritchard, 1963]. The action of tides, winds and other physical processes in an estuary make it a complex system.

#### 1.1.1 Classification of estuaries

Estuaries can be classified based on geomorphology, tidal range and salinity distribution. Based on geomorphology [Pritchard, 1952, 1967; Russell, 1967], estuaries are classified into Coastal plain estuaries, Fjords and Bar-built estuaries. Estuary geomorphology strongly affect the transport of pollutants and ultimately impacts water quality characteristics [Martin and McCutcheon, 1999; Dyer, 1973]. There are other types of estuaries which are formed by tectonic activity, volcanic eruptions etc.

Based on tidal range, if the tidal range is less than 2 *m* in an estuary then it is called



micro-tidal estuary. The tidal ranges are between 2 to 4 *m* in the meso-tidal estuaries and those estuaries, where tidal range is higher than 4 *m* are called macro-tidal estuaries [McCann, 1980; Dyer et al., 2000].

Salinity distribution in an estuary varies from place to place due to their geographical locations, prevailing climate systems and tidal range. The estuaries, based on salinity, are classified into stratified estuaries, partially mixed estuaries and well mixed estuaries [Pritchard, 1955, 1967; Bowden, 1967; Fischer, 1972; Dyer, 1973, 1997]. Hansen and Rattray [1966] classified an estuary based on the salinity variations in the vertical direction and the circulation due to the difference in density. Tidal currents are weak in stratified estuaries because of large river discharge. The low density freshwater from the river side flow above seawater and a sharp boundary is created between these two water masses. In partially mixed estuaries, saline water and freshwater mix partially due to increased tidal activity. Tidal activities generate turbulence and partial mixing take place between freshwater and saline water. Differential pressure forces due to landward moving saline water and seaward moving freshwater from the upstream end give rise to longitudinal density currents and consequent mixing both longitudinally and vertically [Fischer, 1972]. If tides are large, freshwater and saline water mix from surface to bottom and these type of estuaries are called well mixed estuaries.

### 1.1.2 Physical processes in an estuary

Ocean tides often dominate the mixing in estuaries [Gross, 1972]. Ocean tides are defined as the periodic rise and fall of sea surface caused by the gravitational attraction of moon and sun on earth. The gravitational attraction of other planets on earth are negligible because of their distant locations. Tide created in the ocean penetrates into rivers as a disturbance, the shape and size of rivers being such that they do not respond directly to the tidal forces. The disturbance takes the form of a progressive wave, markedly affected by friction and completely damped eventually [Godin, 1988]. Tide, river discharge,

bathymetry, wind, Coriolis force etc. control the processes in an estuary [Fischer et al., 1979]. Circulation and transport mechanisms in estuaries are complex and subject to a large spatial and temporal variability derived from the interaction of river discharge, tides and winds. These forces drive the gravitational circulation and turbulent diffusion which are the main processes controlling the transport of properties in estuaries [Mantovanelli et al., 2004]. Bathymetry in an estuary regulate the speed of propagation of tides. Shallow regions of estuaries enable vertical mixing more effective than that of deeper regions. Freshwater inflow into an estuary normally has a significant impact on mixing and the increased freshwater inflow can change the character of an estuary from well mixed to partially mixed or stratified [Martin and McCutcheon, 1999].

## 1.2 The study area

India has a vast coastline of over 7000 *km* and the major Indian cities, Mumbai, Kolkata and Chennai are situated along these coasts. There are more than 100 major and medium estuarine channels along the east and west coast of India. The estuaries along the east coast of India are long and wide whereas the estuaries along the west coast are smaller. Ganges-Brahmaputra Delta region along the east coast of India is the largest estuarine network in India. Since ancient times, estuaries in India have been a focal point of activities for human settlement, development of ports and harbours, transportation of men and material and for trade and commerce [Qasim, 2003].

The estuaries along the west coast of India are unique in their physical and biogeochemical features. Kochi Backwaters is one of the largest estuarine systems along this region and the other important estuarine systems along this coast are Ashtamudi estuary, Kali river, Mandovi and Zuari estuarine system, Mumbai Harbour and Thane Creek system and a number of small estuaries like Sabarmati, Tapti, Narmada etc. Monsoon is a typical feature of this region. The south-westerly winds blowing from the Indian

Figure 1.1 Map of the west coast of India

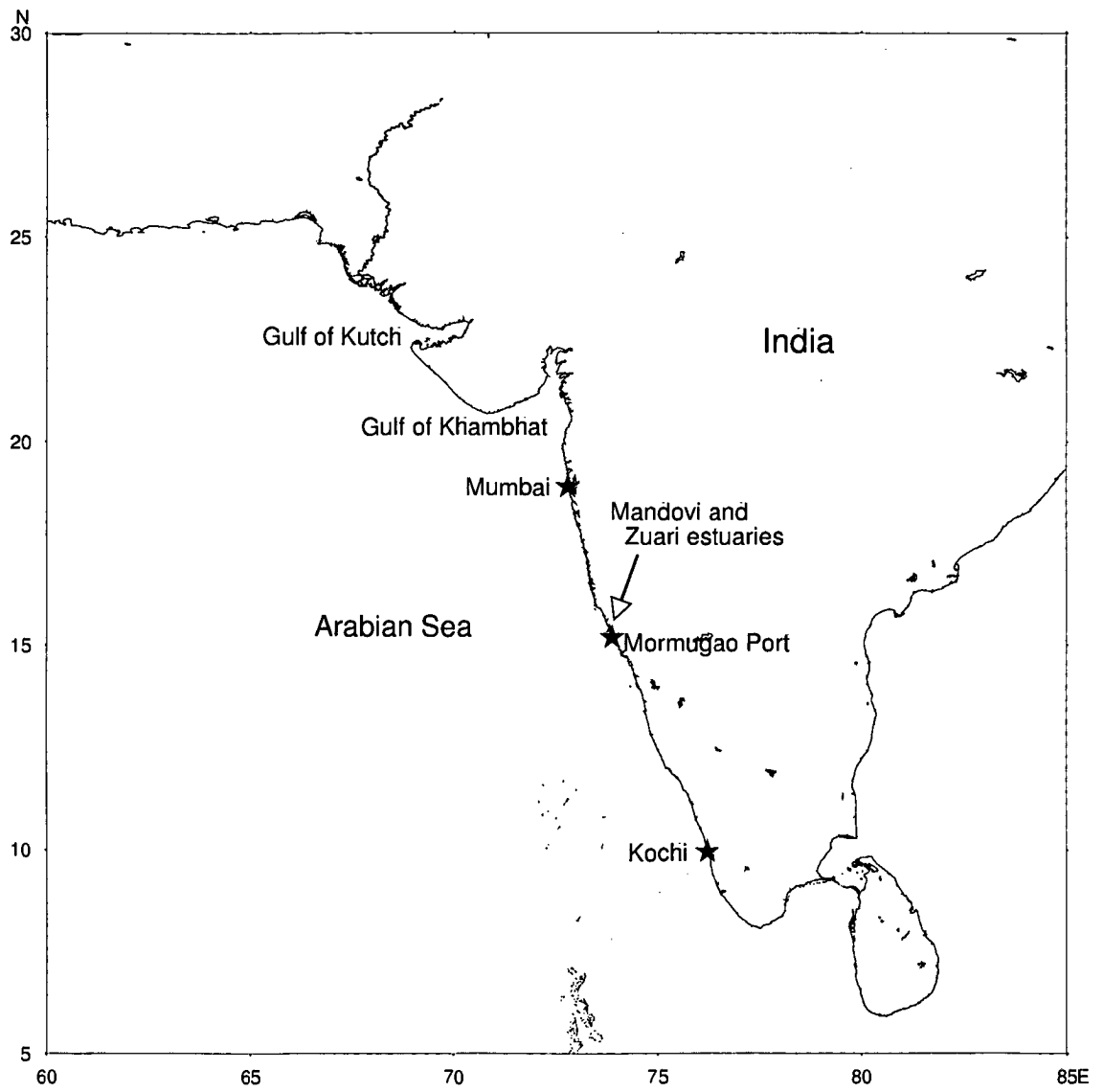
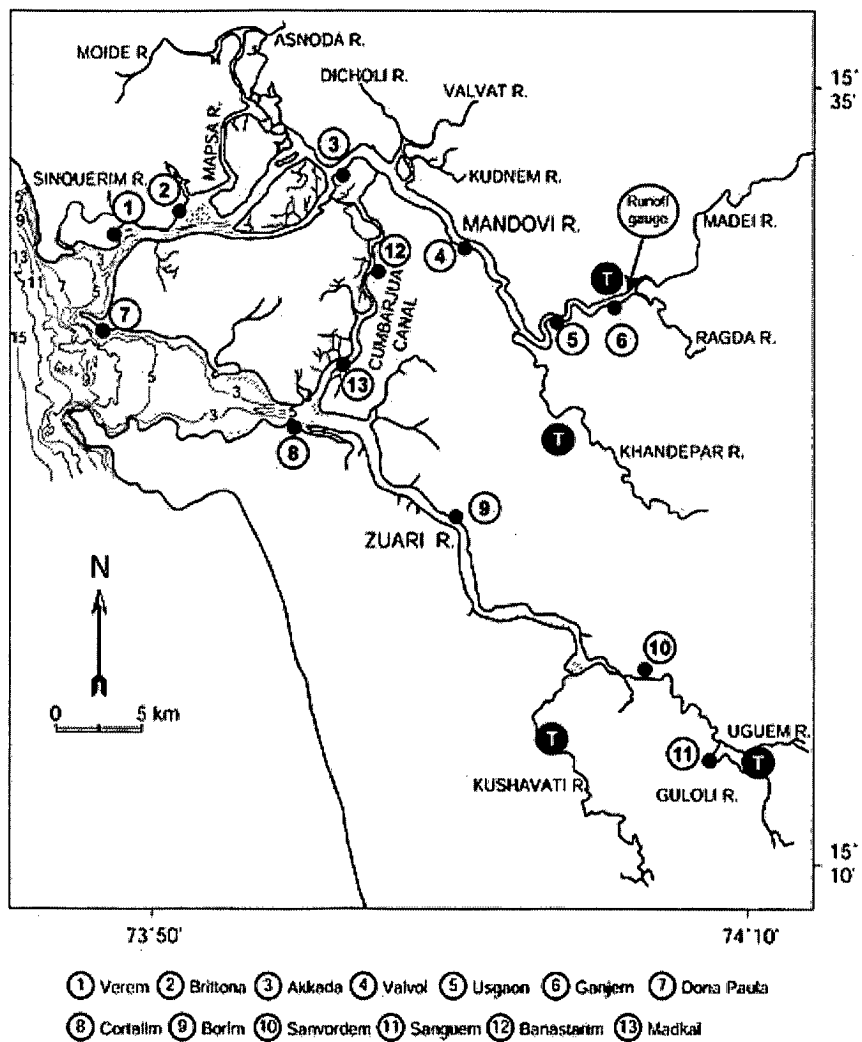


Figure 1.2 Map of the Mandovi and Zuari estuaries

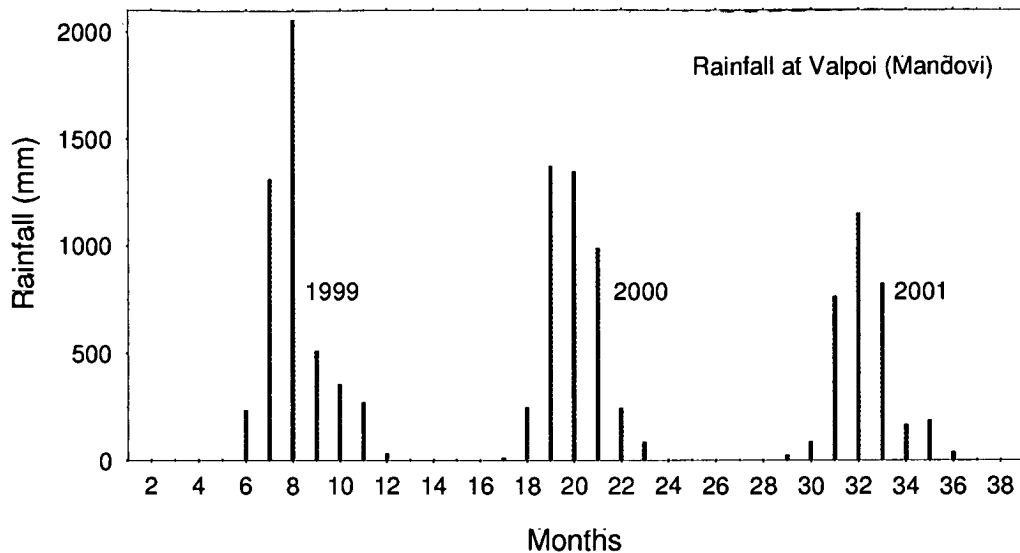


Ocean bring heavy rainfall into the Indian subcontinent during southwest monsoon (June to September) and these estuaries receive heavy river discharge during this period hence they are often called as “monsoonal estuaries”. Salinity distribution in these estuaries undergoes intraseasonal variations during southwest monsoon. Rainfall and subsequent river discharge during this period flushes out salinity very fast from these estuaries into the Arabian sea. Thermodynamics of the water column of these coastal regions of the Arabian sea is greatly affected by the rainfall and subsequent freshwater inflow [Shankar and Shetye, 1999, 2001; Shenoi et al., 2002; Shankar et al., 2004, 2005; Suprit and Shankar, 2008].

The understanding of estuarine dynamics is very important in many aspects because, apart from their role on influencing the physics and bio-geochemistry of the adjacent seas, their role in determining regional ecology and economy are also indispensable. Tidal dynamics, salinity distribution, flushing time etc. in an estuary are to be studied in detail for navigation, fishing, dredging and also, to determine oil spills, disposal of sewage and other potentially harmful wastes.

For the present study, the Mandovi and Zuari estuaries (Figures 1.1 and 1.2) are chosen. These estuaries represent the other estuarine systems on the west coast of India in terms of tidal characteristics, channel convergence, heavy freshwater discharge etc. In addition, the Mandovi and Zuari estuaries play a vital role on regional economy as these channels are exclusively used for transportation of iron and manganese ores from their upstream regions to the nearest port, Mormugao which is one of the major Ports along the west coast of India. The length of the Mandovi and Zuari estuaries are about 50 *km* each and have their upstream regions in the Western Ghats (Mountain ranges along the west coast of India). The Mandovi and Zuari estuaries are shallow channels with average depth of about 5 *m*. The width at the mouth of Mandovi and Zuari estuarine system is about 9 *km* and the width narrow down to 200 *m* at their upstream regions. A narrow canal, Cumbarjua canal, connects these estuaries at a distance of 14 *km* from the mouth of the

**Figure 1.3** Observations of rainfall during 1999–2001 at Valpoi in the Mandovi estuary. The months on the x-axis starts from January, 1999. The rainfall data were obtained from India Meteorological Department.



Mandovi and 11 *km* from the mouth of Zuari. The length of the Cumbarjua canal is about 17 *km* and has an average width of 0.5 *km*. A number of tributaries such as Sinquerim River, Mapusa River, Khandepar River join to the Mandovi estuary while Kushavati and Sanguem Rivers join to the Zuari estuary. As mentioned earlier, southwest monsoon is a unique feature of this region and the Mandovi and Zuari estuaries receive heavy river discharge during this period. The normal rainfall of this region is about 2500–3000 *mm* in a year and 80% of the total rainfall occurs during the southwest monsoon. Figures 1.3 and 1.4 show the observations of rainfall during 1999–2001 at Valpoi and Sanguem stations respectively in the Mandovi and Zuari estuaries. Rainfall reaches to its peak during July and August and river discharge from the upstream ends of these rivers is about 400  $m^3 s^{-1}$  during this period (see Figure 1.5).

Based on tidal range, the Mandovi and Zuari are meso-tidal estuaries. Tides in these estuaries are semidiurnal mixed type and the tidal range is about 2 *m*. The studies on

**Figure 1.4** Observations of rainfall during 1999–2001 at Sanguem in the Zuari estuary. The months on the x-axis starts from January, 1999. The rainfall data were obtained from India Meteorological Department.

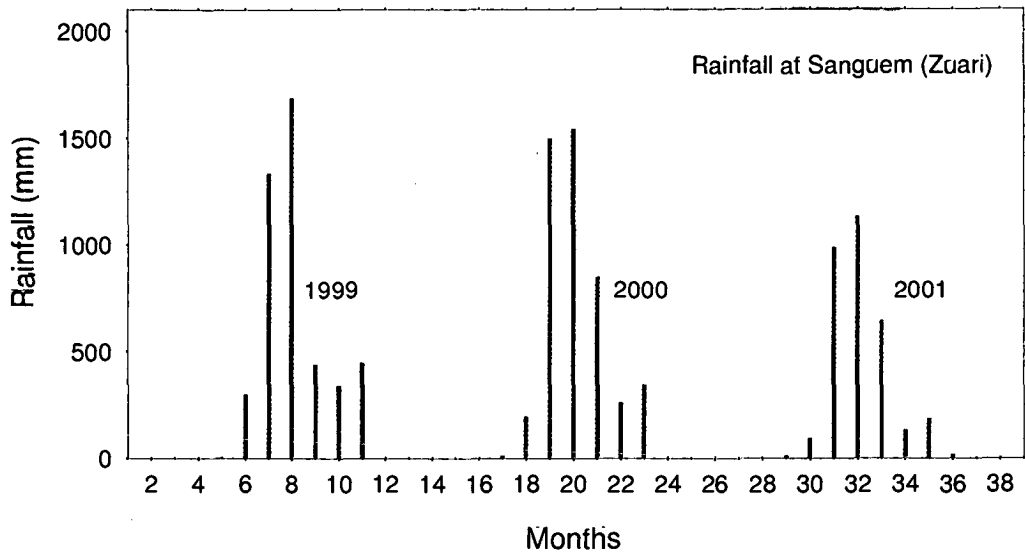
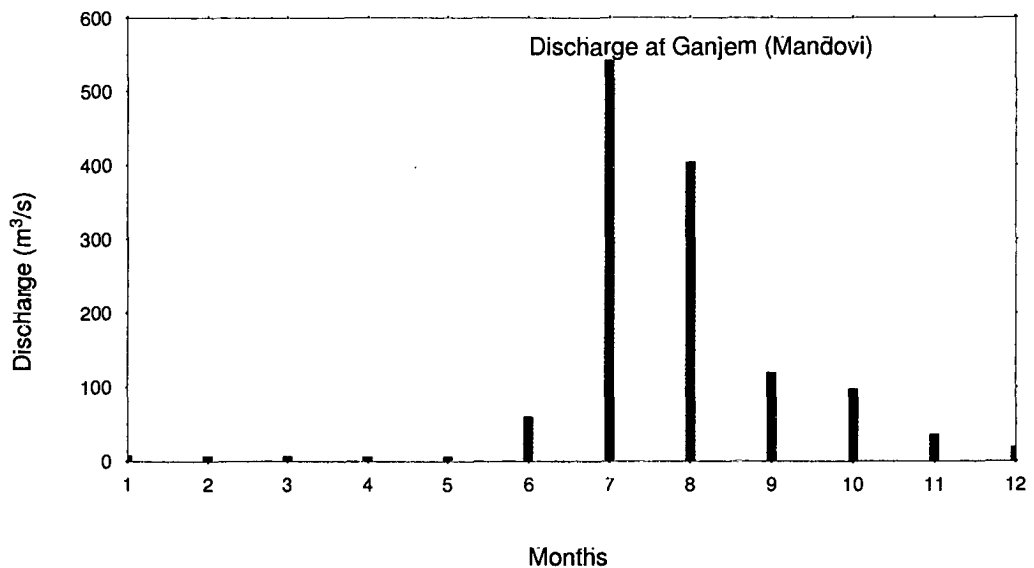


**Figure 1.5** River discharge for Ganjem in the Mandovi estuary. The months on the x-axis starts from January 1993. The river discharge data were obtained from Central Water Commission, Government of India.



hydrography of the Mandovi and Zuari estuaries started in early 1970s. The previous studies on tides and salinity in these estuaries were limited to observations. Dehadrai [1970]; Dehadrai and Bhargava [1972]; Das et al. [1972]; Murty and Das [1972]; Singbal [1973]; Thomas et al. [1975]; Varma et al. [1975]; DeSousa [1977]; DeSousa et al. [1981]; DeSousa [1999b] investigated some of the environmental features and the influence of tide in regulating the flow in these estuaries. Tidal amplitude in the Mandovi and Zuari remains unchanged upto about 40 *km* from the mouth, and then drops sharply over the next 10 *km* [Shetye et al., 1995]. Sundar and Shetye [2005] calculated amplitude and phase of the major tidal constituents in the Mandovi and Zuari estuaries using sea level measured during March–April 2003 at different stations in these estuaries. They found that the five major constituents  $M_2$ ,  $S_2$ ,  $N_2$ ,  $K_1$  and  $O_1$  have amplitudes more than 10 *cm* at the mouth of these estuaries and the amplitude and phase of these major constituents increase from mouth to the upstream regions before topographic effect comes to play.

The Mandovi and Zuari are partially mixed estuaries and the longitudinal distribution of salinity in these estuaries are subjected to large variations during a year. Near the mouth, during a tidal cycle, salinity remains almost constant (35 *psu*) between November and May. But salinity at the mouth varies from 7 to 22 *psu* during June to September. [Qasim and Sengupta, 1981; Shetye et al., 1995]. Heavy precipitation and land runoff from June to September bring about large changes in temperature, salinity, flow pattern, dissolved oxygen and nutrients when the estuary becomes freshwater dominated [Qasim and Sengupta, 1981]. Sandbars are formed at the mouth of the Mandovi estuary during this period and the formation of these sandbars halts the traffic in the Mandovi from June to September. But the navigation in the Zuari and Cumbarjua canal is uninterrupted during this period. By the end of September, the effect of river discharge is reduced and saline water intrudes towards upstream regions. By February, the downstream regions of these estuaries become an extension of the sea. The heavy rainfall and subsequent freshwater inflow into the catchment area during June to September hereafter referred to as 'wet



season' stratifies the downstream regions consisting of about 10–12 *km* from the mouth of the estuaries. From 12 *km*, to the upstream regions of about 35 *km* the estuaries become completely freshwater dominated. During the post monsoon (October to January), the saline water intrudes further into upstream regions. February to May, hereafter referred to as 'dry season', these estuaries are vertically well mixed throughout the regions. Shetye and Murty [1987] used a one dimensional numerical model for the simulation of salinity in the Zuari estuary. Unnikrishnan et al. [1997] used a one dimensional network model consisting of all the tributaries of the estuarine system for the simulation of tidal decay at the upstream regions during wet season in the Mandovi and Zuari estuaries. As mentioned previously, tide is a major driving force in an estuary and tidal asymmetry can change the duration of flood and ebb in an estuary. Though many studies [Unnikrishnan et al., 1999a; Shetye, 1999; Unnikrishnan and Luick, 2003; Sundar and Shetye, 2005] were conducted to understand the variation of major diurnal and semidiurnal constituents in the gulfs and estuaries on the west coast of India, no detailed study was undertaken to know the variations of overtides ( $M_4$ ,  $M_6$ ) and compound tides ( $MS_f$ ,  $MK_3$ ,  $MN_4$ ,  $MS_4$ ) in these gulfs and estuaries. Overtides and compound tides have major role on tidal asymmetry inside the estuaries.

### 1.2.1 Objectives

The aim of the present thesis is to determine the characteristics of tidal propagation and salinity distribution in the Mandovi and Zuari estuaries using a hybrid network numerical model. The main objective are (i) to study the tidal characteristics such as the longitudinal variation of tidal amplitudes during dry and wet seasons, freshwater influence on tides and the tidal asymmetry caused by overtides and compound tides (ii) to study the longitudinal variation of salinity distribution and freshwater influence on salinity distribution and (iii) to study the intraseasonal variations of salinity in the Mandovi estuary during southwest monsoon with the help of salinity measurements made in the estuary.

In addition to this first chapter there are four more chapters in this thesis and the outline of these chapters is given below.

## 1.2.2 Chapter 2

Chapter 2 of the thesis deals with data and methodology. This chapter contains a detailed description of a numerical model developed for the present study. A hybrid network numerical model was developed to simulate tides, tidal currents and salinity distribution in the Mandovi and Zuari estuaries. A hybrid network model consisting of a vertically averaged 2D model and an area averaged 1D model was used. The vertically averaged 2D model was used for the downstream regions in the Mandovi and Zuari estuaries. An area averaged 1D model was used for the upstream regions in the Mandovi and Zuari estuaries and Cumbarjua canal. A finite difference numerical scheme was used for solving partial differential equations of motion, continuity and advection-diffusion equation of salinity. The bathymetry data of the Mandovi, Zuari and Cumbarjua channels were obtained by digitizing the bathymetry maps (1968–1969) of minor ports survey organization, Ministry of Shipping and Transport, Government of India. The monthly mean averaged discharge data (1993) of Ganjem, an upstream station in the Mandovi estuary were used for prescribing river discharge at the upstream boundaries in the Mandovi and Zuari estuaries. The continuous measurements of tides and salinity made in April and August 1993 were used for validation of the model and tidal measurements in March–April, 2003 were used to study the tidal asymmetry in these estuaries. In addition, we made salinity measurements along the longitudinal sections in the Mandovi estuary during the selected days of 2005–2007, which were used to study the intraseasonal variations of salinity during southwest monsoon.

### 1.2.3 Chapter 3

Chapter 3 describes the tidal characteristics in the Mandovi and Zuari estuaries. This chapter describes the results of simulation of tides, tidal currents and the influence of river discharge on tides. Also, the harmonic analysis of major diurnal and semidiurnal constituents, overtides, compound tides and the  $M_4/M_2$  amplitude ratio and relative surface phase ( $2M_2 - M_4$ ) are also discussed. The simulation of tides during dry and wet seasons in 1993, the study of freshwater effect on tides and the simulation of tidal currents were carried out using the hybrid network numerical model described in Chapter 2. To study tidal asymmetry in the Mandovi and Zuari estuaries, the 35-days observations of tide made in March–April, 2003 [Sundar and Shetye, 2005] were used for the harmonic analysis, and this 1-month duration of data was sufficient to resolve major diurnal and semidiurnal constituents, overtides and compound tides. The harmonic analysis of both observed and simulated tides was carried out using Tidal Analysis Software Kit-2000 [Bell et al., 2000]. To find the difference between observed and simulated tides, the complex difference module was calculated. The complex difference module gives synthetic information about the difference in both amplitude and phase between the observation and simulation. It is found that the model simulated tides successfully during dry and wet seasons in the Mandovi and Zuari estuaries. The results from the study show that fairly strong tidal currents in the absence of river discharge mix the water column vertically in the Mandovi and Zuari estuaries during dry season. During wet season, the velocity associated with river discharge prevents upstream propagation of tides. The rapid increase of the first and second harmonics of  $M_2$  and compound tides inside these estuaries show the nonlinear response of the Mandovi and Zuari estuarine systems to tidal forcing. The variation of  $M_4/M_2$  amplitude ratio from the mouth to head indicates that tide is subjected to more asymmetry in the Zuari than that in the Mandovi. The increase of the first harmonic of  $M_2$  and decrease of relative surface phase ( $2M_2 - M_4$ ) inside the Mandovi and Zuari estuaries show that these estuaries are flood dominant.

### 1.2.4 Chapter 4

Chapter 4 deals with the simulations of salinity distribution in the Mandovi and Zuari estuaries. The simulation of the longitudinal variation of salinity during dry and wet seasons, freshwater effect on salinity distribution and the intraseasonal variations of salinity during wet season are described in this chapter. The flushing time using freshwater fraction method in the Mandovi and Zuari was calculated using the hybrid numerical model. Tidally averaged salinity and residual currents over a period of  $M_2$  tide were also calculated to quantify the freshwater influence on salinity. The measurements of salinity in the Mandovi estuary during the selected days of 2005–2007 were used to study intraseasonal variations of salinity during wet season. The residual circulation in the Mandovi and Zuari estuaries was also determined.

### 1.2.5 Chapter 5

The results and significant findings from present study described in the previous chapters are summarized in this chapter. The limitations of the present approach and suggestions for further studies to improve the present understanding are also given in this chapter.

# **Chapter 2**

## **Data and Methodology**

### **2.1 Introduction**

This chapter gives a detailed account of the development of a hybrid network numerical model, which was developed for simulations of tides and salinity distribution in the Mandovi and Zuari estuaries. The data sets used for prescribing boundary conditions, validation of the model etc. are also described in this chapter. A finite difference numerical scheme was used for solving partial differential equations of motion, continuity and advection diffusion equation of salinity. The details of the data sets used for the present study and the formulation of a hybrid network numerical model are given in the following sections.

### **2.2 Data sets**

Numerical modelling of physical phenomena such as tidal circulation and salinity distribution in an estuary require a number of data sets, which include bathymetry data, surface elevation data, salinity data, river discharge data etc. for prescribing open boundary conditions, model validation etc.

### **2.2.1 Bathymetry data**

Bathymetry data of the Mandovi, Zuari and Cumbarjua canal were obtained by digitizing the bathymetry maps (1968–1969) of minor ports survey organization, Ministry of Shipping and Transport, Government of India. The one dimensional upstream regions in the Mandovi, Zuari and Cumbarjua canal were schematized into 75, 81 and 32 segments respectively based on the description given by [Harleman and Lee, 1969].

### **2.2.2 Tides and salinity measurements during April and August 1993**

Shetye et al. [1995] made continuous measurements of tides and salinity during 7–9 April and 19–21 August 1993 in the Mandovi, Zuari and Cumbarjua canal. Sea level obtained from the above observations were used for the model validation.

### **2.2.3 Measurements of tides during March–April 2003**

Sea level measurements were carried out at 13 locations in the Mandovi, Zuari and the Cumbarjua canal. These measurements were part of the ICMAM (Integrated Coastal and Marine Area Management) under the Ministry of Earth Sciences, Government of India. There are six stations in the Mandovi estuary; five stations in the Zuari estuary and two stations in the Cumbarjua Canal where continuous measurements of tides using tide poles were carried out during 10 March to 13 April 2003.

### **2.2.4 Salinity measurements in the Mandovi during 2005–2007**

An important characteristic of southwest monsoon is the breaks in rainfall during this period. The break during rainfall reduce river discharge, which in turn causes intrusion of salinity to further upstream regions in the Mandovi and Zuari estuaries. Saline water is pushed back into the sea when the rainfall once again becomes active. To study this intraseasonal variations of salinity during this period, we carried out salinity measurements

along the longitudinal sections in the Mandovi estuary during the selected days of 2005–2007. This data were analysed to study the intraseasonal variations of salinity during wet season.

### **2.2.5 River discharge data**

The monthly mean averaged discharge data in 1993 at Ganjem, an upstream station in Mandovi estuary were obtained from Central Water Commission, Government. of India.

### **2.2.6 Rainfall data**

Rainfall data during 1999–2001 at Valpoi and Sanguem stations respectively in the Mandovi and Zuari estuaries, and rainfall data at Panaji near the mouth of the Mandovi and Zuari estuaries, during the selected days of 2005–2007 were obtained from India Meteorological Department.

## **2.3 Numerical model**

Numerical models have a variety of applications in scientific and engineering fields. Numerical models are widely used for the simulations of physical processes in ocean and have many applications in the coastal regions and estuaries. To simulate tidal circulation, sedimentation, salinity distribution etc. in an estuary, various modelling techniques such as physical modelling, analytical modelling etc. are used. Though physical modelling techniques are useful for the predictions of the estuarine processes, this approach is expensive and have limitations in scaling some physical parameters. Analytical modelling is another tool to study the estuarine systems and many studies were carried out in estuaries using analytical models [Ketchum, 1950, 1951a,b, 1954, 1955; Ippen and Harleman, 1961; Hansen and Rattray, 1965].

Simulation of estuarine processes requires proper representation of bottom topography, irregular coastline etc. The limitations of analytical modelling is that it assumes a regular geometry of systems. The geometry of an estuarine system has an important role on circulation and phase speed of waves. An improper representation of geometry does not show the important characteristics of estuarine dynamics.

Advances in computer technology in 1950s made the solution of equations, which represent the systems easy and fast and many models were developed using one dimensional equations of motion, continuity and advection diffusion equation of salinity [Lamoen, 1949; Hansen, 1956; Harleman et al., 1968; Bella and Dobbins, 1968; Dronkers, 1969]. Some of the studies carried out using one dimensional modelling approach are described in the following sections.

Lamoen [1949] used a one dimensional numerical model to simulate tides and tidal currents in the Panama Canal and Hansen [1956] proposed a numerical model for the non-linear tidal propagation in Ems estuary, Germany. The finite difference explicit numerical scheme was used in the model. Later on, a one dimensional numerical approach was proposed by Harleman et al. [1968] to simulate dispersion coefficient in Potomac estuary. Posmentier and Raymond [1979] used a one dimensional model and the coefficient of longitudinal diffusion for salt was calculated from the distribution of salinity observed in the Hudson estuary. Their results suggested that the density induced, gravitational, vertical circulation does not dominate the longitudinal diffusion of salt in the Hudson estuary. A one dimensional hydrodynamical model was used by Uncles and Jordan [1980] to describe the crosssectionally averaged Stokes drift and Eulerian residual (tidally averaged) currents in a section of the Severn estuary between Porthcawl and Sharpness.

A time dependent, one dimensional, advection diffusion equation was used by Holloway [1981] to predict salinity distribution in the vertically well mixed upper regions of the Bay of Fundy. Tidal asymmetries at Nauset Inlet was studied using a one dimensional numerical model by Speer and Aubrey [1985]. Thatcher and Harleman [1981]



used another one dimensional model to study the salinity fields in Delaware estuary and Shetye and Murty [1987] used a one dimensional model to estimate the annual salt budget in the Zuari estuary on the west coast of India. Giese and Jay [1989] used a one dimensional harmonic transport model, which provides a qualitative explanation for and accurate quantitative predictions of along channel variations in tidal properties in terms of the momentum balance.

Savenije [1993] proposed a predictive steady state salt intrusion model in alluvial estuaries. Their method applies equally well to density or tide driven mixing and it can be used for estuaries with a wide range of shapes, as long as the estuary is alluvial and the longitudinal variation of the cross sectional area can be described by an exponential function. Li and Elliot [1993] used an array of one dimensional models to simulate the vertical structure of tidal currents and temperature of North sea. They used a turbulence closure scheme proposed by Mellor and Yamada [1974].

Unnikrishnan et al. [1997] used a network numerical model in the Mandovi and Zuari estuaries to simulate the tidal decay during wet season. Gillibrand and Balls [1998] formulated a one dimensional salt intrusion model to investigate the hydrography of the Ythan estuary, a small shallow macro-tidal estuary in the north east of Scotland. Their model successfully simulated salinity distributions for periods of high and low river flow, and was used to illustrate how total oxidized nitrogen concentrations fluctuated in response to variations in river flow. A box model was developed by Pritchard [1969] to simulate tides.

Most of these studies were carried out to understand the basic dynamical processes in the estuarine systems. Though one dimensional models are successful in simulating tidal hydrodynamics to a great extent, its inability to represent the changes of circulation and mixing in the lateral and vertical directions, which are significant in many of the estuarine systems, are the major limitations of this modelling approach.

The development of new generation computers since 1970s paved the way for devel-

opment of two dimensional simulations of estuarine systems fast and less costly. Two dimensional models can simulate circulation in wide bays and estuaries much better than one dimensional models. [Leendertse, 1967] developed a two dimensional model and he used a finite difference scheme to solve partial differential equations. Later, many two dimensional vertically and laterally averaged models were developed.

[Reid and Bodin, 1968] used a two dimensional numerical storm surge model in Galveston Bay. They simulated tide in the Bay without including the surface stress term in the equations. Heaps [1969] developed a numerical model for the North sea.

Two dimensional models were developed by [Leendertse, 1970; Leendertse and Gritton, 1971a,b] for the simulations of water levels and velocities in well mixed estuaries. Prandle and Crookshank [1974] used two dimensional and one dimensional models using a finite difference scheme to simulate tides in the St. Lawrence River. They used two dimensional model and one dimensional models for wider and narrow regions respectively.

A two dimensional numerical model in the longitudinal and vertical plane was developed by Hamilton [1975] to study the vertical structure of current and salinity in the Rotterdam Waterway. Laterally averaged equations were used in the model and the equations were approximated by a finite difference initial value method. Ross et al. [1977] developed a vertically integrated numerical model for water quality and sediment transport and this model was also used for hurricane surge computation. Blumberg [1977] developed a real time numerical model to simulate the dynamics of Potomac River estuary. The model output showed that simulations of surface elevation, velocity and salinity fields were in good agreement with that of observations.

Blumberg [1978] carried out numerical experiments to get the detailed features of tidal characteristics in an estuary. The simulations were carried out for two cases, one for varying density and another for constant density. In this study, it was found that the discharge through any section, the tidal range, and the tidal phases were independent of the density structure. However, the tidal amplitudes, the mean elevation and the vertical

structure of longitudinal velocity changed considerably in the various experiments.

[Johns, 1978] developed a parametrization scheme for modelling turbulence in marine systems and an application was made to the determination of tidal structure in an elongated channel. Prandle [1978] used a two dimensional vertically integrated numerical model to simulate the distribution of residual flow and the variation in mean sea level in the southern North Sea.

A nonlinear numerical tidal model by Bowman and Chiswell [1982] was used in Hau-raki Gulf to determine the water levels, velocities, shallow water tides, residual circulation, energy dissipation rates and vorticity. Falconer et al. [1986] developed a depth averaged model for the simulation of tidal circulation in Rattray Island. Hamilton [1990] carried out simulations of time and depth dependent salinity and current fields of the Columbia River estuary using a multi channel, laterally averaged estuary model.

Lee et al. [1993] used a depth averaged model to study the pollutant dispersal in Masan bay Korea. The numerical model used for the simulation was a modified version of [Falconer et al., 1986]. Rady et al. [1994] used a model to examine the astronomical tides in the Gulf of Suez, Egypt. A vertically averaged two dimensional model was used for simulations of tides.

Unnikrishnan et al. [1999b] developed a two dimensional barotropic numerical model based on shallow water wave equations to simulate the sea level and tidal circulation in the shelf regions of the central west coast of India including Gulf of Khambhat, west coast of India. Their study showed that the circulation in the region is dominated by barotropic tides.

[Wang et al., 2004] calculated the residence time of the Danshuei River through a series of numerical experiments using a laterally integrated two dimensional hydrodynamic eutrophication model (HEM-2D). There are many other laterally averaged models for modelling transport processes in narrow rivers and estuaries [Chen, 1989, 1990, 2003, 2004a,b; Chen et al., 2000; Chen, 2007].

The high power computing availability nowadays facilitates the simulations of three dimensional nature of the estuarine systems. Some of these kind of models used for the simulations of tidal hydrodynamics, salt transports are those of Leendertse et al. [1973]; Oey et al. [1985] and Ji et al. [2007].

### **2.3.1 Numerical model for simulations of tides and salinity in the Mandovi and Zuari estuaries**

Three dimensional models are generally too complex for routine applications and their use is still confined to situations where the detailed spatial definition is essential [Lewis, 1997]. The Mandovi and Zuari estuaries are very shallow and narrow estuaries and the proper schematization is easier in a 1D formulation at the upstream regions and a 2D formulation for the wider regions near the mouth. If the significant variations of estuarine processes occur in horizontal plane, a vertically integrated modelling approach can be employed. In the present study, for the simulation of tides and salinity, a hybrid network numerical model consisting of 2D and 1D models was used. The 2D numerical model in the hybrid model is the modified form of a vertically averaged 2D numerical model described by Unnikrishnan et al. [1999b]. The 2D model was used for simulating tides and salinity in the downstream regions in the Mandovi and Zuari estuaries. The cross sectional area of the Mandovi and Zuari estuaries decrease rapidly toward the upstream directions. Hence for the simulation of tides and salinity at these narrow upstream regions, we developed an area averaged 1D model using the formulation given by [Harleman and Lee, 1969; Thatcher and Harleman, 1972]. The 2D and 1D models were coupled at a distance of about 15 and 12 *km* for the Mandovi and Zuari respectively from the mouth of these estuaries (Figure 2.1).

### 2.3.2 2D model equations

The vertically averaged equations of momentum, continuity and advection diffusion equation of salinity were used in the 2D model. A Cartesian coordinate system was used for the present model domain where x and y-axis are positive toward east and north respectively.

The momentum equation in the transport form can be written as follows

$$\frac{\partial U}{\partial t} + \frac{\partial(uU)}{\partial x} + \frac{\partial(vU)}{\partial y} = -g(h+\eta)\frac{\partial\eta}{\partial x} + fV + A_H\nabla^2U - C_DU\frac{\sqrt{U^2+V^2}}{(h+\eta)^2} \quad (2.1)$$

$$\frac{\partial V}{\partial t} + \frac{\partial(uV)}{\partial x} + \frac{\partial(vV)}{\partial y} = -g(h+\eta)\frac{\partial\eta}{\partial y} - fU + A_H\nabla^2V - C_DV\frac{\sqrt{U^2+V^2}}{(h+\eta)^2} \quad (2.2)$$

The continuity equation can be written as

$$\frac{\partial\eta}{\partial t} + \frac{\partial U}{\partial x} + \frac{\partial V}{\partial y} = 0 \quad (2.3)$$

Advection diffusion equation of salinity is written as follows

$$\frac{\partial S}{\partial t} + \frac{\partial(uS)}{\partial x} + \frac{\partial(vS)}{\partial y} = K_x\frac{\partial^2 S}{\partial x^2} + K_y\frac{\partial^2 S}{\partial y^2} \quad (2.4)$$

Where  $U = u(h+\eta)$  and  $V = v(h+\eta)$

### 2.3.3 Equations in 1D model

The equations used in the one dimensional model are area averaged momentum and continuity equations and advection diffusion equation of salinity [Harleman and Lee, 1969; Thatcher and Harleman, 1972].

The one dimensional momentum equation can be written as

$$\frac{\partial Q}{\partial t} + \frac{2Q}{A}q - \frac{2bQ}{A} \frac{\partial \eta}{\partial t} = -gA \frac{\partial(z_0 + h + \eta)}{\partial x} - g \frac{Q |Q|}{AC^2R} \quad (2.5)$$

The continuity equation is written as follows

$$b \frac{\partial \eta}{\partial t} + \frac{\partial Q}{\partial x} - q = 0 \quad (2.6)$$

Chezy coefficient is calculated using the formula given below.

$$C = \frac{(1.49)}{n} R^{\frac{1}{6}} \quad (2.7)$$

Where  $n$  is the manning coefficient

Area averaged advection diffusion equation of salinity can be written as

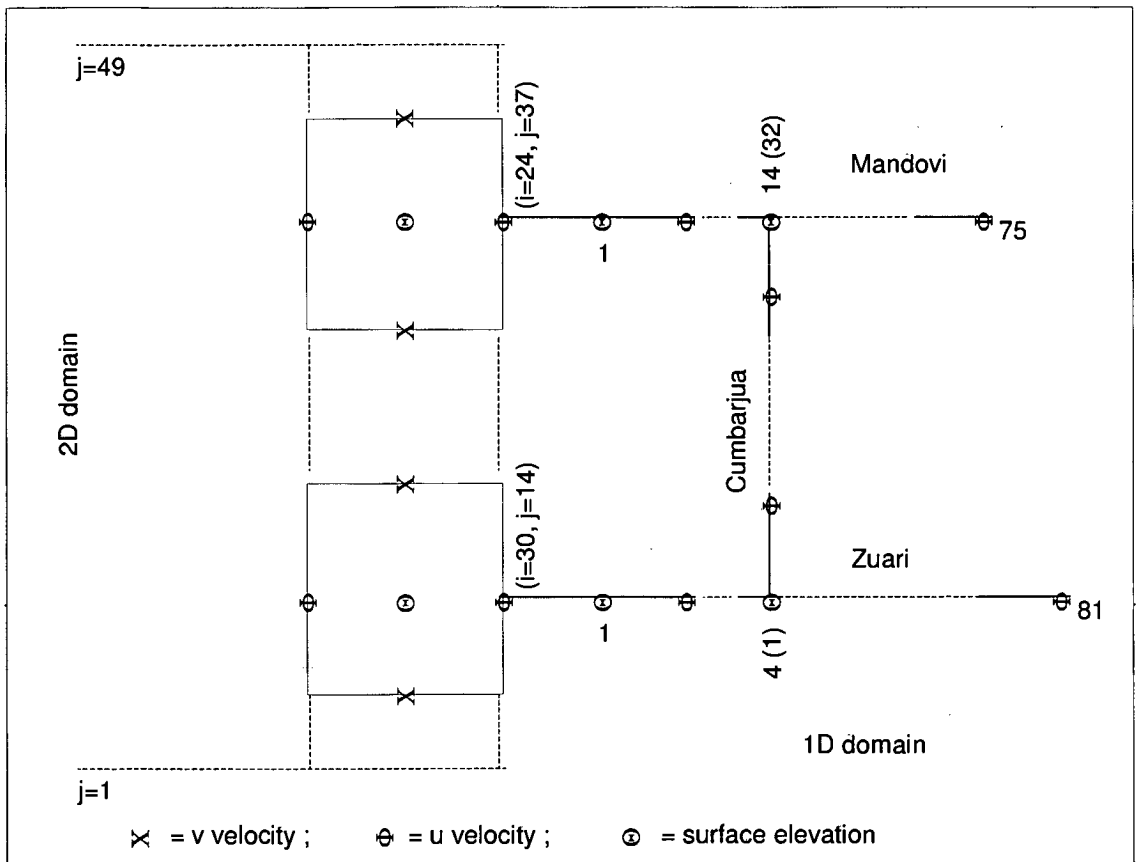
$$A \frac{\partial S}{\partial t} + \frac{\partial(QS)}{\partial x} = AK_x \frac{\partial^2 S}{\partial x^2} \quad (2.8)$$

### 2.3.4 Finite difference scheme

There are many numerical methods such as finite difference method, finite element method etc. for solving the partial differential equations. Finite difference schemes are widely



**Figure 2.2** Schematic diagram showing the coupling between 2D and 1D models and two 1D models.





used numerical schemes because they give less complexity compared to other numerical schemes.

Hydrodynamic modelling of estuaries normally requires the physical dimensions to be approximated by a computational grid [Martin and McCutcheon, 1999]. There are various types of model grids and a grid is selected for approximating the solutions of differential equations based on what kind of numerical scheme is used. In the present model, an Arakawa C grid [Arakawa and Lamb, 1977; Thubum, 2007] was used (see Figure 2.2). Arakawa C grid is a staggered grid and  $u$  and  $v$  velocities are computed at the grid boundaries and free surface elevation and salinity are computed at the centre of the grid. The advantage of using this grid is that it enables the user to include barriers, across which no flow is allowed. Also, a zero velocity boundary condition can be applied at the closed boundaries [Grzechnik, 2000].

The leapfrog scheme was used to march in time. The leapfrog scheme is a three time level scheme having second order accuracy. Despite its three time level structure, the leapfrog scheme is efficient because it requires derivative computations only once at each time step. It is neutrally stable, with no dissipation error [Zhou, 2002].

The continuity equation in finite difference form can be written as

$$\frac{\eta_{i,j}^{n+2} - \eta_{i,j}^n}{2\Delta t} = - \left( \frac{U_{i,j}^{n+1} - U_{i-1,j}^{n+1}}{\Delta x} \right) - \left( \frac{V_{i,j}^{n+1} - V_{i,j-1}^{n+1}}{\Delta y} \right) \quad (2.9)$$

Advection diffusion equation of salinity in finite difference form can be written as

$$\begin{aligned} \frac{S_{i,j}^{n+2} - S_{i,j}^n}{2\Delta t} = & -\frac{1}{\Delta x} \left\{ (u_{i,j}^{n+1}) \left( \frac{S_{i+1,j}^{n+1} - S_{i,j}^{n+1}}{2} \right) + (u_{i-1,j}^{n+1}) \left( \frac{S_{i,j}^{n+1} - S_{i-1,j}^{n+1}}{2} \right) \right\} \\ & -\frac{1}{\Delta y} \left\{ (v_{i,j}^{n+1}) \left( \frac{S_{i,j+1}^{n+1} - S_{i,j}^{n+1}}{2} \right) + (v_{i,j-1}^{n+1}) \left( \frac{S_{i,j}^{n+1} - S_{i,j-1}^{n+1}}{2} \right) \right\} \\ & + K_x \left( \frac{S_{i+1,j}^n + S_{i-1,j}^n - 2S_{i,j}^n}{\Delta x^2} \right) + K_y \left( \frac{S_{i,j+1}^n + S_{i,j-1}^n - 2S_{i,j}^n}{\Delta y^2} \right) \end{aligned} \quad (2.10)$$

The momentum equation along the x-axis in finite difference form can be written as

$$\begin{aligned} \frac{U_{i,j}^{n+2} - U_{i,j}^n}{2\Delta t} = & -\frac{1}{\Delta x} \left\{ \left( \frac{u_{i,j}^{n+1} + u_{i+1,j}^{n+1}}{2} \right) \left( \frac{U_{i,j}^{n+1} + U_{i+1,j}^{n+1}}{2} \right) - \left( \frac{u_{i-1,j}^{n+1} + u_{i,j}^{n+1}}{2} \right) \left( \frac{U_{i-1,j}^{n+1} + U_{i,j}^{n+1}}{2} \right) \right\} \\ & -\frac{1}{\Delta y} \left\{ \left( \frac{v_{i+1,j}^{n+1} + v_{i,j}^{n+1}}{2} \right) \left( \frac{U_{i,j}^{n+1} + U_{i,j+1}^{n+1}}{2} \right) - \left( \frac{v_{i+1,j-1}^{n+1} + v_{i,j-1}^{n+1}}{2} \right) \left( \frac{U_{i,j}^{n+1} + U_{i,j-1}^{n+1}}{2} \right) \right\} \\ & -\frac{g}{\Delta x} \left\{ \left( \frac{h_{i,j} + h_{i+1,j}}{2} + \frac{\eta_{i,j}^{n+1} + \eta_{i+1,j}^{n+1}}{2} \right) (\eta_{i+1,j}^{n+1} - \eta_{i,j}^{n+1}) \right\} \\ & + f \left\{ \left( \frac{V_{i,j}^{n+1} + V_{i+1,j}^{n+1} + V_{i,j-1}^{n+1} + V_{i+1,j-1}^{n+1}}{4} \right) \right\} \\ & + A_H \left\{ \left( \frac{U_{i+1,j}^n - 2U_{i,j}^n + U_{i-1,j}^n}{\Delta x^2} \right) + \left( \frac{U_{i,j+1}^n - 2U_{i,j}^n + U_{i,j-1}^n}{\Delta y^2} \right) \right\} \\ & - C_D (U_{i,j}^n) \left\{ \sqrt{\left( \frac{(U_{i,j}^n)^2 + (V_{i,j}^n)^2}{(h_{i,j} + \eta_{i,j}^n)^2} \right)} \right\} \end{aligned} \quad (2.11)$$

Momentum equation along the y-axis in finite difference form is written as

$$\begin{aligned}
\frac{V_{i,j}^{n+2} - V_{i,j}^n}{2\Delta t} = & -\frac{1}{\Delta x} \left\{ \left( \frac{u_{i,j}^{n+1} + u_{i,j+1}^{n+1}}{2} \right) \left( \frac{V_{i,j}^{n+1} + V_{i+1,j}^{n+1}}{2} \right) - \left( \frac{u_{i-1,j}^{n+1} + u_{i-1,j+1}^{n+1}}{2} \right) \left( \frac{V_{i-1,j}^{n+1} + V_{i,j}^{n+1}}{2} \right) \right\} \\
& -\frac{1}{\Delta y} \left\{ \left( \frac{v_{i,j}^{n+1} + v_{i,j+1}^{n+1}}{2} \right) \left( \frac{V_{i,j}^{n+1} + V_{i,j+1}^{n+1}}{2} \right) - \left( \frac{v_{i,j}^{n+1} + v_{i,j-1}^{n+1}}{2} \right) \left( \frac{V_{i,j}^{n+1} + V_{i,j-1}^{n+1}}{2} \right) \right\} \\
& -\frac{g}{\Delta y} \left\{ \left( \frac{h_{i,j} + h_{i,j+1}}{2} + \frac{\eta_{i,j}^{n+1} + \eta_{i,j+1}^{n+1}}{2} \right) (\eta_{i,j+1}^{n+1} - \eta_{i,j}^{n+1}) \right\} \\
& -f \left\{ \left( \frac{U_{i,j}^{n+1} + U_{i,j+1}^{n+1} + U_{i-1,j}^{n+1} + U_{i-1,j+1}^{n+1}}{4} \right) \right\} \\
& + A_H \left\{ \left( \frac{V_{i+1,j}^n - 2V_{i,j}^n + V_{i-1,j}^n}{\Delta x^2} \right) + \left( \frac{V_{i,j+1}^n - 2V_{i,j}^n + V_{i,j-1}^n}{\Delta y^2} \right) \right\} \\
& - C_D (V_{i,j}^n) \left\{ \sqrt{\frac{\left( (U_{i,j}^n)^2 + (V_{i,j}^n)^2 \right)}{\left( h_{i,j} + \eta_{i,j}^n \right)^2}} \right\}
\end{aligned} \tag{2.12}$$

One dimensional equations of momentum, continuity and salt equation were also solved in a similar fashion.

### 2.3.5 Coupling of numerical models

The 2D model domain extends to 15 and 12 km in the Mandovi and Zuari estuaries respectively from the mouth (see Figure 2.1). A 1D model was used for the upstream regions of the Mandovi and Zuari estuaries and for the Cumbarjua canal.

### 2.3.6 Coupling between 2D and 1D models

Surface elevation and salinity at the 1<sup>st</sup> grid point of the 1D domain of the Mandovi and Zuari were calculated using the following formulation

$$\eta_i^{n+2} = \eta_i^n - \left( \frac{2\Delta t}{\Delta x b_i} \right) \left( Q_i^{n+1} - b_i \left( U_{i-1,j}^{n+1} \right) \right) \quad (2.13)$$

$$\begin{aligned} S_i^{n+2} = & S_i^n - \left( \frac{\Delta t}{\Delta x A_i} \right) \left\{ Q_i^{n+1} (S_{i+1}^{n+1} - S_i^{n+1}) + A_i u_{i-1,j}^{n+1} (S_i^{n+1} - S_{i-1,j}^{n+1}) \right\} \\ & + K_x \left( \frac{2\Delta t}{\Delta x^2} \right) (S_{i-1,j}^n + S_{i+1}^n - 2S_{i,j}^n) \end{aligned} \quad (2.14)$$

Where  $U_{i-1,j}^{n+1}$  and  $S_{i-1,j}^{n+1}$  are respectively transport and salinity from 2D model. In the above equation, (i-1) corresponds to 24 and j corresponds to 37 in the Mandovi. In the Zuari, (i-1) corresponds to 30 and j corresponds to 14.  $Q_i^{n+1}$  and  $S_i^{n+1}$  are respectively transport and salinity from 1D models. Note that  $Q_i^{n+1}$  and  $S_i^{n+1}$  are general notations used for transport and salinity in 1D models in the above equations. But for the following calculations,  $Q_i^{n+1}$  and  $S_i^{n+1}$  are replaced by  $Qm_i^{n+1}$ ,  $Qz_i^{n+1}$ ,  $Qc_i^{n+1}$  and  $Sm_i^{n+1}$ ,  $Sz_i^{n+1}$ ,  $Sc_i^{n+1}$  respectively for the Mandovi, Zuari and Cumbarjua canal.

### 2.3.7 Coupling between two 1D models

Calculation of surface elevation and salinity at the 4<sup>th</sup> grid point in the Zuari and 1<sup>st</sup> grid point in the Cumbarjua (see the 4(1) grid point in Figure 2.2) were made as follows

$$\eta z_i^{n+2} = \eta z_i^n - \left( \frac{2\Delta t}{\Delta x b z_i} \right) (Q z_i^{n+1} + Q c_i^{n+1} - Q z_{i-1}^{n+1}) \quad (2.15)$$

$$\begin{aligned} S z_i^{n+2} = & S z_i^n - \left( \frac{\Delta t}{2\Delta x A_i} \right) \\ & \{ Q z_i^{n+1} (S z_{i+1}^{n+1} - S z_i^{n+1}) + Q z_{i-1}^{n+1} (S z_i^{n+1} - S z_{i-1}^{n+1}) + Q c_i^{n+1} (S c_{i+1}^{n+1} - S z_i^{n+1}) \} \\ & + K_x \left( \frac{2\Delta t}{\Delta x^2} \right) \{ (S z_{i-1}^n + S z_{i+1}^n - 2S z_i^n) + (S c_{i+1}^n + S c_i^n - 2S c_i^n) \} \end{aligned} \quad (2.16)$$

As shown in the Figure 2.2, the 4<sup>th</sup> grid point in the Zuari and 1<sup>st</sup> grid point in the Cumbarjua are same. Therefore,

$$\eta c_i^{n+2} = \eta z_i^{n+2} \quad (2.17)$$

$$S c_i^{n+2} = S z_i^{n+2} \quad (2.18)$$

Calculation of surface elevation and salinity at the 14<sup>th</sup> grid point in the Mandovi and 32<sup>nd</sup> grid point in the Cumbarjua (see the 14(32) grid point in Figure 2.2) were calculated in a similar fashion.

$$\eta m_i^{n+2} = \eta m_i^n - \left( \frac{2\Delta t}{\Delta x b m_i} \right) (Q m_i^{n+1} - Q c_i^{n+1} - Q m_{i-1}^{n+1}) \quad (2.19)$$

$$\begin{aligned}
Sm_i^{n+2} = & Sm_i^n - \left( \frac{\Delta t}{2\Delta x A_i} \right) \\
& \{ Qm_i^{n+1} (Sm_{i+1}^{n+1} - Sm_i^{n+1}) + Qm_{i-1}^{n+1} (Sm_i^{n+1} - Sm_{i-1}^{n+1}) + Qc_i^{n+1} (Sc_{i+1}^{n+1} - Sm_i^{n+1}) \} \\
& + K_x \left( \frac{2\Delta t}{\Delta x^2} \right) \{ (Sm_{i-1}^n + Sm_{i+1}^n - 2Sm_i^n) + (Sc_{i-1}^n + Sc_i^n - 2Sc_i^n) \}
\end{aligned} \tag{2.20}$$

The 14<sup>th</sup> grid point in the Mandovi and 32<sup>nd</sup> grid point in the Cumbarjua are same (see Figure 2.2). Therefore,

$$\eta c_i^{n+2} = \eta m_i^{n+2} \tag{2.21}$$

$$Sc_i^{n+2} = Sm_i^{n+2} \tag{2.22}$$

Note that (see Equation 2.15) for calculation of surface elevation at the junction of the Zuari and Cumbarjua, the transport at first grid point of the Cumbarjua was added but that of Mandovi, the transport at the last grid point of the Cumbarjua was subtracted (see Equation 2.19), as per sign convention used, the flow in the Cumbarjua canal is taken as positive from the Zuari side to the Mandovi side.

### 2.3.8 Freshwater influx inclusion in the model

Freshwater influx was included in the model by calculating transport from the river discharge data at the upstream end of the model domain. Transport at the upstream end of the model domain was calculated as follows.

$$q_n^{n+1} = \frac{D}{\Delta x} \quad (2.23)$$

Where  $q$  is freshwater influx per unit channel length ( $m^2s^{-1}$ )

### 2.3.9 Stability criterion of the numerical scheme

The stability of the scheme was determined by Courant-Friedrichs-Lewy (CFL) stability criterion, which can be written as follows

$$\Delta t \leq \frac{(\Delta x, \Delta y)}{\sqrt{2g(h + \eta)}} \quad (2.24)$$

Where  $\Delta t$  is the time step, which was chosen as 15 seconds in the present model.  $\Delta x$  and  $\Delta y$  are space increments in  $x$  and  $y$ -directions, which were chosen as 500  $m$ . The grid spacing between  $x$  and  $y$ -directions should be minimised so that it can resolve the effect of irregular coastlines of the estuaries and bays better, but the reduction in grid spacing leads to small time step and this in turn consumes more computational time. In the present model, the  $\Delta x$  and  $\Delta y$  were chosen as 500  $m$  to represent islands and embayments of the Mandovi and Zuari estuaries more accurately.

### **2.3.10 Initial and Boundary conditions**

At the western boundary (open boundary) of the model, surface elevation and salinity were defined as a function of time, while zero flux conditions were applied in the eastern, southern and northern boundaries. For the simulation of surface elevation and tidal currents, the model was initialized with zero surface elevation and velocity throughout the network. At upstream end points of the model domain, transport was calculated according to the river discharge rate. For the simulation of longitudinal distribution of salinity, the model was initialized with constant salinity at different sections of the model domain based on the observations available in 1993.



## **Chapter 3**

# **Simulations of tides in the Mandovi and Zuari estuaries**

### **3.1 Introduction**

In this chapter, the simulations of tides, tidal currents, freshwater influence on tides and the studies on tidal asymmetries are described. Tidal estuaries serve as vital components to coastal ecosystems throughout the world. They usually have complex geometry and strongly nonlinear tidal dynamics [McLaughlin et al., 2003]. As mentioned previously, tide is the main driving mechanism in the estuaries. The Mandovi and Zuari estuaries are meso-tidal estuaries where tidal range is about 1.5 and 2.3 *m* during neap and spring tides respectively. The numerical model, boundary conditions used for the simulations and the results are described in the following sections.

#### **3.1.1 Numerical model**

The hybrid network numerical model described in Chapter 2 was used for the simulations of tidal amplitude, tidal currents etc. in the Mandovi, Zuari and Cumbarjua canal. Sim-

ulations of tidal currents were carried out in the 2D domain of the Mandovi and Zuari estuaries. The details of the equations and numerical scheme used in the model have been explained in Chapter 2.

### 3.1.2 Initial and boundary conditions

Tide, for forcing the model at the open boundary was predicted from the known tidal constituents at Mormugao (Figure 1.2) using Tidal Analysis Software Kit-2000. At the western boundary (open boundary) of the model, surface elevation was defined as a function of time, while zero flux conditions were applied in the eastern, southern and northern boundaries. The model was initialised with zero surface elevation and velocity throughout the network. At the upstream end of the model domain, transport was calculated from the available river discharge rate.

### 3.1.3 The coefficients used in the model

The coefficient of horizontal diffusion of momentum,  $A_H$ , was chosen to be  $500 \text{ m}^2 \text{ s}^{-1}$  in the present model. There was no considerable variation in amplitude at different stations in the estuaries when the bottom drag coefficient,  $C_D$ , in the model was allowed to vary from 0.001 to 0.003, however, the value of 0.002 showed better agreement between observed and simulated tides. Hence we used 0.002 as a constant value for bottom drag coefficient in the downstream regions of the model. At the upstream regions, the channels bathymetry plays an important role on tides. So the Manning coefficient in 1D model was allowed to vary from 0.015 to 0.035.

## 3.2 Results

To simulate tides, the model was run for different cases. First, for the simulation of longitudinal variation of tides during dry and wet seasons and influence of river discharge

on tides. Second, for the simulation of tidal currents and third, for the simulation of tidal constituents. The details of the simulations and the results are described in the following sections.

For simulation of tides, the hybrid network model with initial and boundary conditions was run for 6 days each for dry and wet seasons. The model was forced with sea surface elevation at the open boundary as described previously. During wet season, the Mandovi and Zuari estuaries receive huge amount of fresh water. Figure 1.5 shows the discharge at Ganjem in 1993. The river discharge was about  $400 \text{ m}^3 \text{ s}^{-1}$  during July and August (Bars correspond to 7 and 8 along the x-axis). Hence, river discharge of  $400 \text{ m}^3 \text{ s}^{-1}$  was introduced at upstream end of the model domain. The model was run for 6 days (12 tidal cycles). The first 3 days were considered for spin-up and the remaining 3 days simulations were used for the comparison with the observations.

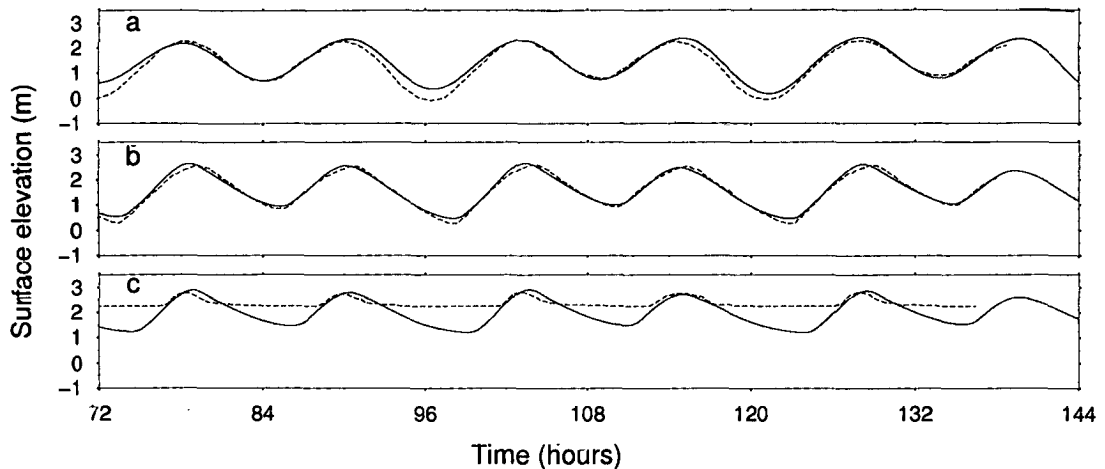
### 3.2.1 Simulations of tides in the Mandovi estuary

Figure 3.1 shows the simulated tides during dry season in the Mandovi estuary. There is a good agreement between the simulations and observations at Mormugao (Figure 3.1 a) and Volvoi (Figure 3.1 b) and at Ganjem (Figure 3.1 c), the simulations are reasonably good. What is noticed from the Figure 3.1 is that, when tide reaches at Ganjem, tidal range is reduced to less than  $0.5 \text{ m}$  from  $2.1 \text{ m}$ . The simulations of tide during wet season are also reasonably well in the Mandovi (Figure 3.3). The presence of tidal oscillations is negligible at Ganjem during wet season.

### 3.2.2 Simulations of tides in the Zuari estuary and Cumbarjua canal

Observed and simulated tides during dry and wet seasons in the Zuari estuary and Cumbarjua canal are shown in Figures 3.3 and 3.4 respectively. The model could simulate the observed tides well in both dry and wet seasons in the Zuari estuary. The magnitude of

**Figure 3.1** Observed (dotted line) and simulated (solid line) tides at different stations in the Mandovi estuary in April 1993. The panels a, b and c represent Mormugao, Volvoi and Ganjem respectively. 72 *hours* shown on the x-axis correspond to 0.0 *hours* (IST) on 07/04/1993.



the tidal amplitude at Banastarim in the Cumbarjua canal (Figures 3.3 b and 3.4 b) are almost equal to that of Zuari. This shows that tide is propagated to the Cumbarjua canal from Zuari without any dissipation in amplitudes. At Sanguem, an upstream end station in the Zuari estuary (Figures 3.3 c), tidal amplitude during dry season is not reduced as in the case of Ganjem in the Mandovi.

### 3.2.3 Simulations of tidal currents

Tidal observations carried out during April and August 1993 were used for the validation of model. The simulations of tides were reasonably well in these estuaries and the simulation of tide showed that the model could be used for the simulation of tidal currents in these estuaries. For the simulation of tidal currents, the model was run for 1 month and the simulations were carried out during the spring and neap tides in April 1993. The purpose of running the model in the month of April was to determine the tidal currents in the absence of river discharge. To simulate tidal currents, the model was forced at open

**Figure 3.2** Observed (dotted line) and simulated (solid line) tides at different stations in the Mandovi estuary in August 1993. The panels a, b and c represent Mormugao, Volvoi and Ganjem respectively. 72 hours shown on the x-axis correspond to 0.0 hours (IST) on 19/08/1993.

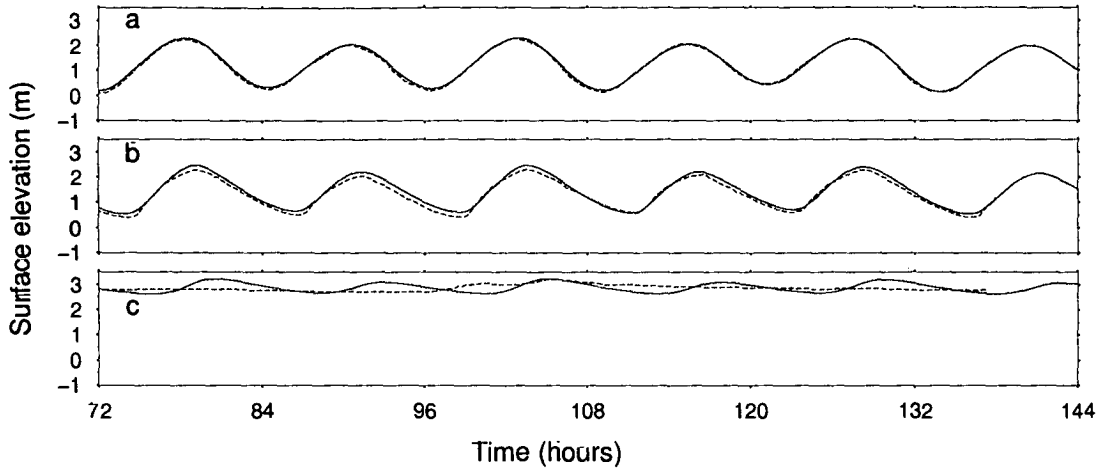


**Figure 3.3** Observed (dotted line) and simulated (solid line) tides at different stations in the Zuari estuary and Cumbarjua canal in April 1993. The panels a, b and c represent Mormugao, Banastarim and Sanguem respectively. 72 hours shown on the x-axis correspond to 0.0 hours (IST) on 07/04/1993.

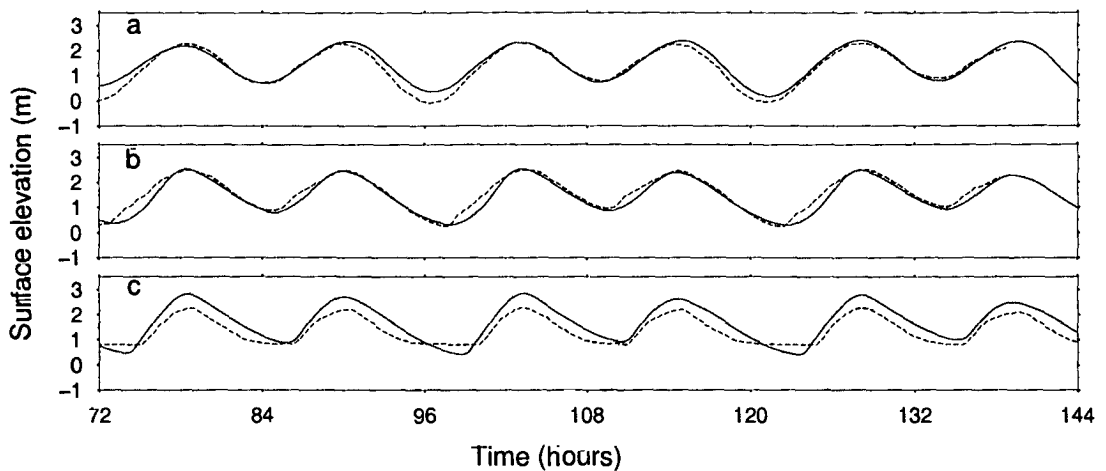
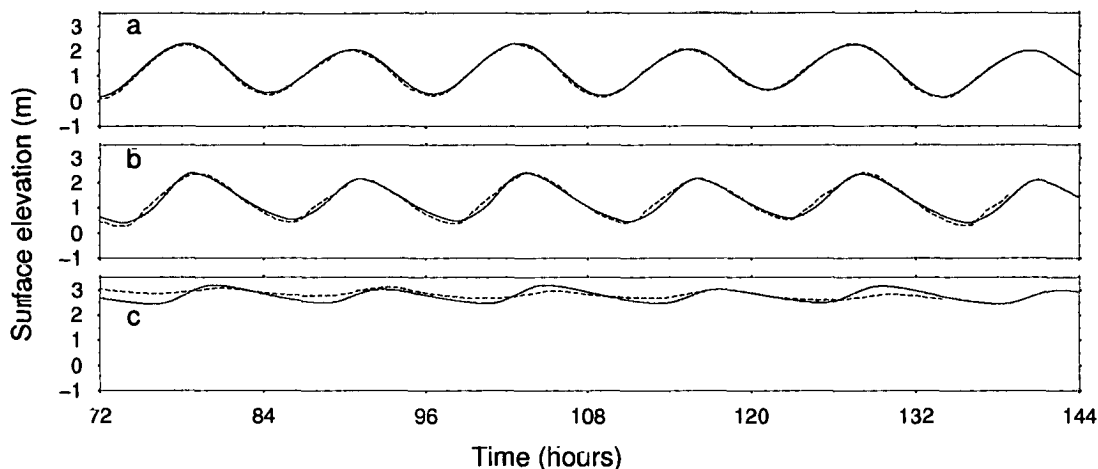


**Figure 3.4** Observed (dotted line) and simulated (solid line) tides at different stations in the Zuari estuary and Cumbarjua canal in August 1993. The panels a, b and c represent Mormugao, Banastarim and Sanguem respectively. 72 hours shown on the x-axis correspond to 0.0 hours (IST) on 19/08/1993.



boundary with sea surface elevation as a function of time.

Tidal ranges in both the Mandovi and Zuari estuaries are about 2.3 and 1.5 m during spring and neap tides respectively. Tidal currents simulated for spring tide are shown in Figures 3.5–3.7. Fairly strong tidal currents of about  $0.80 \text{ m s}^{-1}$  were found during this period in the downstream regions of these estuaries. The magnitude of tidal currents are reduced to about  $0.4 \text{ m s}^{-1}$  during the neap tide (Figure 3.8–3.10). The magnitude of tidal currents are high in the Zuari than compared to Mandovi. This is because of the higher depth in the Zuari compared to Mandovi. Tidal current observations [DeSousa, 1999a, 2000], at Campal, near the mouth of the Mandovi estuary were carried out on 15–16 April 1999. These measurements of tidal currents show that the magnitude of tidal currents is of about  $1.0 \text{ m s}^{-1}$  during spring tide whereas the observations during neap tide (12–13 February 2000) show that the magnitude of these currents are of about  $0.65 \text{ m s}^{-1}$ . The simulated currents are slightly lower than that of those observed.

To study the tidal currents during wet season, the tidally averaged currents over a  $M_2$

**Figure 3.5** Tidal currents during the spring tide in the Mandovi and Zuari estuaries. The currents shown are only for the 2D domain of the 1D and 2D model domain. The sea surface elevation predicted for April 1993 at Mormugao was used for prescribing boundary condition at the open boundary. The timings shown are with respect to the occurrence of high tide at Mormugao.

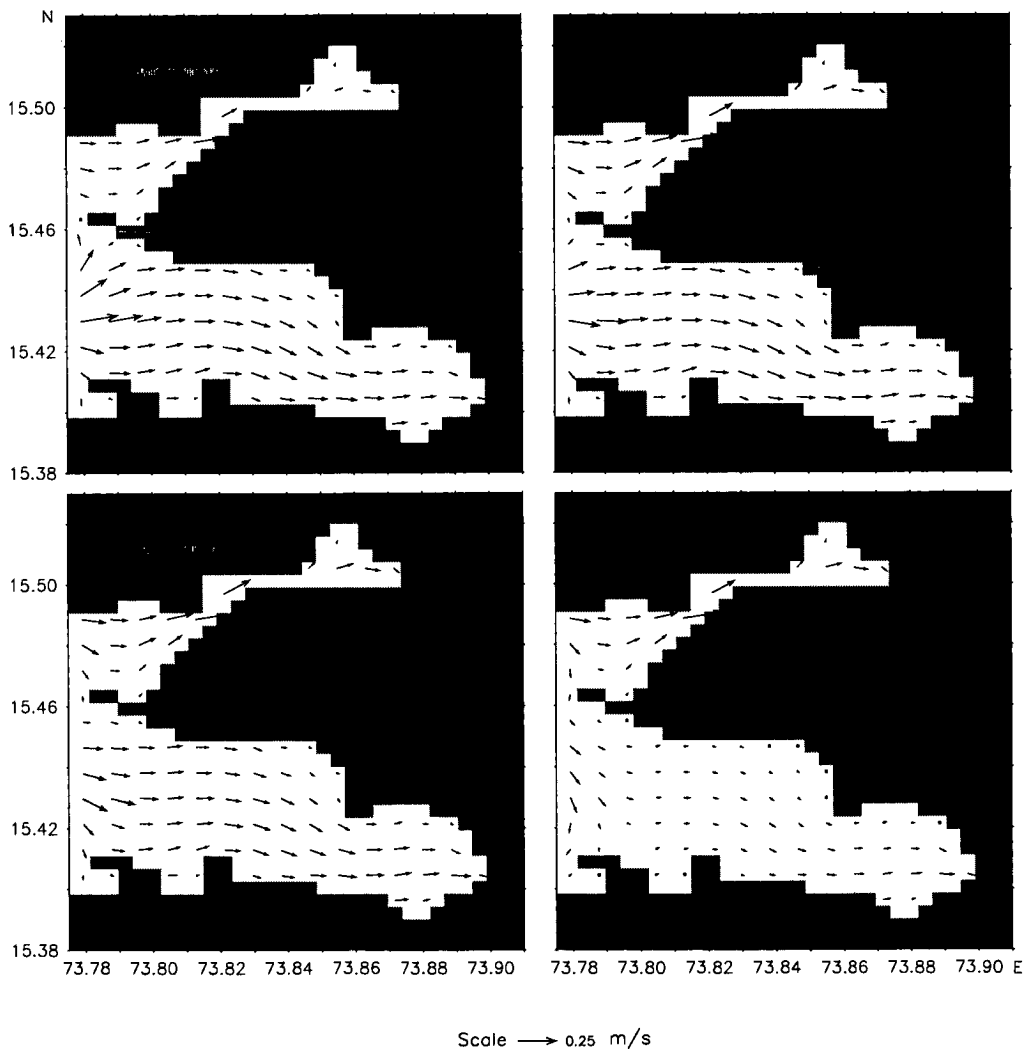


**Figure 3.6** (Continued) Tidal currents during the spring tide in the Mandovi and Zuari estuaries. The currents shown are only for the 2D domain of the 1D and 2D model domain. The sea surface elevation predicted for April 1993 at Mormugao was used for prescribing boundary condition at the open boundary. The timings shown are with respect to the occurrence of high tide at Mormugao.

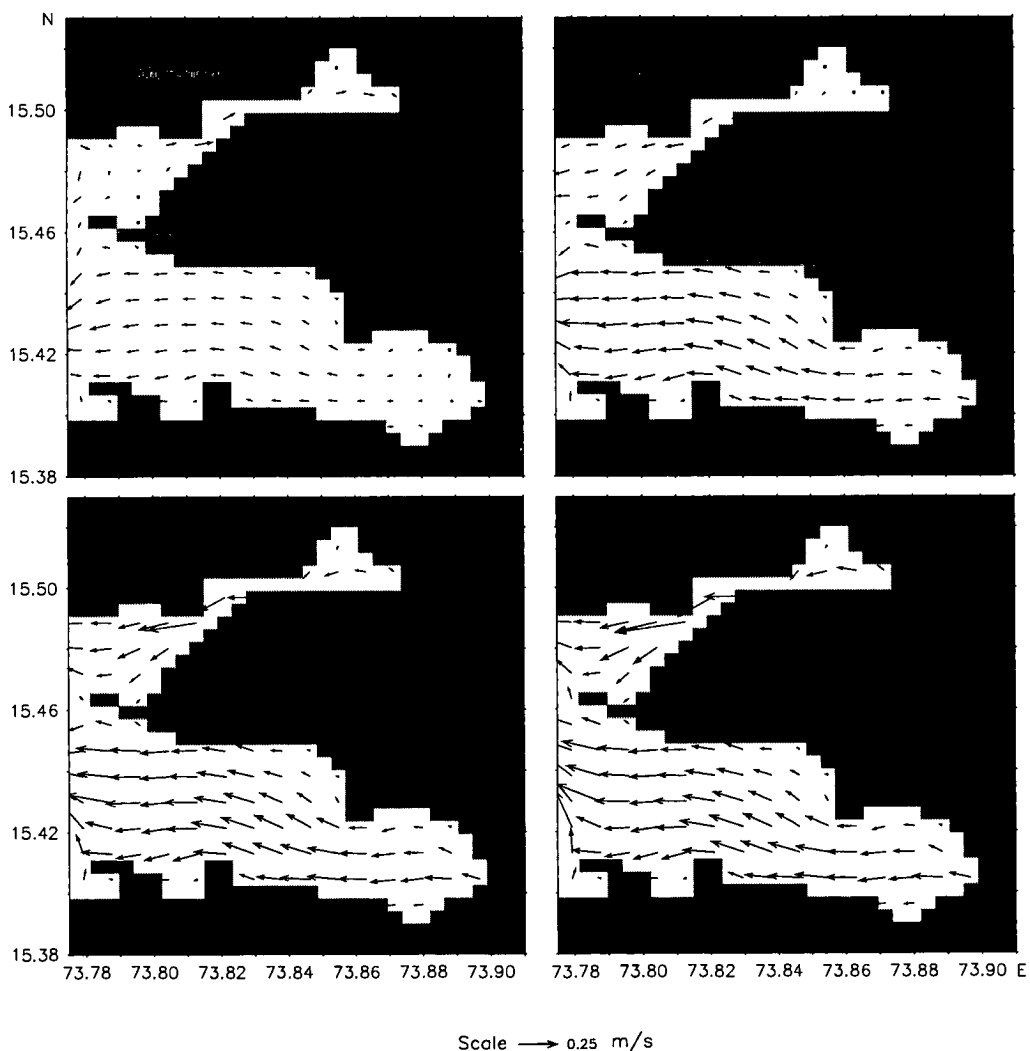




**Figure 3.7 (Continued)** Tidal currents during the spring tide in the Mandovi and Zuari estuaries. The currents shown are only for the 2D domain of the 1D and 2D model domain. The sea surface elevation predicted for April 1993 at Mormugao was used for prescribing boundary condition at the open boundary. The timings shown are with respect to the occurrence of high tide at Mormugao.

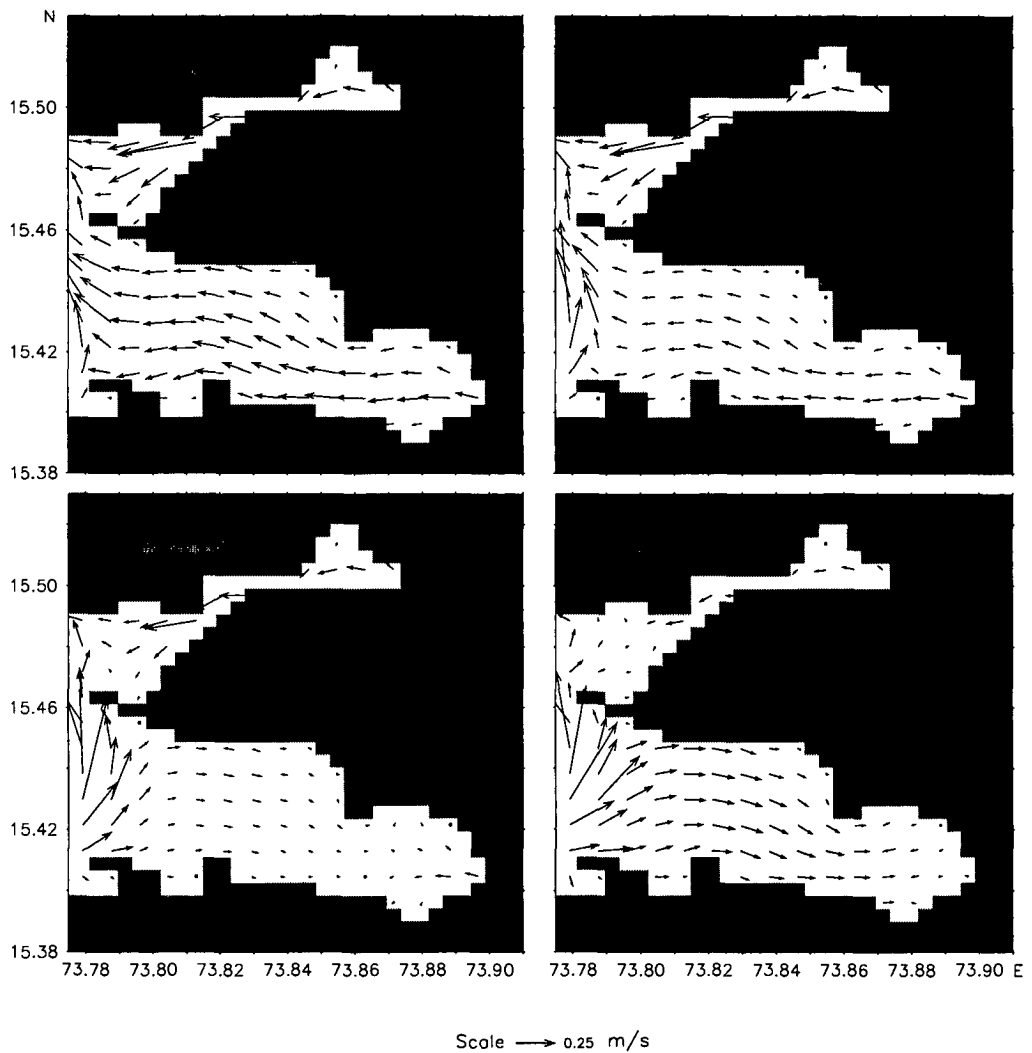


**Figure 3.8** Tidal currents during the neap tide in the Mandovi and Zuari estuaries. The currents shown are only for the 2D domain of the 1D and 2D model domain. The sea surface elevation predicted for April 1993 at Mormugao was used for prescribing boundary condition at the open boundary. The timings shown are with respect to the occurrence of high tide at Mormugao.

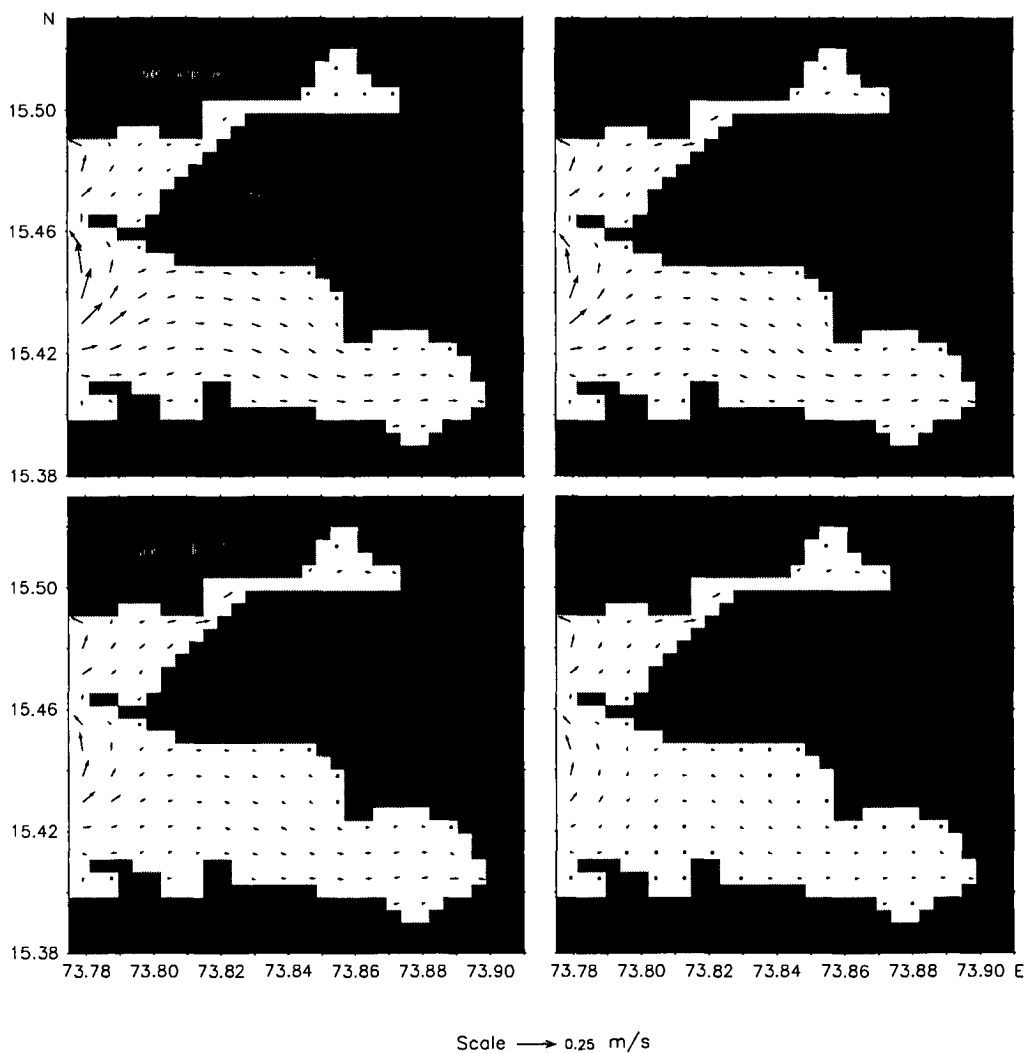


**Figure 3.9 (Continued)** Tidal currents during the neap tide in the Mandovi and Zuari estuaries. The currents shown are only for the 2D domain of the 1D and 2D model domain. The sea surface elevation predicted for April 1993 at Mormugao was used for prescribing boundary condition at the open boundary. The timings shown are with respect to the occurrence of high tide at Mormugao.

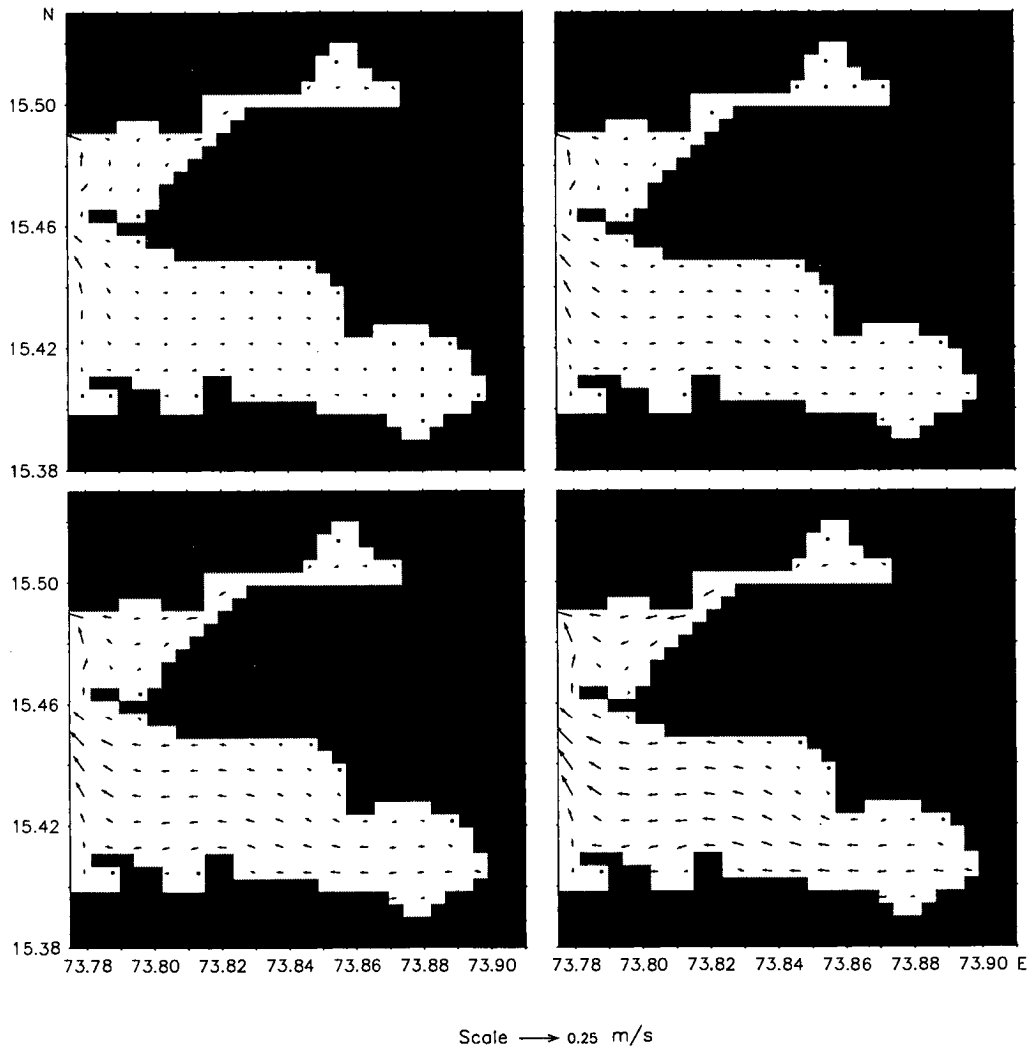
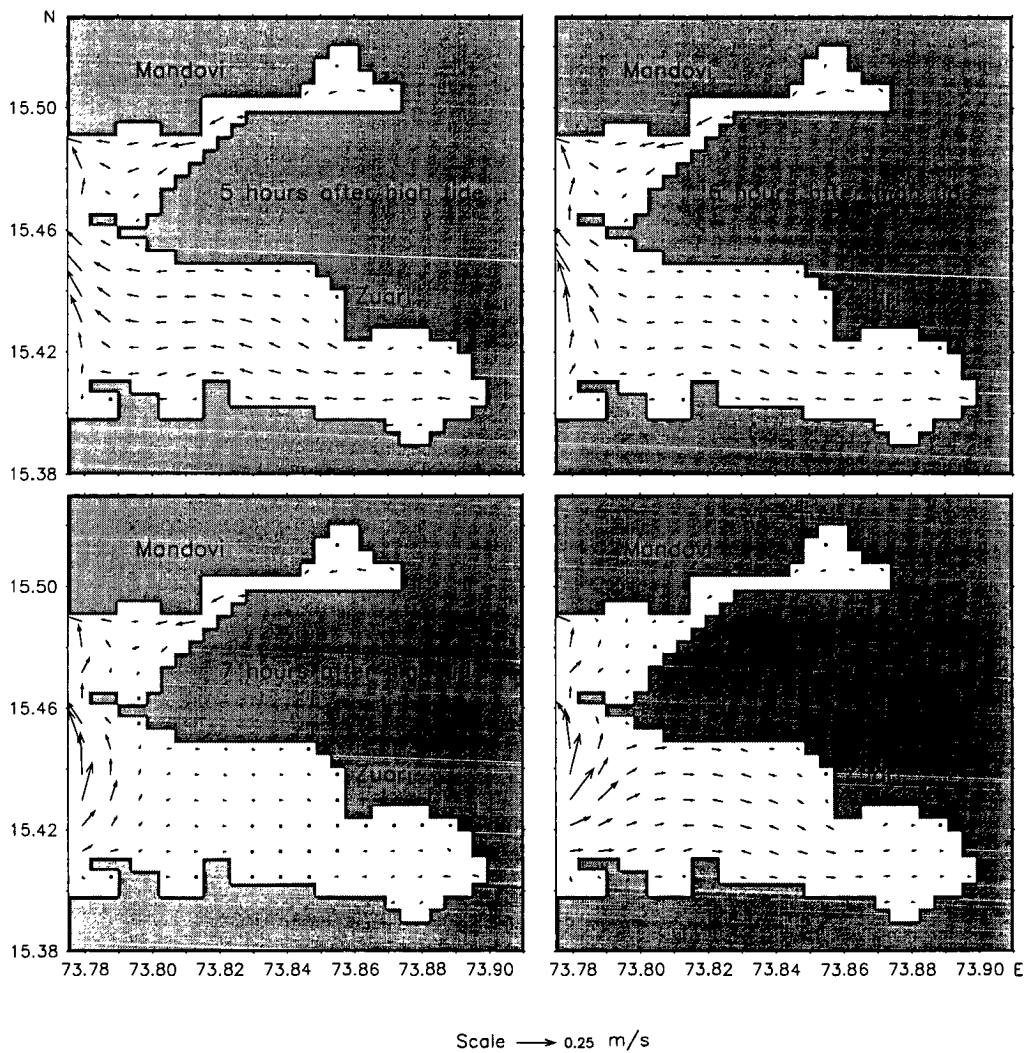


**Figure 3.10 (Continued)** Tidal currents during the neap tide in the Mandovi and Zuari estuaries. The currents shown are only for the 2D domain of the 1D and 2D model domain. The sea surface elevation predicted for April 1993 at Mormugao was used for prescribing boundary condition at the open boundary. The timings shown are with respect to the occurrence of high tide at Mormugao.



tidal period was calculated for varying river discharges. The details of the simulations residual currents and flushing time are explained in Chapter 4 of this thesis.

### 3.3 Tidal asymmetry

One of the main objectives of this thesis was to study the tidal asymmetries in the Mandovi and Zuari estuaries. Tidal spectrum consists of large number of constituents and amplitude and phase of these constituents are subjected to distortion when they propagate from ocean to estuaries. Bottom friction, channel geometry and other physical processes cause tidal distortion in an estuary. Tidal asymmetry has important effects on both the geological evolution of shallow estuaries and the navigability of estuarine channels [Aubrey and Speer, 1985; Speer and Aubrey, 1985]. The mutual interference of an astronomical tide and a shallow water tide can give rise to tidal asymmetry [Kang and Jun, 2003]. To study the tidal asymmetry in these estuaries, the simulations of observed tides during March–April 2003 were carried out. Thereafter, the harmonic analysis of observed and simulated tides was carried out. Tidal constituents derived from harmonic analysis were analysed to study the nonlinear response of the Mandovi and Zuari estuarine system to tidal forcing.

#### 3.3.1 Simulation of tides measured during March–April 2003

The model was run for 42 days (3 March–13 April 2003) to simulate tides at 13 stations in the Mandovi and Zuari estuaries. Even in April, there is a small fresh water influx ( $10\text{--}15\text{ m}^3\text{s}^{-1}$ ) into the Mandovi and Zuari estuaries from the upstream ends; hence river discharge of  $10\text{ m}^3\text{s}^{-1}$  was introduced at the upstream end boundaries in the Mandovi and Zuari estuaries. The model was spun up over a period of 7 days (3–9 March 2003) and the simulated tides of the remaining days (10 March–13 April 2003) were compared with those observed. The observed and simulated tides at 13 stations in the main channels

of the Mandovi and Zuari and in the Cumbarjua are plotted in Figures 3.11– 3.13. The model has reproduced the tidal observations reasonably well in almost all the stations. Verem station in the Mandovi is about 5 km from the mouth where tide is about 1.5 and 2.3 m during neap and spring tide respectively. Tidal ranges remain almost the same at Britona (9 km), Akkada (20 km), Volvoi (33 km) and Usgao (41 km) with slight increase in amplitude toward the upstream regions. But when tide reaches Ganjem (50 km), the tidal oscillation is visible only during spring tide. Similarly, tides at Dona Paula (0 km), Cortalim (12 km), Borim (21 km) and Sanvordem (45 km) also remain unchanged, but the magnitude of tide gets distorted at Sanguem (55 km). The simulation of tides at Banastarim (15 km) and Madkai (24.5 km) in the Cumbarjua are also well reproduced by the model.

### 3.3.2 Harmonic analysis of tides

The purpose of harmonic analysis of tide is to find out the amplitude and phase of each individual constituents from a long tidal record (1 month or more) so that each constituent's role on the tidal distortion in an estuary can be studied in detail. In the present study, Tidal Analysis Software Kit-2000 was used for harmonic analysis of tides. The 35-day data of observed and simulated tides were used for harmonic analysis, and this 1-month's duration of data was sufficient to resolve the major diurnal and semidiurnal constituents; overtides and compound tides.

### 3.3.3 Complex difference module

To find the difference between observed and simulated tidal constituents, the complex difference module was computed. The complex difference module gives synthetic information about the difference in both amplitude and phase between the observation and simulation. The mean difference of this module over major diurnal and semidiurnal con-

**Figure 3.11** Observed (dotted line) and simulated (solid line) tides in the Mandovi estuary during 10 March–13 April 2003. 144 hours on the x-axis correspond to 0.0 hours (IST) on 10 March 2003.

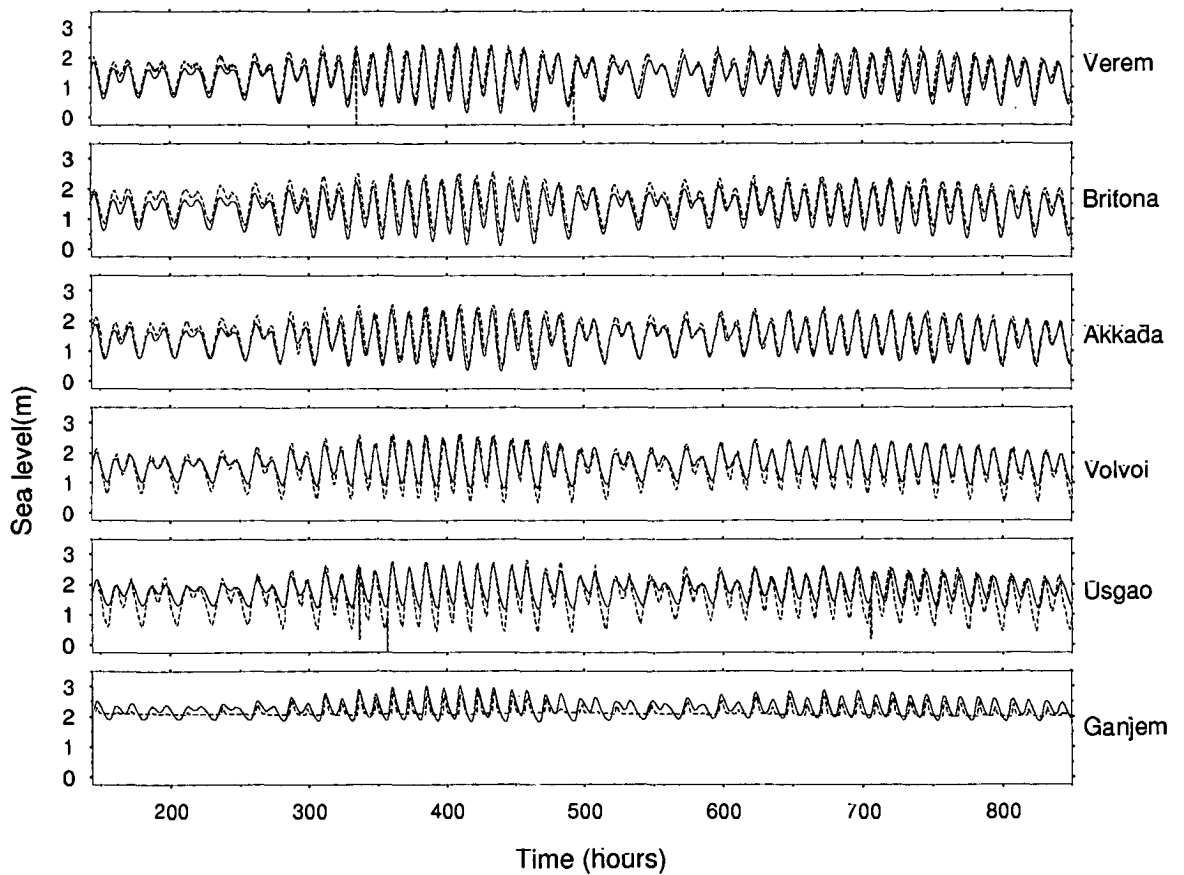


**Figure 3.12** Observed (dotted line) and simulated (solid line) tides in the Zuari estuary during 10 March–13 April 2003. 144 *hours* on the x-axis correspond to 0.0 *hours* (IST) on 10 March 2003.

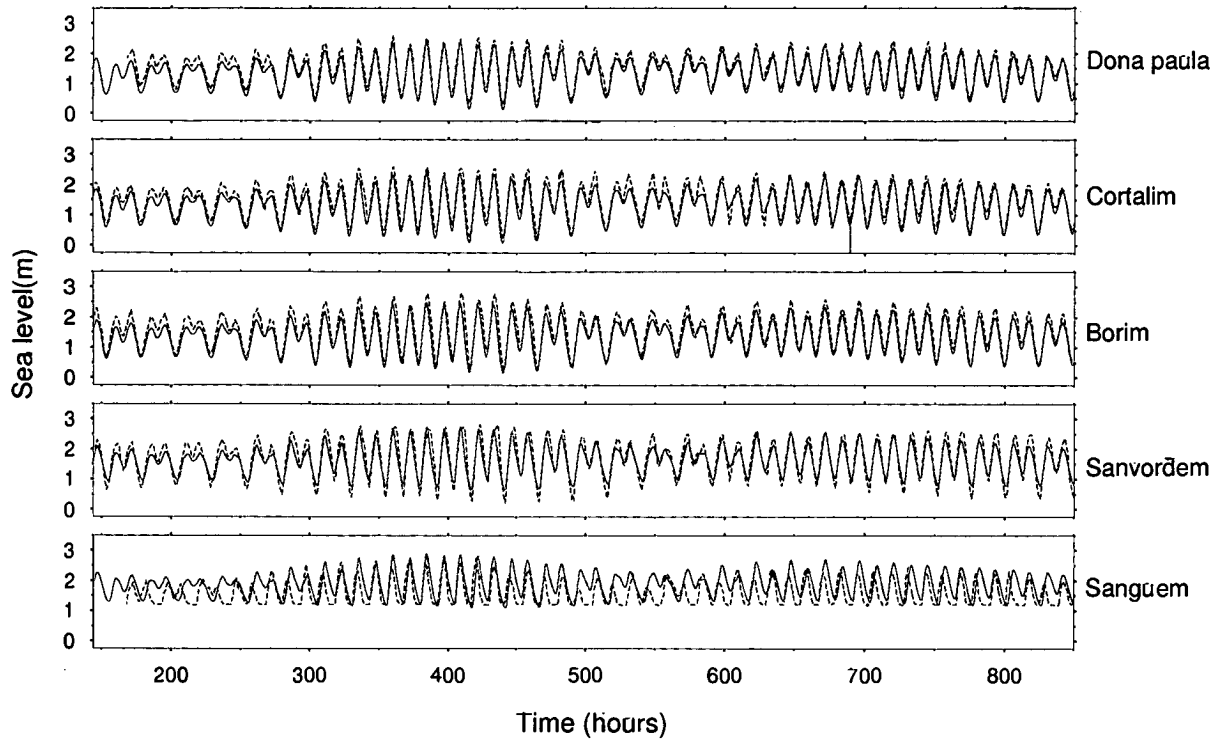
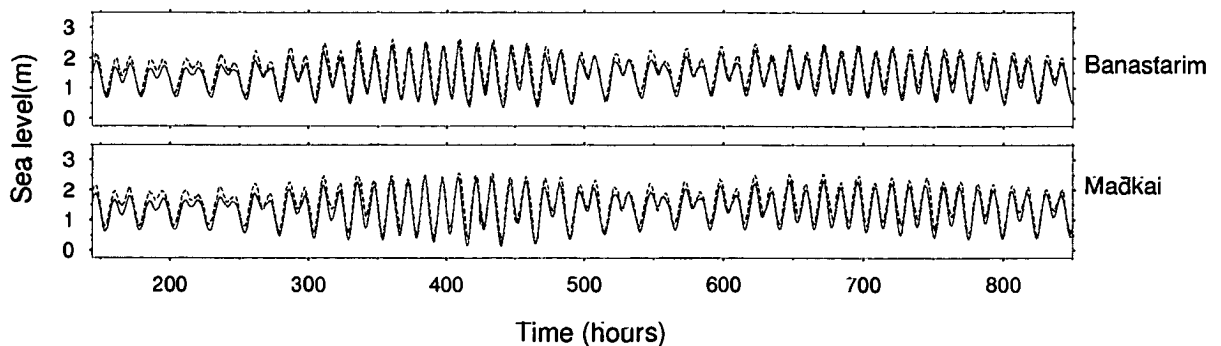


**Figure 3.13** Observed (dotted line) and simulated (solid line) tides in the Cumbarjua canal during 10 March–13 April 2003. 144 *hours* on the x-axis correspond to 0.0 *hours* (IST) on 10 March 2003.





stituents, over tides and compound tides was also calculated to get the mean estimate of the accuracy of the model at each station. The amplitudes and phases of observed and simulated tidal constituents and the complex difference module are given in Tables 3.1 and 3.2. The five major diurnal and semidiurnal constituents in Tables 1 and 2, are plotted in Figure 3.14. Overtides and compound tides are shown in Figures 3.15 and 3.16 respectively. As discussed earlier,  $M_2$  is the dominant tidal constituent with amplitude of more than 50 *cm* both in the Mandovi and Zuari estuaries. The other dominant constituents are  $K_1$ ,  $S_2$ ,  $O_1$  and  $N_2$  (see Tables 3.1 and 3.2).

**Table 3.1** Amplitudes (Amp), Phases (Pha) and Complex difference module (Diff) of tidal constituents in the Mandovi estuary. The number in bracket shown for each station name is the distance (*km*) from the mouth of the estuary.

Constituents ( <i>cm</i> )		Verem[5]			Britona [9]			Akkada [20]			Volvoi [33]			Usgao[41]			Ganjem [50]		
		Obs	Model	Diff	Obs	Model	Diff	Obs	Model	Diff	Obs	Model	Diff	Obs	Model	Diff	Obs	Model	Diff
$O_1$	<b>Amp</b>	<b>14.9</b>	<b>17</b>	<b>2.6</b>	<b>14.7</b>	<b>17</b>	<b>2.4</b>	<b>14.5</b>	<b>16.4</b>	<b>1.9</b>	<b>14.3</b>	<b>14.7</b>	<b>1.7</b>	<b>15</b>	<b>13.5</b>	<b>1.9</b>	<b>2.3</b>	<b>12.5</b>	<b>13.36</b>
	<i>Pha</i>	51.2	57.1		54.7	57.8		60.8	62.7		62.7	69.6		67.1	71.9		327.9	75.1	
$K_1$	<b>Amp</b>	<b>35.5</b>	<b>32.5</b>	<b>4.5</b>	<b>33.7</b>	<b>32.6</b>	<b>2</b>	<b>34.1</b>	<b>32.2</b>	<b>2.11</b>	<b>33.5</b>	<b>31.3</b>	<b>5.4</b>	<b>36.6</b>	<b>30.5</b>	<b>7.09</b>	<b>6.1</b>	<b>28.6</b>	<b>22.64</b>
	<i>Pha</i>	61.5	69.2		67	69.9		75	76.6		77.5	86.3		83.2	89.4		82.1	93	
$N_2$	<b>Amp</b>	<b>12.3</b>	<b>12.4</b>	<b>1.8</b>	<b>12.4</b>	<b>12.5</b>	<b>4.3</b>	<b>12.8</b>	<b>12.3</b>	<b>5.3</b>	<b>14.3</b>	<b>12.1</b>	<b>3.7</b>	<b>15.8</b>	<b>12.1</b>	<b>5.3</b>	<b>2.8</b>	<b>11.6</b>	<b>8.8</b>
	<i>Pha</i>	299.5	291		312.3	292.4		329.1	304.8		336.3	323.2		345.1	329		333.9	335	
$M_2$	<b>Amp</b>	<b>53.2</b>	<b>54.2</b>	<b>1.7</b>	<b>52.4</b>	<b>54.4</b>	<b>10.88</b>	<b>55.3</b>	<b>54.2</b>	<b>14.33</b>	<b>61.1</b>	<b>55.1</b>	<b>7.9</b>	<b>63.6</b>	<b>55.6</b>	<b>10</b>	<b>12.1</b>	<b>53.9</b>	<b>42.71</b>
	<i>Pha</i>	318.2	316.7		329.6	318.1		345.5	330.5		353.3	348.2		0	354.2		20.92	1.1	
$S_2$	<b>Amp</b>	<b>18.2</b>	<b>20.8</b>	<b>3</b>	<b>17.4</b>	<b>20.9</b>	<b>4.19</b>	<b>17.9</b>	<b>20.4</b>	<b>5.5</b>	<b>19.6</b>	<b>20.1</b>	<b>1.4</b>	<b>20.6</b>	<b>20.3</b>	<b>2.6</b>	<b>5.7</b>	<b>19.7</b>	<b>4</b>
	<i>Pha</i>	358.1	2.8		11.1	4.2		32.5	17.5		41.3	37.4		51	43.5		48.9	49.9	
mean diff of major constituents				<b>2.7</b>			<b>4.7</b>			<b>5.8</b>			<b>4</b>			<b>5.4</b>			<b>18.3</b>
$M_4$	<b>Amp</b>	<b>0.6</b>	<b>1.3</b>	<b>0.7</b>	<b>1.5</b>	<b>1.3</b>	<b>0.9</b>	<b>1.2</b>	<b>0.5</b>	<b>1.5</b>	<b>1.7</b>	<b>2.8</b>	<b>2.5</b>	<b>2.3</b>	<b>4.3</b>	<b>2.1</b>	<b>6.4</b>	<b>6.1</b>	<b>10</b>
	<i>Pha</i>	25.1	18.1		72.2	24.5		284.8	359		199.2	261.6		237.2	267.2		35	287.4	
$M_6$	<b>Amp</b>	<b>0.4</b>	<b>0.8</b>	<b>0.6</b>	<b>0.6</b>	<b>0.8</b>	<b>0.4</b>	<b>0.9</b>	<b>0.9</b>	<b>1.0</b>	<b>1.9</b>	<b>1.1</b>	<b>1.4</b>	<b>2.2</b>	<b>1.1</b>	<b>1.4</b>	<b>2.6</b>	<b>1.2</b>	<b>1.8</b>
	<i>Pha</i>	301	251		292.5	255.5		5	291.1		44	352.2		67.5	33.7		44.5	84.2	
mean diff of overtides				<b>0.6</b>			<b>0.7</b>			<b>1.2</b>			<b>2</b>			<b>1.7</b>			<b>5.9</b>
$MSf$	<b>Amp</b>	<b>4.3</b>	<b>3.6</b>	<b>2.3</b>	<b>4.5</b>	<b>3.6</b>	<b>2.8</b>	<b>4.8</b>	<b>3.4</b>	<b>1.4</b>	<b>5</b>	<b>4.1</b>	<b>0.9</b>	<b>4.8</b>	<b>4.7</b>	<b>1.4</b>	<b>4.1</b>	<b>5.4</b>	<b>1.9</b>
	<i>Pha</i>	342.1	309.1		349	309.2		329.8	326		5.1	0.4		354.3	11.9		40	22.6	
$MK_3$	<b>Amp</b>	<b>0.7</b>	<b>1.4</b>	<b>1.7</b>	<b>0.3</b>	<b>1.4</b>	<b>1.3</b>	<b>1</b>	<b>2</b>	<b>1.3</b>	<b>2.2</b>	<b>3.5</b>	<b>2.15</b>	<b>2.3</b>	<b>4.3</b>	<b>2</b>	<b>3</b>	<b>4.9</b>	<b>4.7</b>
	<i>Pha</i>	245.5	350.6		279.9	351.3		326.9	1.8		329.1	5.1		12.7	9.4		86.8	17.9	
$MN_4$	<b>Amp</b>	<b>0.5</b>	<b>0.5</b>	<b>0.06</b>	<b>0.7</b>	<b>0.5</b>	<b>0.5</b>	<b>0.1</b>	<b>0.2</b>	<b>0.2</b>	<b>0.8</b>	<b>1.2</b>	<b>1.0</b>	<b>1.7</b>	<b>2.0</b>	<b>1</b>	<b>2.5</b>	<b>2.8</b>	<b>3.8</b>
	<i>Pha</i>	25.1	18.1		72.2	24.5		284.8	359		199.2	261.6		237.2	267.2		12.55	279.8	
$MS_4$	<b>Amp</b>	<b>0.5</b>	<b>1.7</b>	<b>2.1</b>	<b>0.8</b>	<b>1.7</b>	<b>2.2</b>	<b>0.6</b>	<b>2.1</b>	<b>2.4</b>	<b>1.8</b>	<b>3.8</b>	<b>3.3</b>	<b>2.5</b>	<b>5.1</b>	<b>2.6</b>	<b>5.8</b>	<b>6.5</b>	<b>6.3</b>
	<i>Pha</i>	166	10.2		132.6	12.1		253.4	12.6		292.9	354.4		344.1	355.1		63.31	1.4	
mean diff of compound tides				<b>1.5</b>			<b>1.7</b>			<b>1.3</b>			<b>1.8</b>			<b>1.7</b>			<b>4.2</b>

**Table 3.2** Amplitudes (Amp), Phases (Pha) and Complex difference module (Diff) of tidal constituents in the Zuari estuary. The number in bracket shown for each station name is the distance (*km*) from the mouth of the estuary.

Constituents ( <i>cm</i> )		Dona Paula [0]			Cortalim [12]			Borim [21]			Sanvordem [45]			Sanguem [55]		
		Obs	Model	Diff	Obs	Model	Diff	Obs	Model	Diff	Obs	Model	Diff	Obs	Model	Diff
$O_1$	<b>Amp</b>	<b>16.9</b>	<b>17</b>	<b>0.44</b>	<b>14.7</b>	<b>17.1</b>	<b>2.78</b>	<b>13.9</b>	<b>16.7</b>	<b>3.72</b>	<b>16.2</b>	<b>15.4</b>	<b>1.43</b>	<b>7.6</b>	<b>9.7</b>	<b>14.86</b>
	<i>Pha</i>	55.6	57.04		62.6	57.5		52.1	61.3		62.9	67.2		190.6	72.7	
$K_1$	<b>Amp</b>	<b>32.4</b>	<b>32.4</b>	<b>0.7</b>	<b>35.5</b>	<b>32.7</b>	<b>4.9</b>	<b>38.8</b>	<b>32.8</b>	<b>6.7</b>	<b>37.4</b>	<b>32.2</b>	<b>5.9</b>	<b>17.9</b>	<b>22.9</b>	<b>37</b>
	<i>Pha</i>	67.7	69.1		63.1	70		70	74.9		78.3	82.9		220.9	90.6	
$N_2$	<b>Amp</b>	<b>12.4</b>	<b>12.4</b>	<b>0.6</b>	<b>12.3</b>	<b>12.8</b>	<b>0.5</b>	<b>15.8</b>	<b>13.1</b>	<b>4.7</b>	<b>13.9</b>	<b>14</b>	<b>5.1</b>	<b>12.1</b>	<b>9.9</b>	<b>4.2</b>
	<i>Pha</i>	288.1	290.9		292.3	292.5		318	302.2		339.3	317.9		308.5	327.6	
$M_2$	<b>Amp</b>	<b>54</b>	<b>53.9</b>	<b>2.1</b>	<b>59.9</b>	<b>55.9</b>	<b>4.3</b>	<b>63.8</b>	<b>57.7</b>	<b>10</b>	<b>69.7</b>	<b>62.6</b>	<b>11.36</b>	<b>42.6</b>	<b>44.5</b>	<b>29.9</b>
	<i>Pha</i>	313.7	316		319.6	318		335	327.4		350.1	342.4		317.2	357.3	
$S_2$	<b>Amp</b>	<b>20.7</b>	<b>20.7</b>	<b>1</b>	<b>19.8</b>	<b>21.5</b>	<b>1.7</b>	<b>21.6</b>	<b>21.9</b>	<b>2.7</b>	<b>22.9</b>	<b>23.5</b>	<b>7.1</b>	<b>13.6</b>	<b>17.1</b>	<b>14.9</b>
	<i>Pha</i>	359.7	2.6		3.1	4.4		22	14.7		48.8	31.2		345.9	42.8	
Mean diff of major constituents				<b>1</b>			<b>2.8</b>			<b>5.6</b>			<b>6.2</b>			<b>20.2</b>
$M_4$	<b>Amp</b>	<b>1.2</b>	<b>1.2</b>	<b>0.1</b>	<b>2.7</b>	<b>1.4</b>	<b>2.2</b>	<b>3.6</b>	<b>1.0</b>	<b>2.6</b>	<b>4.9</b>	<b>5.2</b>	<b>5.3</b>	<b>6.3</b>	<b>5.1</b>	<b>2.0</b>
	<i>Pha</i>	40.8	46		117.1	62.5		140.6	131		157.3	221		251	267.9	
$M_6$	<b>Amp</b>	<b>0.7</b>	<b>0.7</b>	<b>0.1</b>	<b>0.4</b>	<b>1</b>	<b>0.6</b>	<b>0.8</b>	<b>1.1</b>	<b>0.7</b>	<b>1.8</b>	<b>1.7</b>	<b>0.1</b>	<b>1.7</b>	<b>1.3</b>	<b>1.2</b>
	<i>Pha</i>	242.4	250.6		284	256		327.9	283.6		44.3	42.5		63.3	108.9	
Mean diff of overtides				<b>0.1</b>			<b>1.4</b>			<b>1.6</b>			<b>2.7</b>			<b>1.6</b>
$MSf$	<b>Amp</b>	<b>3.6</b>	<b>3.6</b>	<b>0</b>	<b>2.3</b>	<b>3.6</b>	<b>2.5</b>	<b>5.1</b>	<b>3.5</b>	<b>3.2</b>	<b>4.2</b>	<b>4.1</b>	<b>1.5</b>	<b>10.3</b>	<b>5.1</b>	<b>5.4</b>
	<i>Pha</i>	308.9	308.9		354	310.1		2.4	323.7		15.7	354.3		16.3	28.9	
$MK_3$	<b>Amp</b>	<b>1.4</b>	<b>1.4</b>	<b>0.11</b>	<b>0.8</b>	<b>1.5</b>	<b>1.2</b>	<b>1.2</b>	<b>1.9</b>	<b>2.3</b>	<b>3.6</b>	<b>3.7</b>	<b>2.6</b>	<b>5.2</b>	<b>3.4</b>	<b>7.3</b>
	<i>Pha</i>	346.3	351		47.4	348		250.3	348.5		305.8	348.8		133.2	16.8	
$MN_4$	<b>Amp</b>	<b>0.5</b>	<b>0.5</b>	<b>0.05</b>	<b>1.2</b>	<b>0.5</b>	<b>0.9</b>	<b>1.4</b>	<b>0.3</b>	<b>1.1</b>	<b>2.4</b>	<b>1.9</b>	<b>2.5</b>	<b>3.9</b>	<b>2.3</b>	<b>1.6</b>
	<i>Pha</i>	11.3	16.4		77.7	34.7		135.7	107.7		144.7	215		258.3	266	
$MS_4$	<b>Amp</b>	<b>1.7</b>	<b>1.7</b>	<b>0.1</b>	<b>0.5</b>	<b>1.7</b>	<b>2</b>	<b>2.1</b>	<b>1.5</b>	<b>3.5</b>	<b>4.5</b>	<b>4.4</b>	<b>5.8</b>	<b>4.2</b>	<b>5.4</b>	<b>5.1</b>
	<i>Pha</i>	3.9	9.6		136.8	12.3		198	0		244.3	326.8		283.8	347.7	
Mean diff of compound tides				<b>0.08</b>			<b>1.6</b>			<b>2.5</b>			<b>3.1</b>			<b>4.9</b>

**Table 3.3** Amplitudes (Amp), Phases (Pha) and Complex difference module (Diff) of tidal constituents in the Cumbarjua canal. The number in bracket shown for each station name is the distance (*km*) from the mouth of the estuary.

Constituents ( <i>cm</i> )		Madkai [15]			Banastarim [24.5]		
		Obs	Model	Diff	Obs	Model	Diff
$O_1$	<b>Amp</b>	<b>14.3</b>	<b>15.9</b>	<b>3.7</b>	<b>14.1</b>	<b>16.7</b>	<b>5.4</b>
	<i>Pha</i>	56.4	69.4		42.6	60.5	
$K_1$	<b>Amp</b>	<b>34.5</b>	<b>32.7</b>	<b>7.7</b>	<b>34.8</b>	<b>32.6</b>	<b>2.2</b>
	<i>Pha</i>	72	84.8		73.5	73.7	
$N_2$	<b>Amp</b>	<b>13.3</b>	<b>11.8</b>	<b>1.7</b>	<b>14.4</b>	<b>12.8</b>	<b>1.6</b>
	<i>Pha</i>	322.4	318		298.5	299.7	
$M_2$	<b>Amp</b>	<b>55.7</b>	<b>54.8</b>	<b>2.3</b>	<b>57.6</b>	<b>56.3</b>	<b>1.3</b>
	<i>Pha</i>	340.4	342.7		325.4	325.1	
$S_2$	<b>Amp</b>	<b>18.4</b>	<b>19.9</b>	<b>2.2</b>	<b>19.6</b>	<b>21.4</b>	<b>2.1</b>
	<i>Pha</i>	26.4	31.2		15.4	12	
mean diff of major constituents				<b>3.57</b>			<b>2.5</b>
$M_4$	<b>Amp</b>	<b>2</b>	<b>3</b>	<b>4.7</b>	<b>0.5</b>	<b>1</b>	<b>0.7</b>
	<i>Pha</i>	116.9	257.9		149.6	101.2	
$M_6$	<b>Amp</b>	<b>1.5</b>	<b>0.8</b>	<b>0.7</b>	<b>0.3</b>	<b>1.1</b>	<b>0.8</b>
	<i>Pha</i>	318.2	308.7		270.6	274.2	
Mean diff of overtides				<b>2.7</b>			<b>0.7</b>
$MSf$	<b>Amp</b>	<b>5</b>	<b>3.6</b>	<b>2.8</b>	<b>6.5</b>	<b>3.5</b>	<b>3.5</b>
	<i>Pha</i>	3.2	328.9		343	321.3	
$MK_3$	<b>Amp</b>	<b>0.9</b>	<b>3.7</b>	<b>3.2</b>	<b>1.8</b>	<b>1.7</b>	<b>3</b>
	<i>Pha</i>	295.8	351		228.3	349.7	
$MN_4$	<b>Amp</b>	<b>0.8</b>	<b>1.2</b>	<b>1.9</b>	<b>0.2</b>	<b>0.3</b>	<b>0.1</b>
	<i>Pha</i>	99.3	259.2		47.6	73.5	
$MS_4$	<b>Amp</b>	<b>1</b>	<b>3.8</b>	<b>4.4</b>	<b>0.5</b>	<b>1.4</b>	<b>1.9</b>
	<i>Pha</i>	210.1	336		193.9	8.6	
Mean diff of compound tides				<b>3.1</b>			<b>2.1</b>

### 3.3.4 Major diurnal and semidiurnal constituents

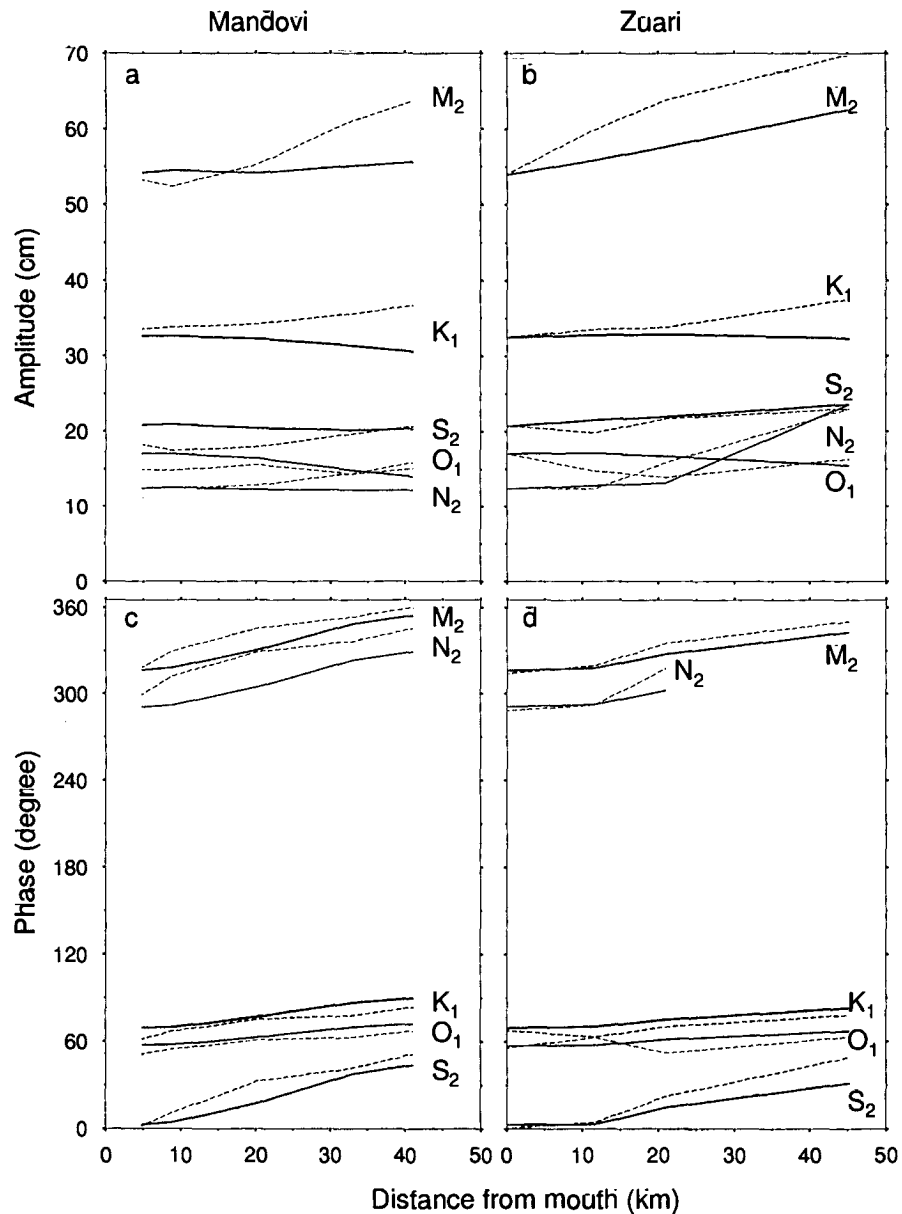
Figure 3.14 shows the observed and simulated amplitudes and phases of five major tidal constituents. The observed amplitude of  $M_2$  in the Mandovi is 53 *cm* at Verem and the amplitude increases to about 63 *cm* at Usgao. Thus, the increase of  $M_2$  tide when it reaches the upstream regions is about 10 *cm*. In the Zuari, the amplitude of  $M_2$  is about 54 *cm* at Dona Paula, and the amplitude increases to about 69 *cm* at Sanvordem. Amplitudes of  $K_1$ ,  $S_2$ ,  $O_1$  and  $N_2$  also increase toward the upstream regions. Now if we look at the simulations of these constituents, at Verem, Britona and Akkada, the simulation

of the amplitude of  $M_2$  is reasonably good, but at Volvoi and Usgao, the model underestimates  $M_2$ . In the Zuari, the model reproduces  $M_2$  reasonably well from Dona Paula to Sanvordem (see Figure 3.14b). The simulation of the amplitudes of  $O_1$ ,  $N_2$  and  $S_2$  are also reasonably good in both the Mandovi and Zuari. The model underestimates the amplitude of  $K_1$  at upstream regions, but the model has reproduced the phase increase of diurnal and semidiurnal constituents toward the upstream regions reasonably well both in the Mandovi and Zuari. The mean difference of major constituents at different stations except Ganjem and Sanguem in the Mandovi and Zuari are within the limits of model accuracy (see Tables 3.1 and 3.2). The differences found at Ganjem and Sanguem are very high, and the reasons are explained in the Discussion section.

### 3.3.5 Overtides and compound tides

Overtides are plotted in Figure 3.15, which show the longitudinal variation of amplitude and phase of  $M_4$  and  $M_6$  toward the upstream regions. The simulations of overtides are reasonably good in the Mandovi and Zuari. Both observation and simulation show the rapid increase of  $M_4$  inside the Zuari. The amplitude and phase of  $M_6$ , which is the second harmonic of  $M_2$ , also increases inside these estuaries. The amplitude of  $M_6$  is better simulated than  $M_4$  in both these estuaries. Figure 3.16 shows that  $MSf$  (lunisolar synodic fortnightly constituent) is a significant compound tidal constituent in the Mandovi and Zuari with its amplitude of about 3 cm (see Tables 1 and 3) at the downstream regions and increases about 5 cm at the upstream regions. Two other important compound tides are  $MK_3$  (ter-diurnal tide, derived from the interactions of  $M_2$  and  $K_1$ ) and  $MN_4$  (quarter-diurnal tide which is the result of  $M_2$  and  $N_2$  interactions). The amplitude and phase of  $MK_3$  steadily increase inside these estuaries. The simulations of the amplitude and phase of  $MN_4$  is well matched with that observed in the Mandovi and there is a reasonably good match in the Zuari. The simulation of the amplitude of  $MS_4$  (quarter-diurnal compound tide which is the result of  $M_2$  and  $S_2$  interactions) also has a reasonable match in the

**Figure 3.14** Variation in amplitude (*cm*) and phase (*degree*) of observed (dotted line) and simulated (solid line) five major tidal diurnal and semidiurnal constituents in the Mandovi and Zuari estuaries.



Zuari, but the model overestimates the amplitude in the Mandovi. The mean difference of overtides and compound tides increases marginally from mouth to upstream stations.

### 3.3.6 $M_4/M_2$ amplitude ratio and relative surface phase ( $2M_2 - M_4$ )

$M_4/M_2$  amplitude ratio and relative surface phase ( $2M_2 - M_4$ ) help to determine the nonlinear distortion of tides inside the estuaries. Relative phasing of  $M_4$  to  $M_2$  determines whether an estuary is flood dominant or ebb dominant [Aubrey and Speer, 1985; Speer and Aubrey, 1985; Friedrichs and Aubrey, 1988].  $M_4/M_2$  is almost steady in the Mandovi estuary (see Table 3.4) and it steadily increases in the Zuari from the mouth to upstream regions. The model overestimates  $M_4/M_2$  at the upstream regions in the Mandovi, and the simulation of  $M_4/M_2$  overall is good in the Zuari (see Table 3.5). The relative surface phase decreases toward the upstream regions in both the Mandovi and Zuari estuaries.

**Table 3.4**  $M_4/M_2$  amplitude ratio and relative surface phase ( $2M_2 - M_4$ ) in the Mandovi estuary

	Verem[5]		Britona [9]		Akkada [20]		Volvoi [33]		Usgao[41]		Ganjem [50]	
	Obs	Model	Obs	Model	Obs	Model	Obs	Model	Obs	Model	Obs	Model
$M_4/M_2$	<b>0.01</b>	<b>0.02</b>	<b>0.03</b>	<b>0.02</b>	<b>0.02</b>	<b>0.009</b>	<b>0.02</b>	<b>0.04</b>	<b>0.03</b>	<b>0.07</b>	<b>0.52</b>	<b>0.11</b>
$2M_2 - M_4$ (degree)	222.3	226	207.7	222.5	172.7	259.6	145.6	68.2	100.1	73.6	6.8	74.8

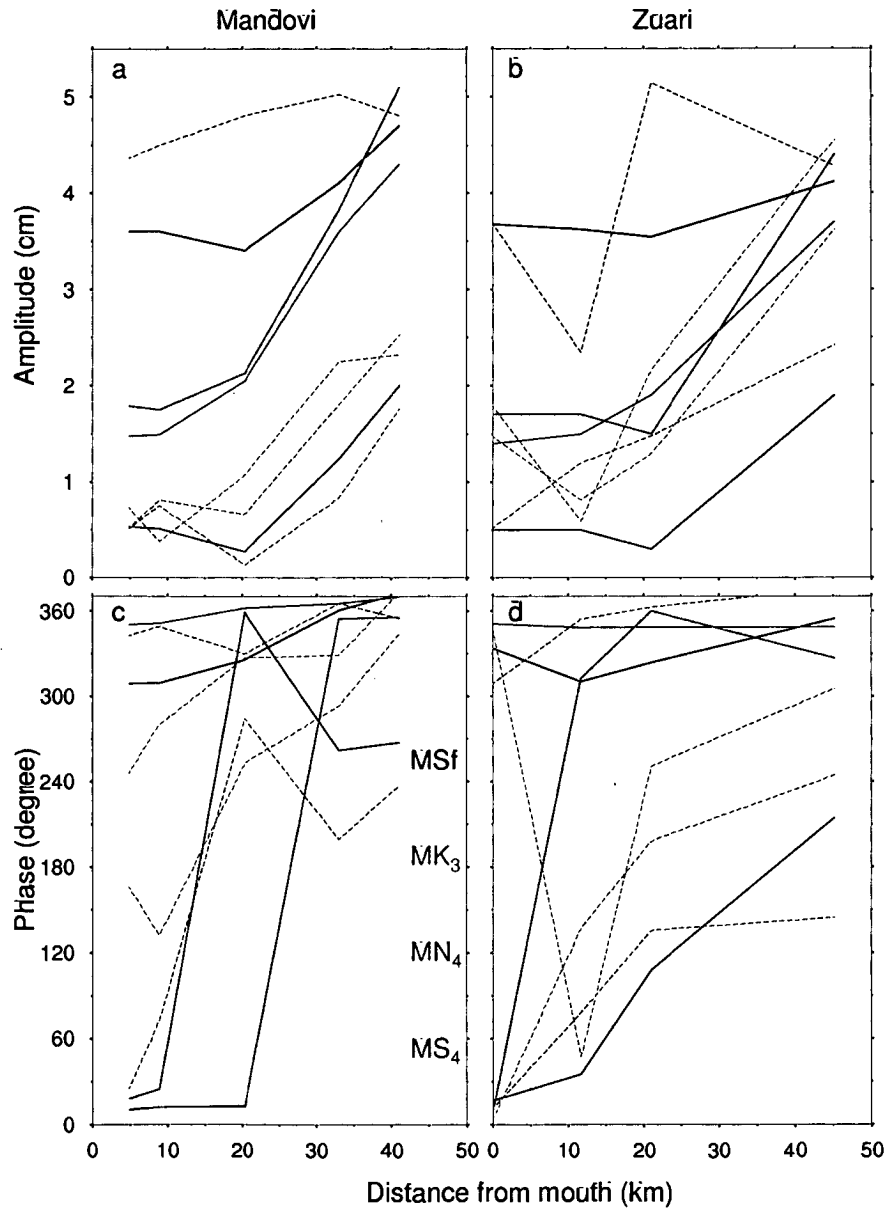
**Table 3.5**  $M_4/M_2$  amplitude ratio and relative surface phase ( $2M_2 - M_4$ ) in the Zuari estuary

	Dona Paula [0]		Cortalim [12]		Borim [21]		Sanvordem [45]		Sanguem [55]	
	Obs	Model	Obs	Model	Obs	Model	Obs	Model	Obs	Model
$M_4/M_2$	<b>0.02</b>	<b>0.02</b>	<b>0.04</b>	<b>0.02</b>	<b>0.05</b>	<b>0.01</b>	<b>0.07</b>	<b>0.08</b>	<b>0.14</b>	<b>0.11</b>
$2M_2 - M_4$ (degree)	222.6	226	162.1	213.5	169.4	163.4	182.9	103.7	23.4	86.7





**Figure 3.16** Variation in amplitude (*cm*) and phase (*degree*) of observed (dotted line) and simulated (solid line) compound tides in the Mandovi and Zuari estuaries.



## 3.4 Discussion

The present study describes tidal circulation in the Mandovi and Zuari estuaries. The study also focuses on the freshwater influence on tides and tidal asymmetries. The model sensitivity to horizontal diffusion of momentum was checked and the coefficient value was allowed to vary between 100 and  $700 \text{ m}^2 \text{ s}^{-1}$ . The increase in amplitude and phase of tidal constituents toward the upstream regions was better simulated for the value of  $500 \text{ m}^2 \text{ s}^{-1}$ . The changes in friction from 0.001 to 0.003 did not show any significant impact on amplitude and phase, however the value, 0.002 showed better agreement between the observed and simulated tides.

### 3.4.1 Longitudinal variation in tidal amplitudes

Tidal amplitudes in the Mandovi and Zuari estuaries slightly increase toward the upstream regions (Figures 3.1 – 3.4). This is due to the rapid decrease in channel's width toward the upstream regions. Ganjem is located at the upstream end of the Mandovi estuary (Figure 3.1c) where the tidal range is about  $0.5 \text{ m}$  during dry season. This indicates that even a small volume of river discharge through a narrow channel is sufficient to prevent tide entering the upstream regions. The channel's elevation from the sea level is also a factor preventing the tidal propagation further toward upstream regions, but at Sanguem (Figure 3.2 c), the tidal amplitude is not decayed much. This is due to two factors (i) the volume of the river runoff in the Zuari is smaller than compared to Mandovi during dry season, and (ii) the width of the channel is larger than that of the Mandovi. During wet season, the tidal oscillations are minimum at these two stations because of heavy fresh water influx ( $300\text{--}500 \text{ m}^3 \text{ s}^{-1}$ ). This was confirmed by the model results when fresh water influx of  $400 \text{ m}^3 \text{ s}^{-1}$  was introduced at upstream boundaries in the Mandovi and Zuari. Tidal amplitude in the Cumbarjua canal (Figures 3.2 b and 3.3 b) is almost similar to that of Zuari. This could be due to the fact that the cross sectional area of the Cumbarjua

canal at the junction with the Zuari is larger than that of the Mandovi. So tide propagates into the Cumbarjua canal freely from the Zuari.

### 3.4.2 Tidal currents and mixing of water column

One of the main purposes of using a 2D and 1D coupled model was to simulate tidal currents in the down stream regions in the Mandovi and Zuari estuaries. Fairly strong tidal currents and the absence of river discharge mixes the water column vertically during the dry season in these estuaries. During wet season, the velocity associated with river discharge prevents upstream propagation of tides [Unnikrishnan et al., 1997]. The tidal influence is very low at the upstream regions during wet season and the saline water gets pushed toward the mouth of these estuaries.

### 3.4.3 Nonlinearity in tidal propagation in the Mandovi and Zuari estuaries

Tidal observations in March–April 2003 show that the tidal amplitude remains almost same with slight increase in the upstream direction in the Mandovi and Zuari estuaries over a long stretch. The previous studies in the Mandovi and Zuari estuaries show that tidal amplitude remains unchanged over a distance of 40 *km* from the mouth and then decays rapidly over the next 10 *km* [Shetye et al., 1995; Unnikrishnan et al., 1997]. The Mandovi and Zuari estuaries are strongly converging channels and this leads to the amplification of tides in the upstream direction. The momentum balance in this type of estuary is primarily between pressure gradient and friction [Friedrichs and Aubrey, 1994], the decay in amplitude due to friction gets cancelled by geometric amplification, which leaves the amplitude, unchanged over 40 *km* in the Mandovi and Zuari estuaries from the mouth. Tidal amplitude gets decayed in the remaining 10 *km* in these estuaries. Unnikrishnan et al. [1997] showed that the decay in amplitude at the upstream regions was because of

the influence of river discharge. The influence of river discharge is visible even in April at Ganjem.

#### **3.4.4 Increase in amplitudes and phases of major constituents**

Harmonic analysis of tides shows that the predominant species of tidal constituents increase inside these estuaries (see Figure 3.14). As we have seen, the Mandovi and Zuari estuaries are not frictionally dominated estuaries; the frictional nature of the estuary is demonstrated by the significant decay of all semidiurnal and diurnal constituents, with associated large phases [Aubrey and Speer, 1985]. The previous studies [Unnikrishnan et al., 1999a; Shetye, 1999; Unnikrishnan and Luick, 2003] show that major diurnal and semidiurnal constituents increase inside the Gulf of Khambhat and Gulf of Kutch because of quarter wave length resonance and geometric effects. Shetye [1999] showed that the large amplification in semidiurnal constituents in the Gulf of Kutch is due to the proximity of their periods to the period at which the gulf resonates. Though we have not estimated the role of co-oscillation of incident and reflected waves in amplitude and phase in the Mandovi and Zuari estuaries, it can be seen from Figures 3.15 and 3.16 that the amplitude and phase variations of the tidal constituents toward the upstream regions are not linear, which is a strong indication of the presence of a reflected wave in these estuaries. Hence the amplification of semidiurnal constituents in the Mandovi and Zuari can be mainly attributed to the balance between pressure gradient and friction as mentioned previously. The superimposition of incident and reflected wave could be the other cause for the increase in semidiurnal constituents in the upstream directions.

### 3.4.5 Increase in amplitude and phase of overtides and compound tides

Nonlinear response to the tidal forcing is reflected in the increase of high frequency  $M_2$  over tide, compound tides and a forced low frequency  $MSf$  constituent throughout the estuary [Aubrey and Speer, 1985]. The increase of  $M_4$  toward the upstream regions in an estuary indicates flood dominance.  $M_4$  increases both in the Mandovi and Zuari estuaries. Similarly, amplitude and phase of  $M_6$  increase inside the estuaries. Increase of  $M_6$  inside the estuaries can be attributed to the quadratic friction [Blanton et al., 2002]. The nonlinear increase of compound tides toward the upstream regions can be seen in Figure 3.16. Both observation and simulation show a consistent increase of amplitude of  $MSf$  in the Mandovi though the model slightly underestimates amplitude in the downstream regions, but the observed amplitude increase of  $MSf$  inside the Zuari is not consistent. The amplitude of  $MN_4$  in the Mandovi and  $MS_4$  in the Zuari decreases in the middle regions of these estuaries and then steadily increase to the upstream directions. This rapid increase in amplitude and phase of the first and second harmonics of  $M_2$  and the nonlinear increase of compound tides show the nonlinear nature of the Mandovi and Zuari estuarine systems to the tidal forcing.

The complex difference module calculated at different stations in the Mandovi and Zuari shows that the mean differences over major diurnal and semidiurnal constituents, overtides, and compound tides gradually increase from the downstream region to the upstream regions. The difference in  $M_2$  is also high toward the upstream stations. For the present study, a 2D square grid was used, which is not well adapted to the irregular configuration of coastlines. The meandering effects of channels influence the amplitude and phase of tide entering into the estuary. The higher difference found in some stations between observed and simulated could be due to these reasons. Now, if we look at the difference calculated at Ganjem and Sanguem, the differences are very high between observed and simulated tidal constituents. Apart from the above cited reasons, there are

other factors such as river discharge, and higher channel elevation with respect to mean sea level, which also prevent tide from entering these upstream stations. River discharge into the Mandovi is more than that of the Zuari. Thus, the tidal characteristics get distorted more at Ganjem than at Sanguem. Tide is visible at Ganjem only during spring tide. Hence the harmonic analysis of tidal signal measured at Ganjem did not resolve the amplitude and phase of tidal constituents accurately.

The increase of  $M_4/M_2$  amplitude ratio toward the upstream regions is marginal, except Ganjem in the Mandovi estuary, (see Table 3.4) the  $M_4/M_2$  is 0.01 at Verem and 0.03 at Usgao. This increase of  $M_4/M_2$  from the mouth to upstream regions shows that tides do not get distorted much toward the upstream regions in the Mandovi whereas at Ganjem, tide gets completely distorted as it is evident from the very high amplitude ratio, which is about 0.5. In the Zuari, tidal amplitude gets distorted toward the upstream regions with the continuous increase of  $M_4/M_2$  from 0.02 to 0.1 (see Table 3.5). The observations of relative surface phase decrease from  $222^\circ$  at Verem to  $6.8^\circ$  at Ganjem in the Mandovi. In the Zuari, the observation of relative surface phase decrease from Dona Paula to Cortalim, but from Cortalim to Sanvordem, the relative surface phase increases and again it decreases at Sanguem (see Tables 3.4 and 3.5). But the model shows a decrease in relative surface phase toward the upstream directions both in the Mandovi and Zuari with exceptions at Akkada and Usgao. Now if we look at the relative phase relationship between  $M_4$  and  $M_2$ , a flood-dominant system has a sea surface phase of  $0^\circ$  to  $180^\circ$  with maximum flood at  $90^\circ$  and ebb-dominant system has sea surface phase of  $180^\circ$  to  $360^\circ$  with maximum ebb at  $270^\circ$  [Friedrichs and Aubrey, 1988]. If we assume a linear relationship in the relative phase mentioned previously, a relative surface phase of about  $220^\circ$  at Verem and Dona Paula, and about  $6^\circ$  at Ganjem, and about  $23^\circ$  at Sanguem show that the relative surface phase decreases toward the upstream regions. The decrease of a relative surface phase toward upstream directions is an indication of flood-dominance. Analysis of sea level observations (see Figure 3.11 and 3.12) also show the flood-dominance in the

Mandovi and Zuari estuaries. Overall, the increase of  $M_4$  and decrease of relative surface phase in both the Mandovi and Zuari show that these estuaries are flood-dominated. But there are some mudflats at the upstream regions in the Zuari estuary, that can increase the duration of ebb, which indicates that the Zuari estuary is less flood-dominant than the Mandovi estuary.

### 3.5 Conclusion

The study shows that tides in the Mandovi and Zuari estuaries undergo longitudinal variation due to geometry of channels, channel elevation with respect to the mean sea level and also due to river discharge from the upstream regions. The hybrid network model used for the study reproduced tides and showed freshwater influence on tides. Harmonic analysis of the observed and simulated tides was carried out to study the nonlinear nature of tidal propagation in the Mandovi and Zuari estuaries. The observations and model results show the consistent increase of amplitude and phases of major diurnal and semidiurnal constituents inside these estuaries. The increase of amplitudes and phases of major tidal constituents inside the estuaries show that the Mandovi and Zuari estuaries are not frictionally dominated estuaries because the frictional effect is balanced by the geometric effect. The increase of overtides and compound tides inside the estuaries show the non-linearity of these estuaries to tidal forcing. The  $M_4/M_2$  amplitude ratio shows that tidal distortion in the upstream regions in the Mandovi is marginal, whereas in the Zuari, the  $M_4/M_2$  amplitude ratio steadily increases in the upstream direction. This higher amplitude ratio indicates strong tidal distortion in the Zuari.

# Chapter 4

## Salinity distribution in the Mandovi and Zuari estuaries

### 4.1 Introduction

This chapter describes salinity distribution in the Mandovi and Zuari estuaries. The longitudinal variations of salinity during dry and wet seasons, the intraseasonal variations of salinity during wet season, tidally averaged salinity and residual currents for varying river discharge and flushing time are discussed in this chapter.

As mentioned in the Chapter 1, salinity distribution in the Mandovi and Zuari estuaries shows large variations during a year. During wet season, heavy rainfall and subsequent river discharge into the catchment area stratifies of about 10–12 *km* from the mouth of these estuaries while the upstream regions of about 40 *km* become completely freshwater. During dry season, these estuaries are vertically well mixed throughout the length.



### 4.1.1 Numerical model

For the simulation of longitudinal distribution of salinity, 2D and 1D advection-diffusion equations of salinity were included in the tidal model. As mentioned earlier, unlike many other estuaries in the world, the Mandovi and Zuari estuaries are very unique in terms of salinity distribution associated with southwest monsoon. These estuaries are vertically well mixed most parts of the year. Only during June to September, the downstream regions of about 10 to 12 *km* from the mouth of these estuaries become partially mixed and the rest of these channels of about 40 *km* become fully freshwater. Hence, the density difference was taken as zero in the present model. The finite difference scheme for solving advection-diffusion equation of salinity and other details of model formulation for the simulation of salinity distribution are described in Chapter 2. The boundary conditions for the simulation of salinity during dry and wet seasons and the results are described in the following sections.

### 4.1.2 Initial and Boundary conditions

At the open boundary of the model, salinity was defined as a function of time, the model was initialized with constant salinity at different sections of the model domain based on the observations in 1993. The observations of salinity available for 3 days each in April and August 1993 were not sufficient to use as open boundary conditions, because the model could not reach the steady state during this time. Since the salinity remains about 35 *psu* throughout the tidal cycles during dry season at the mouth of these estuaries, salinity was defined as a constant value of 35.17 *psu* at the open boundary during dry season to force the model. Salinity varies from 7 to 22 *psu* in a tidal cycle at the mouth during wet season. So salinity was defined as a cosine function that can vary from 7 to 22 *psu* during a tidal cycle ( 12 *hours*). The cosine function used for prescribing the boundary condition in the model is given below.

$$S(t) = 15.0 + 7\cos\omega t \quad (4.1)$$

$$\omega = \frac{2\pi}{T} \quad (4.2)$$

Where  $T$  is the period

### 4.1.3 Diffusion coefficient

The diffusion coefficient for salinity is subjected to seasonal variations from the mouth to upstream regions in the Zuari estuary [Shetye and Murty, 1987]. The model was run for varying salinity diffusion coefficient values range from 10 to 250  $m^2s^{-1}$ . But we used 100 and 150  $m^2s^{-1}$  for the downstream and upstream regions respectively in the present model, because these values gave better match with that of observed.

## 4.2 Results

The model was run for two cases, simulating longitudinal distribution of salinity during dry and wet seasons in the Mandovi and Zuari estuaries and Cumbarjua canal. In the first case, the model was run for simulating salinity distribution during dry season and in the second case, the simulations were carried out for wet season. The model was run for two cases using different boundary conditions at the open boundary during dry and wet seasons.

### 4.2.1 Salinity distribution during dry season

During this season (April), the model was run for 10 days for the simulation of longitudinal distribution of salinity. The model reached steady state after 10 tidal cycles (5 days).

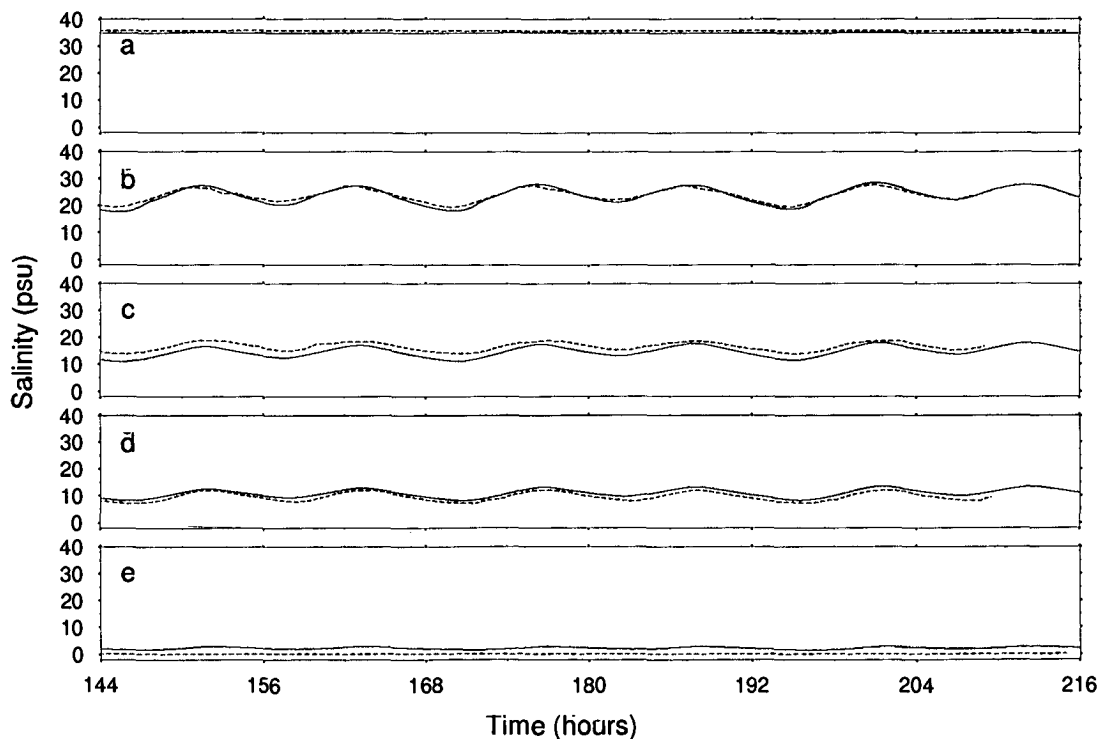
The 6<sup>th</sup> to 8<sup>th</sup> days simulations were used for the comparison. The computed salinity (Figures 4.1 and 4.3) matched well with those observed during dry season at different stations in the Mandovi and Zuari estuaries. Salinity values are more than 20, 10 and 8 *psu* at Sarmanas (20 *km*), Volvoi (33 *km*) and Sonamarg (45 *km*) respectively from mouth to the upstream regions in the Mandovi. But at Ganjem (50 *km*), an upstream end station in the Mandovi, salinity is nearly zero due to the small river discharge ( 10  $m^3 s^{-1}$ ). At this end, the channel cross-sectional area is small and even a weak river discharge can influence salinity considerably [Shetye et al., 1995].

Figure 4.3 shows the salinity in the Zuari estuary and Cumbarjua canal. The simulation of salinity at Cortalim, Banastarim and Sanvordem are also reasonably well matched with that of observations. At Sanguem, both observation and model show that salinity is zero. Figure 4.3b shows salinity distribution in Banastarim, which is a middle station in the Cumbarjua canal where salinity is about 30 *psu*; it indicates that saline water is well transported from the Zuari to Cumbarjua canal by tides during flood.

#### 4.2.2 Salinity distribution during wet season

For the simulations, during wet season (August), salinity was defined as a cosine function at the open boundary and the model was run for 12 days. At the upstream ends of these channels, river discharge of 400  $m^3 s^{-1}$  was introduced. The model reached steady state after 18 tidal cycles (9 days). The 10<sup>th</sup> to 12<sup>th</sup> days simulation of salinity were used for the comparison with the observation. Figures 4.2 and 4.4 show the observed and computed salinity at different stations in the estuarine network during wet season. These panels show that the observed and computed salinity is nearly zero in the upstream regions in the Mandovi and Zuari estuaries.

**Figure 4.1** The longitudinal distribution of salinity at different stations in the Mandovi estuary during dry (April 1993) season. The panels a, b, c, d and e represent Mormugao, Saramanas, Volvoi, Sonamarg and Ganjem respectively. The 144 *hours* on the x-axis correspond to 0.0 *hours* (IST) on 07/04/1993. Dotted and solid lines are observed and model respectively.



**Figure 4.2** The longitudinal distribution of salinity at different stations in the Mandovi estuary during wet (August 1993) season. The panels a, b, c, d and e represent Mormugao, Saramanas, Volvoi, Sonamarg and Ganjem respectively. The 216 *hours* on the x-axis correspond to 0.0 *hours* (IST) on 19/08/1993. Dotted and solid lines are observed and model respectively.

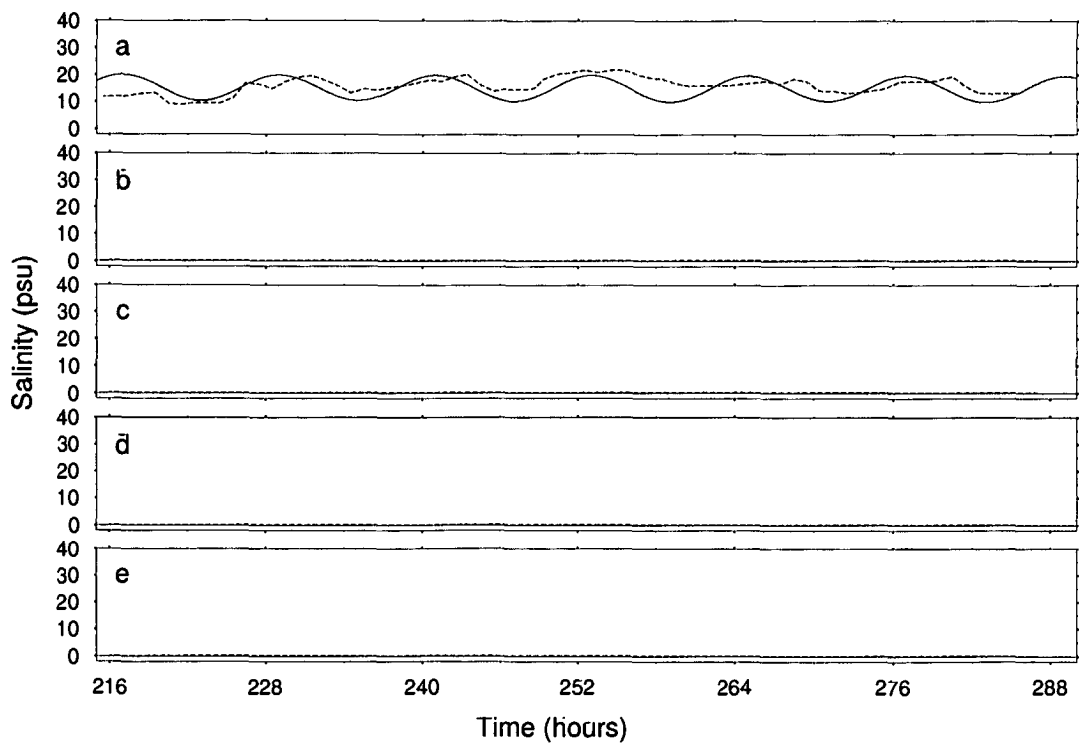


**Figure 4.3** The longitudinal distribution of salinity at different stations in the Zuari estuary and Cumbarjua canal during dry (April 1993) season. The panels a, b, c, d and e represent Mormugao, Cortalim, Banastarim, Sanvordem and Sanguem. The 144 *hours* on the x-axis correspond to 0.0 *hours* (IST) on 07/04/1993. Dotted and solid lines are observed and model respectively.

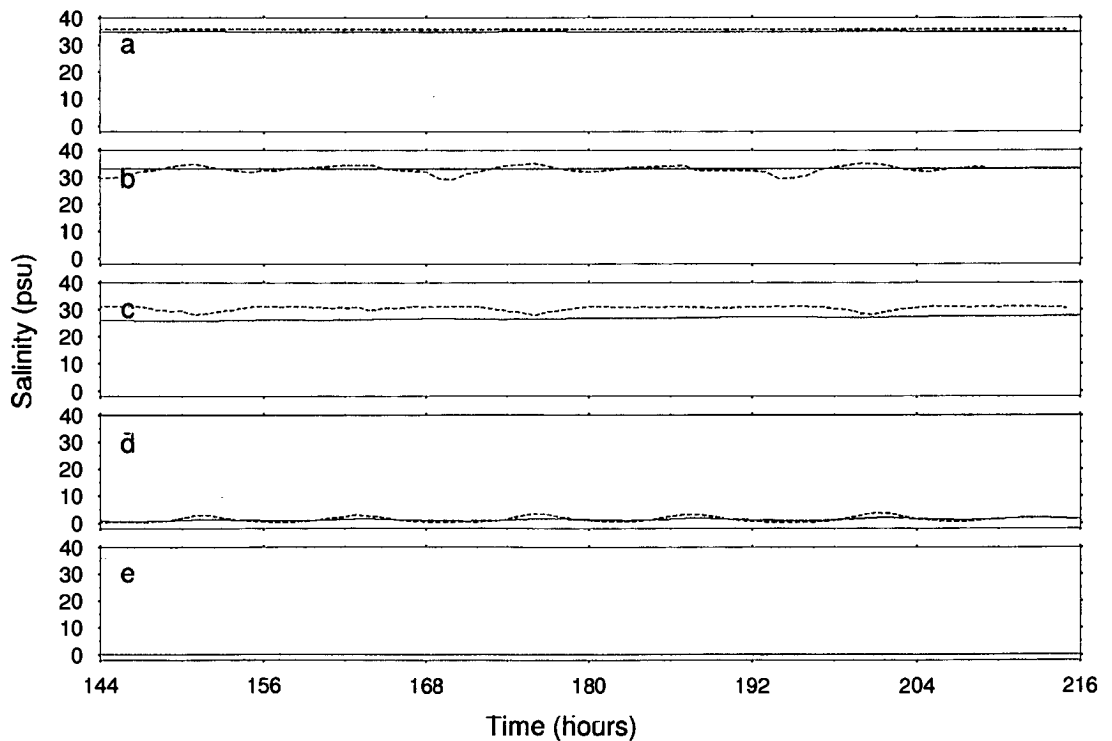
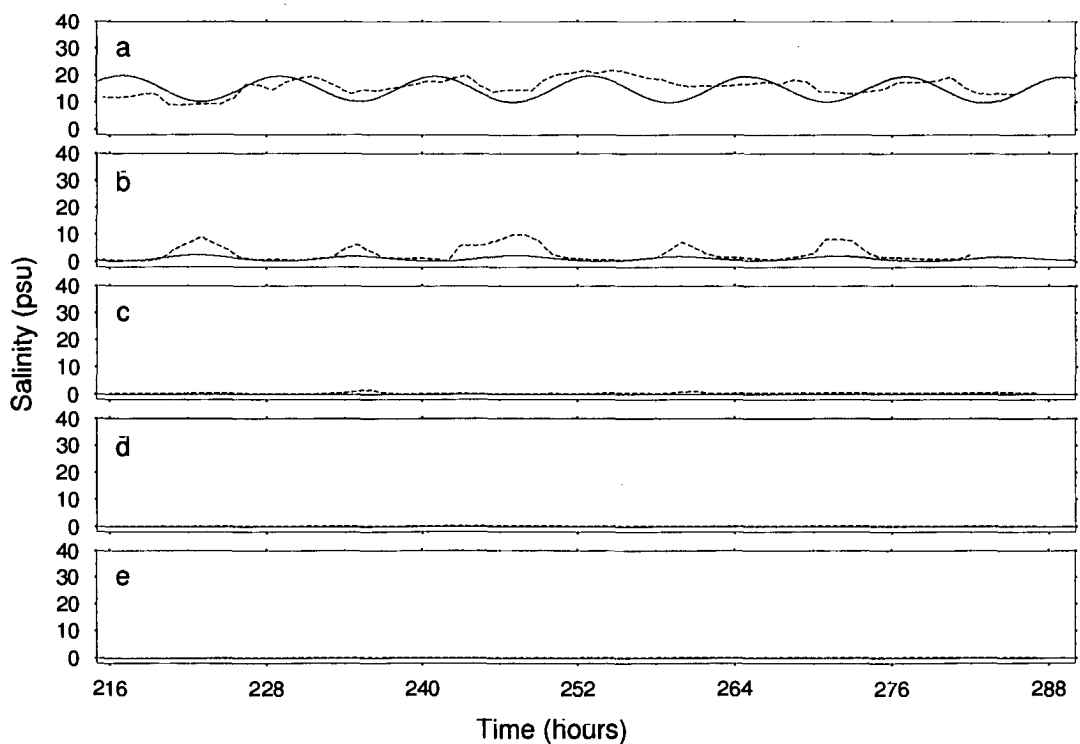


**Figure 4.4** The longitudinal distribution of salinity at different stations in the Zuari estuary and Cumbarjua canal during wet (August 1993) season. The panels a, b, c, d and e represent Mormugao, Cortalim, Banastarim, Sanvordem and Sanguem. The 216 hours on the x-axis correspond to 0.0 hours (IST) on 19/08/1993. Dotted and solid lines are observed and model respectively.



### 4.2.3 Simulation of longitudinal distribution of salinity for varying river discharges

A numerical experiment was carried out for simulating the longitudinal distribution of salinity for varying river discharges in the Mandovi estuary. For this purpose, the model was run for one month with same boundary conditions used for dry season and for each run, river discharges of 0, 10, 25 and  $50 \text{ m}^3\text{s}^{-1}$  were introduced at the upstream end of the model domain of the Mandovi.  $M_2$  tide is the major semidiurnal constituent, which constitutes 50% of the total tide in this region. Hence, the tidally averaged salinity was calculated over a  $M_2$  tidal period. The results of tidally averaged salinity have been shown in Figure 4.5 and the results show that salinity is subjected to large variations in the middle and upstream regions.

## 4.3 Residual currents

Residual currents of  $M_2$  tide in the Mandovi and Zuari estuaries were also calculated for varying river discharges using the numerical model. Residual currents are calculated using the following equation

$$U_r = \frac{1}{T} \int u dt \quad (4.3)$$

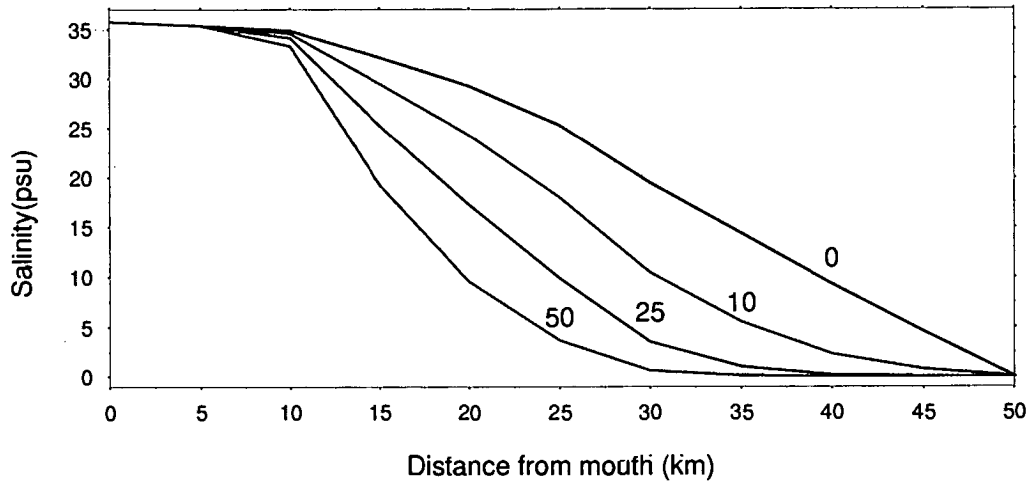
$$V_r = \frac{1}{T} \int v dt \quad (4.4)$$

Where  $U_r$  and  $V_r$  are residual currents,  $u$  and  $v$  are velocities and  $T$  is the period of  $M_2$ , which is 12.42 hours.

For the simulation of residual currents, the model was run over a  $M_2$  tidal period and



**Figure 4.5** Simulations of tidally averaged salinity over  $M_2$  tidal period for varying river discharges in the Mandovi estuary.

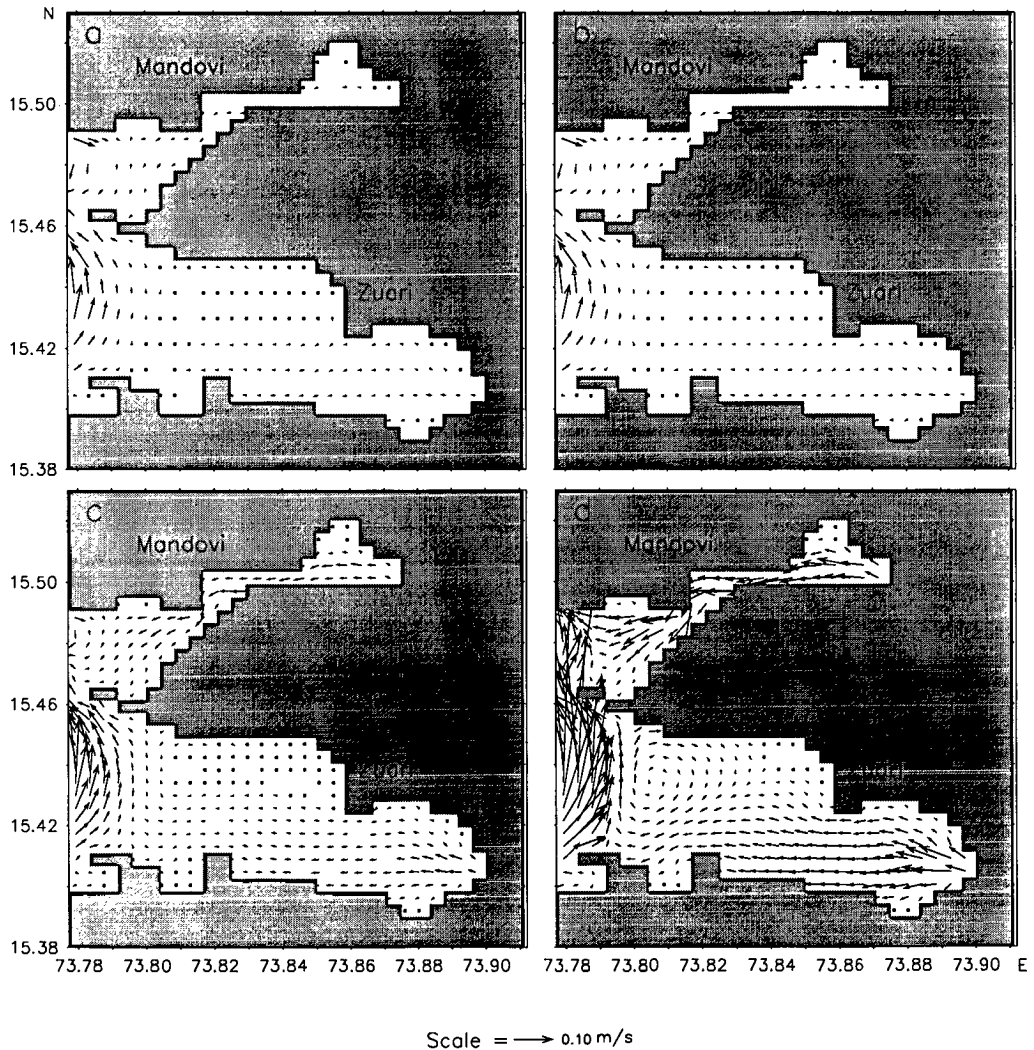


the model run was carried out for river discharges of 0, 10, 100 and 400  $m^3 s^{-1}$ . The results of residual currents for varying freshwater discharges are given in the Figure 4.6. Strong residual currents of about 15–20  $cm s^{-1}$  were found in the estuarine network when river discharge of 400  $m^3 s^{-1}$  was introduced in the model.

#### 4.4 Intraseasonal variations of salinity

As mentioned above, salinity in the Mandovi and Zuari estuaries undergoes large changes during dry and wet seasons. So far, no study was conducted to study the changes on salinity during wet season or whether the breaks during the wet season affect the salinity in the estuary. To study the changes in salinity in detail during wet season, we made salinity measurements along the longitudinal sections in the Mandovi estuary during the selected days of 2005–2007. The measurements of salinity along the longitudinal sections were carried out to understand the salinity variations along the estuary, whereas on 19 September 2006, time series observations (10 hours) were conducted at Old Goa, located

**Figure 4.6** Simulations of residual currents over  $M_2$  tidal period in the Mandovi and Zuari estuaries. The panels a, b, c and d represent the model runs for varying river discharges of 0, 10, 100, 400  $m^3s^{-1}$  respectively.

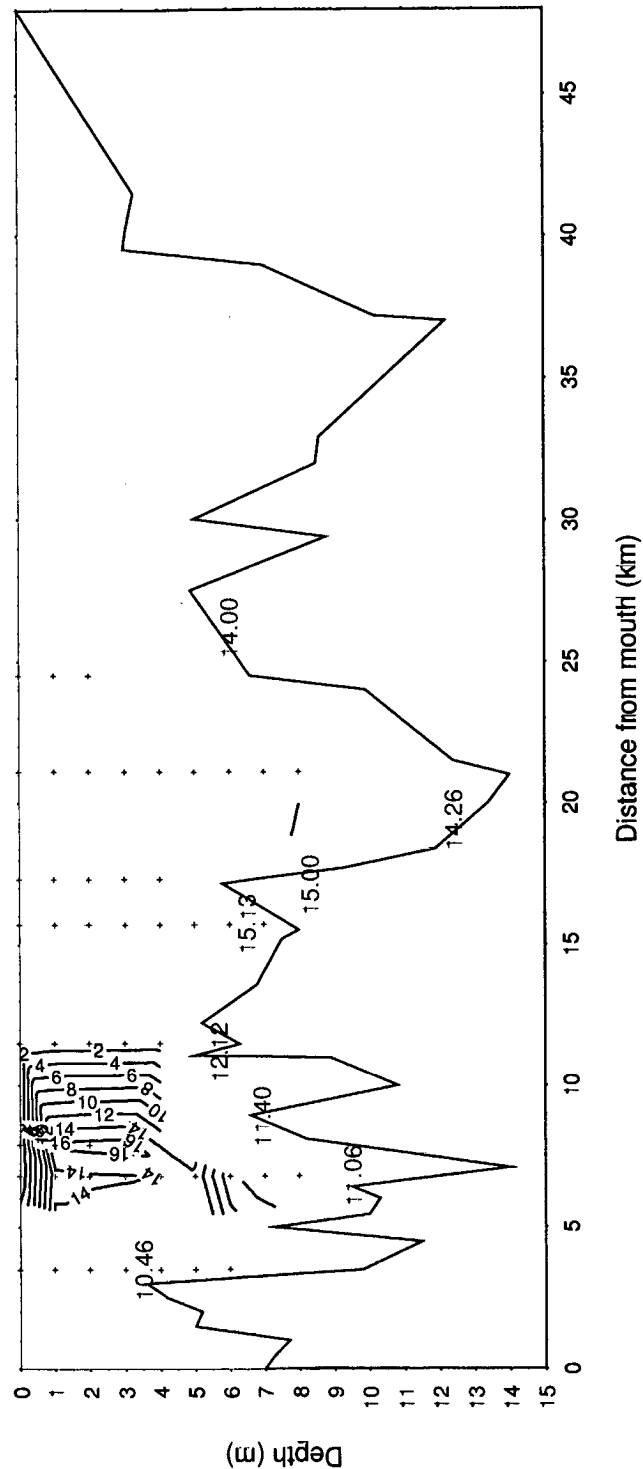


at distance of 15 *km* from the mouth of the Mandovi estuary to understand the salinity variations with time.

The vertical sections of salinity measured on 23 August 2005 is shown in Figure 4.7. The Figure 4.7 shows that salinity remains high (15 *psu*) at the surface in the downstream regions of about 8 *km* from the mouth, and from 12 *km* to further upstream regions, the channel is fully freshwater. Now if we look at the salinity measurements on 13 September 2005 (see Figure 4.8), saline water is further pushed toward the mouth. This was due to high rainfall in September compared to that of August 2005 (see Figure 4.15). During the time of heavy rainfall, salinity intrusion into upstream regions are minimised. This is evident from the continuous measurements of salinity (tidal cycles) made on 19 September 2006, which shows that salinity remains nearly zero from surface to bottom (see Figure 4.9) during two tidal cycles.

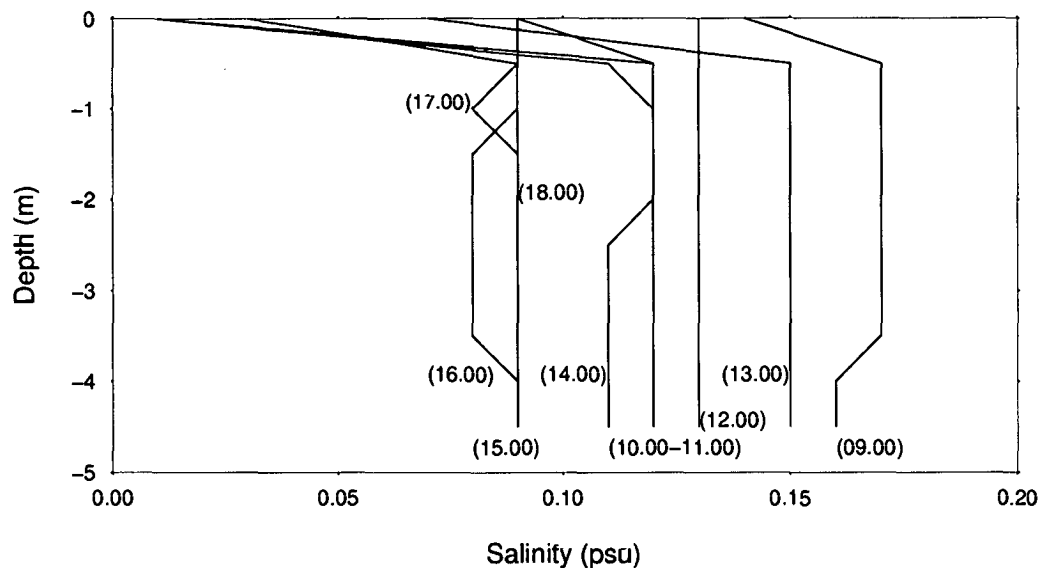
Salinity measurements during the dry season of 2007 show that these estuaries are vertically well mixed. Salinity measurements were carried out on 30 March, 25 May and 1 June 2007 in the Mandovi estuary. Figure 4.10 shows the vertical distribution of salinity along the estuary measured on 30 March 2007. From Figure 4.10, it can be noticed that the water column remains vertically well mixed from the mouth to upstream regions. But the measurements of salinity made on 25 May show that the water column is not fully well mixed (see Figure 4.11). This is not a sustained picture of salinity in May in this estuary, but because of a pre-monsoon shower occurred during the time of salinity measurements (see Figure 4.15e). The normal onset of southwest monsoon over Kerala (southern part of India) is on 1 June and it takes about 10 days to reach Goa. So the Mandovi and Zuari estuaries are well mixed till the 1<sup>st</sup> week of June and this is evident from Figure 4.12. Figure 4.12 also shows that saline water intrudes upto the upstream end of the estuary. Again salinity measurements made during wet season in 2007 show that salinity undergoes intraseasonal variations (Figures 4.13 and 4.14).

Figure 4.7 Vertical distribution of salinity measured on 23 August 2005 in the Mandovi estuary. The time (hours) at which the observations were made are indicated in cyan colour.





**Figure 4.9** Time series measurements of salinity made at Old Goa, located at a distance of 15 km from the mouth in the Mandovi estuary on 19 September 2006. The time (*hours*) at which the observations were made are indicated in the bracket.



## 4.5 Flushing time in the Mandovi and Zuari estuaries

Flushing time is defined as the time required to replace the existing freshwater in an estuary at a rate equal to the river discharge [Officer, 1976]. This method can be used to estimate the estuarine tolerance to the potential harmful substances. The low flushing time keeps an ecosystem free from the adverse effects of pollutants to a great extent. This method also helps to handle oil spills or toxic material in an estuary.

### 4.5.1 Freshwater fraction method

Though there are many methods to calculate flushing time, for the present study, the flushing time was calculated using freshwater fraction method. In this method, the freshwater volume is estimated from the measurements of salinity at different sections in an estuary.

If we assume a linear mixing process, the freshwater fraction  $f$  can be written as

**Figure 4.10** Vertical distribution of salinity measured on 30 March 2007 in the Mandovi estuary. The time (*hours*) at which the observations were made are indicated in cyan colour.

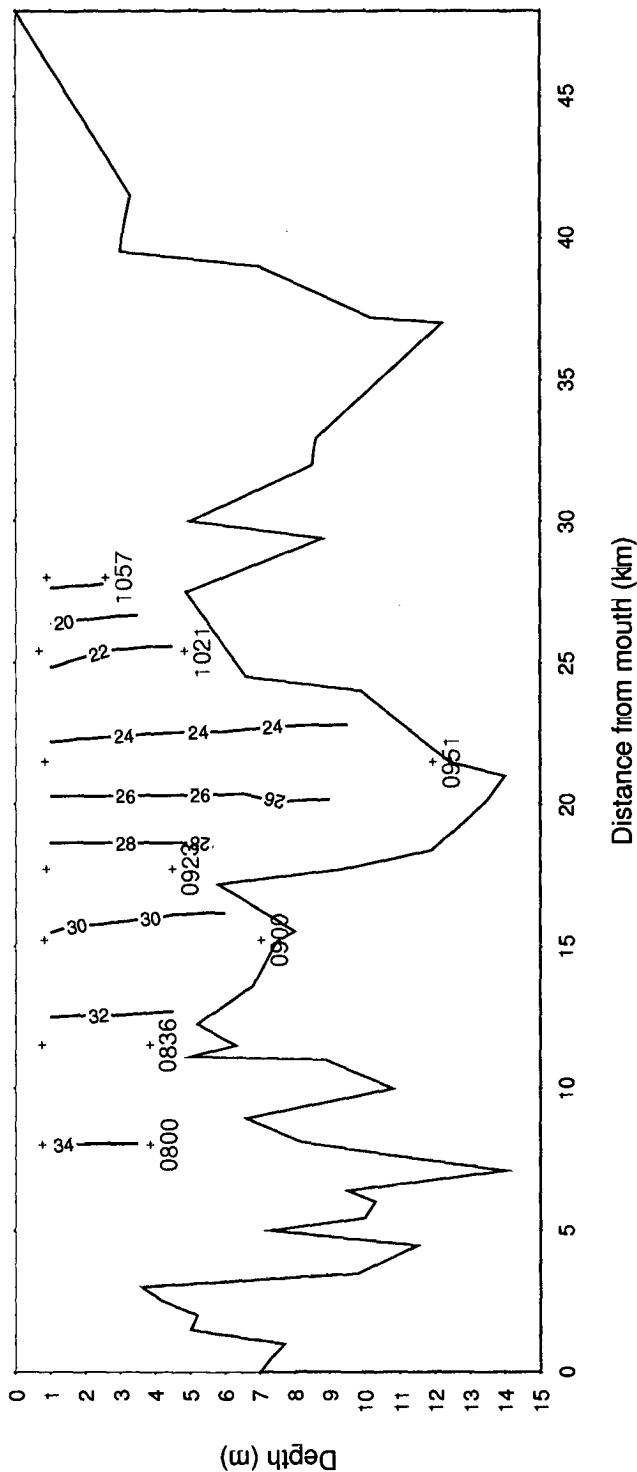
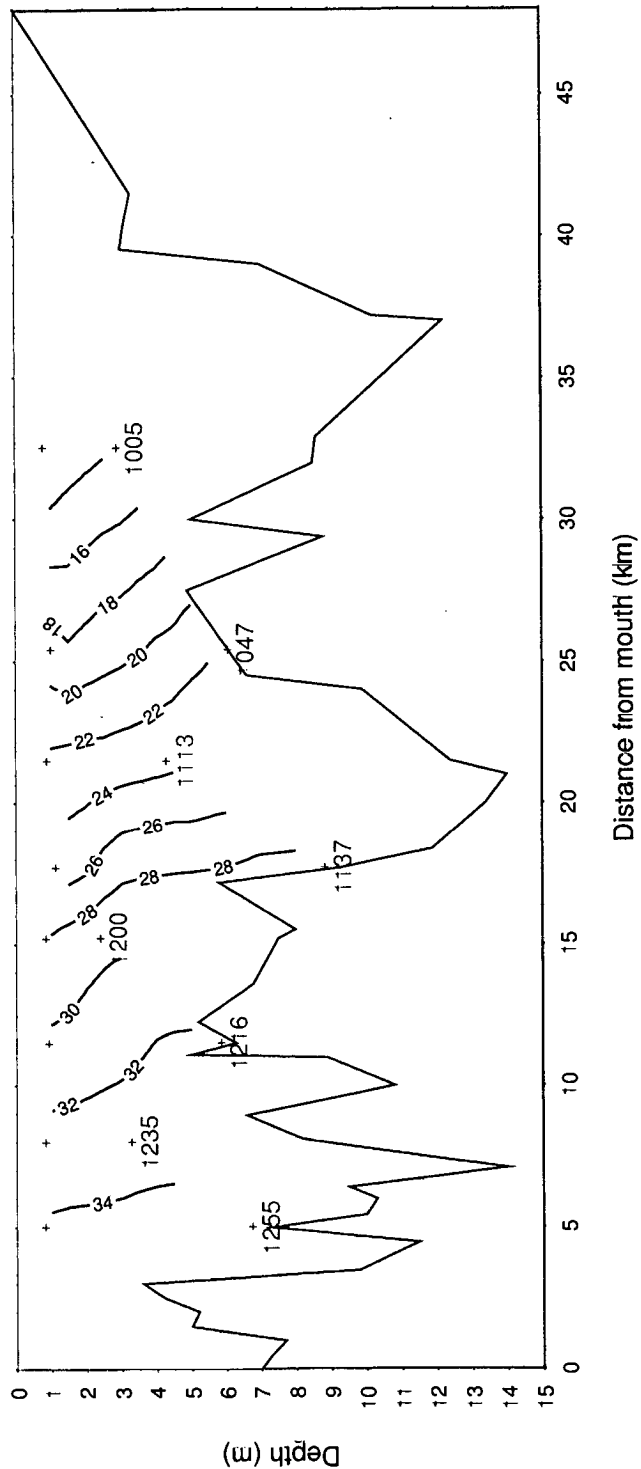
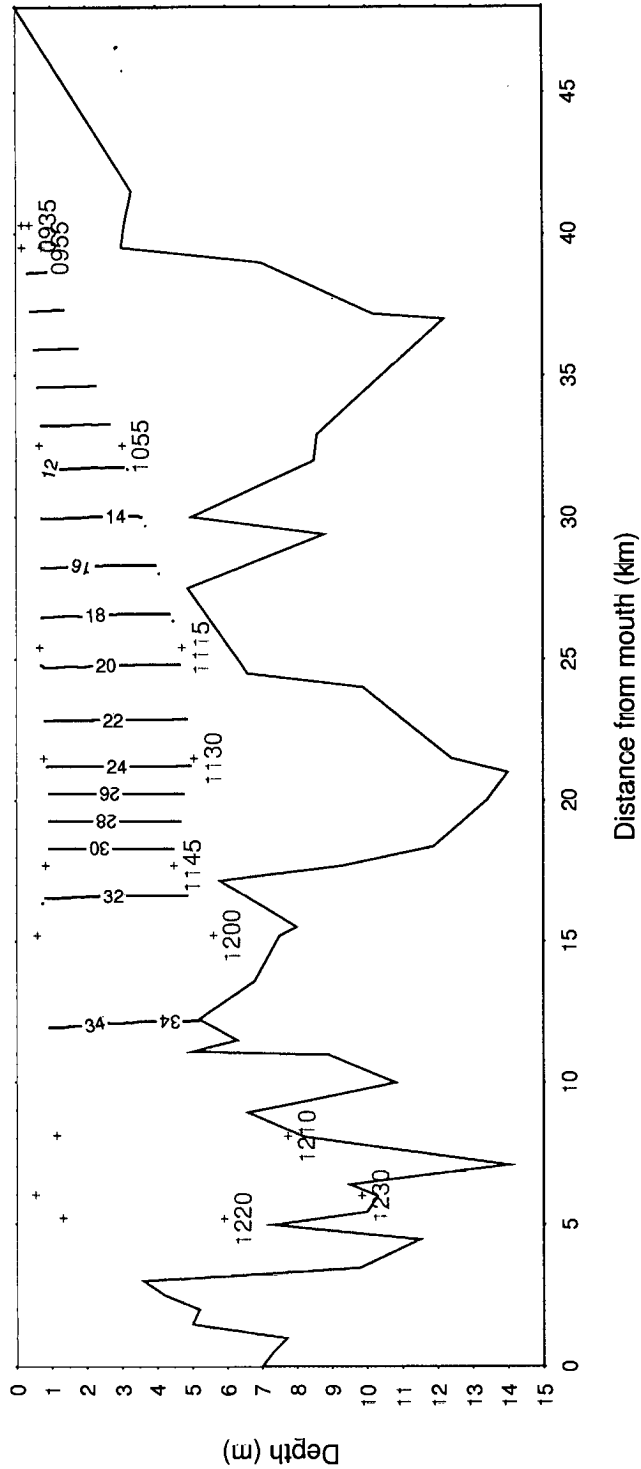


Figure 4.11 Vertical distribution of salinity measured on 25 May 2007 in the Mandovi estuary. The time (*hours*) at which the observations were made are indicated in cyan colour.





**Figure 4.12** Vertical distribution of salinity measured on 1 June 2007 in the Mandovi estuary. The time (*hours*) at which the observations were made are indicated in cyan colour.



**Figure 4.13** Vertical distribution of salinity measured on 27 July 2007 in the Mandovi estuary. The time (*hours*) at which the observations were made are indicated in cyan colour.

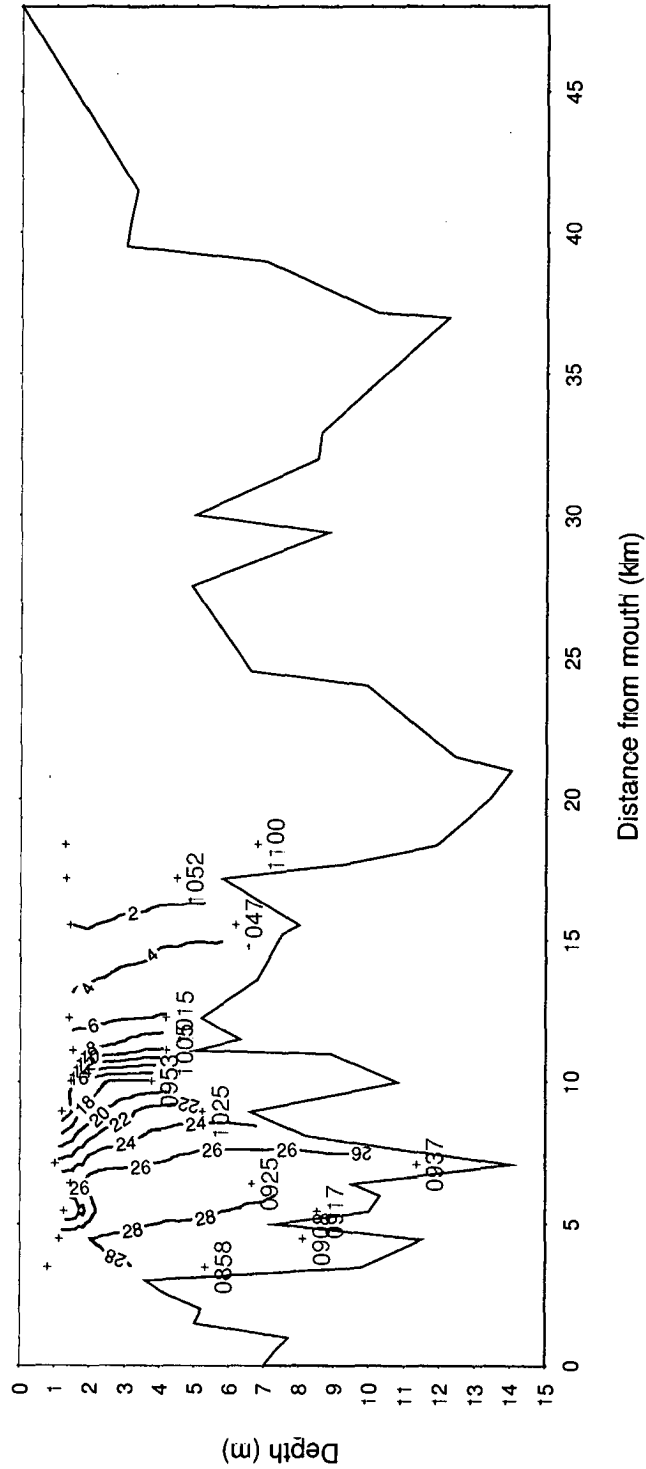


**Figure 4.14** Vertical distribution of salinity measured on 7 September 2007 in the Mandovi estuary. The time (*hours*) at which the observations were made are indicated in cyan colour.

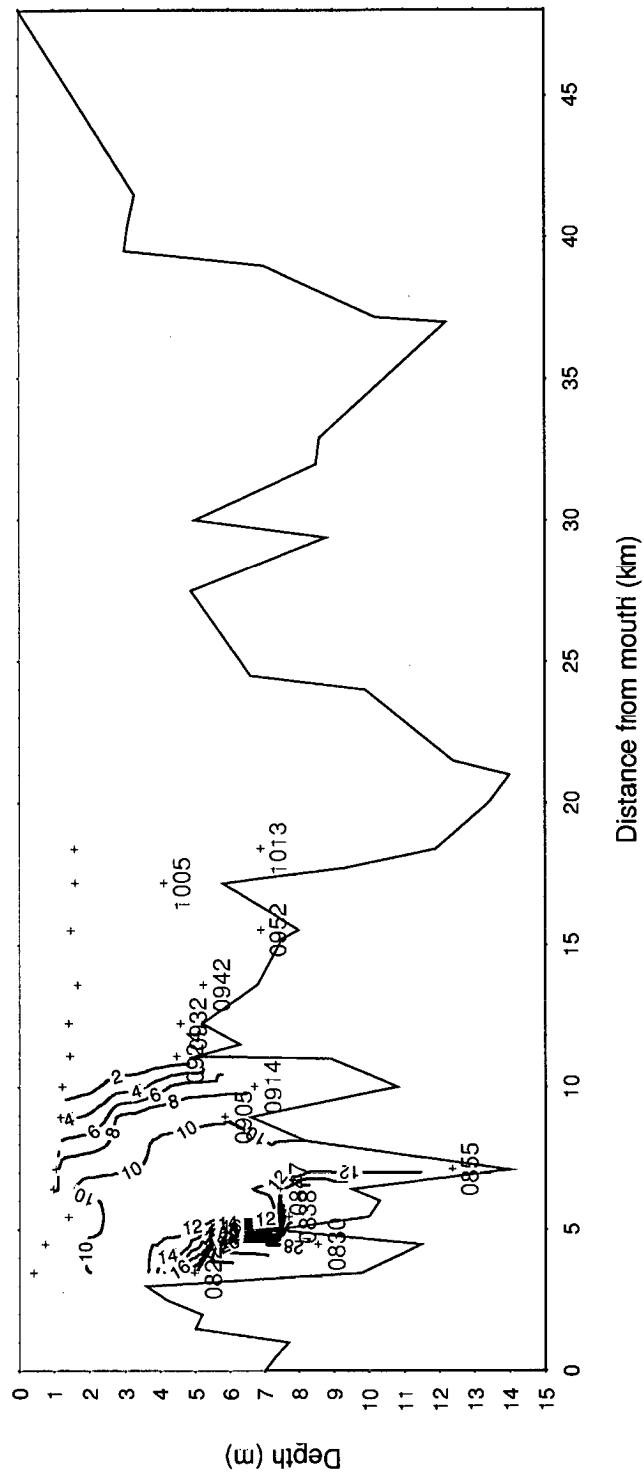
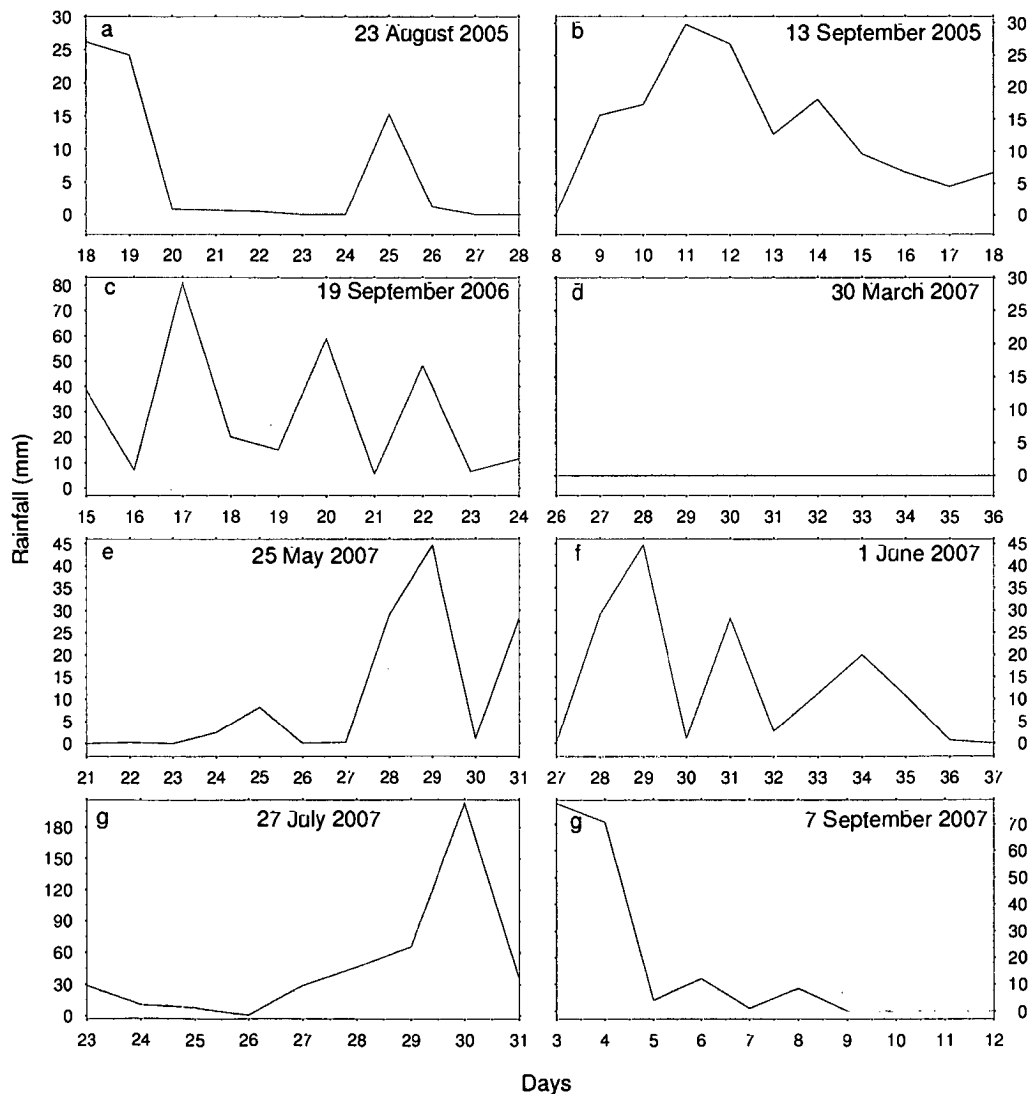


**Figure 4.15** Figure shows rainfall at Panaji (near the mouth of Mandovi) during the time of salinity measurements in the Mandovi estuary. Rainfall is plotted for about 5 days before and after the date (shown in each panel) of salinity measurements. The green and red curves indicate rainfall during wet and dry seasons respectively. The 32<sup>nd</sup> day on the panels d and f are for 1<sup>st</sup> April and June respectively.



follows

$$f = \frac{S_0 - S}{S_0} \quad (4.5)$$

Where  $S_0$  is the normal ocean salinity and  $S$  is the salinity at given location inside the estuary. So the freshwater volume of particular section or an entire estuary is the volume integral of  $f$  and which can written as

$$f^* = \int f dv \quad (4.6)$$

Where  $f^*$  is the average freshwater fraction integrated over  $f$ . So, the flushing time can be written as

$$T = \frac{f^*V}{q} \quad (4.7)$$

Where  $q$  is the freshwater input for the study period and  $V$  is the volume of a section or an entire estuary.

In the present study, for calculating flushing time, the numerical model was run for 41 days each for varying freshwater inputs of 10, 25, 50 and 100  $m^3 s^{-1}$ . After the spin-up of 11 days, the remaining 30 day of salinity was used for computing freshwater fraction at each grid point of the model domain of the Mandovi and Zuari estuaries. The freshwater fraction obtained thus, was averaged over 30 days and the flushing time was calculated using the Equation 4.5. The model results are given the table 4.1 and as well as in Figure 4.16.

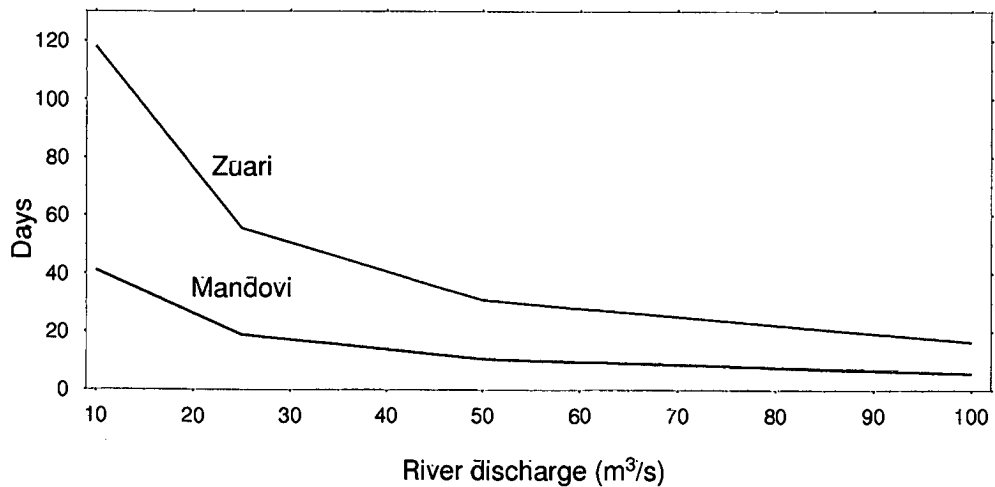
## 4.6 Discussion

The hybrid network model used in the present study could simulate salinity distribution well in the Mandovi and Zuari estuaries during dry season and the simulation of salinity during wet season at upstream regions were also reasonably good. Only at the down

**Table 4.1** Table shows the computed flushing time for varying river discharges in the Mandovi and Zuari estuaries

River discharge $m^3 s^{-1}$	Mandovi <i>Days</i>	Zuari <i>Days</i>
<b>10.0</b>	<b>41.22</b>	<b>117.95</b>
<b>25.0</b>	<b>18.93</b>	<b>055.43</b>
<b>50.0</b>	<b>10.54</b>	<b>030.87</b>
<b>100.0</b>	<b>05.68</b>	<b>016.49</b>

**Figure 4.16** The computed flushing time for varying river discharges in the Mandovi and Zuari estuaries:



stream regions, consisting of about 10–12 *km*, the simulated salinity was underestimated. During wet season, the upstream regions are fully freshwater and hence no stratification and both observation and simulation show that salinity is nearly zero at these regions. The downstream regions consisting of about 10–12 *km* are partially mixed due to heavy river discharge from the upstream regions and incoming saline water driven by tides.

Salinity diffusion coefficient was chosen as 100 and 150  $m^2s^{-1}$  for downstream and upstream regions respectively in the present model. But it was found that the difference between the simulations of salinity for 100 and 150  $m^2s^{-1}$  was minimum.

The continuous measurements of salinity in April and August 1993 were used for the validation of the model. After the validation, this model was used to simulate salinity distribution for varying river discharges. A numerical experiment was carried out for this purpose. The results shows that the salinity distribution undergoes large changes for varying river discharges. Even with river discharge of 50  $m^3s^{-1}$ , salinity distribution remained almost steady upto 5 *km* from the mouth of the Mandovi estuary. Salinity dropped from 10 to 5 *psu* in the middle regions (20 to 35 *km*) and became zero further toward upstream regions when river discharge of 10  $m^3s^{-1}$  was introduced. For river discharges of 50  $m^3s^{-1}$ , salinity drops from 30 to 8 *psu* at about 20 *km* distance from the mouth. From 35 *km* to upstream regions, salinity goes to nearly zero. River discharge in July and August in the Mandovi and Zuari estuaries is about 400  $m^3s^{-1}$ , which can push saline water completely from the upstream regions to the downstream regions. The upstream regions of about 35 *km* become freshwater dominated during wet season.

The simulation of salinity for varying discharge show that the advective transport of salinity toward downstream regions are very strong even for a river discharge of 25  $m^3s^{-1}$ . The longitudinal distribution of salinity both in the Mandovi and Zuari estuaries are almost same. The Mandovi estuary has a lower average salinity than that of Zuari because the Mandovi estuary receives considerable amount of runoff through a large tributary system [Qasim and Sengupta, 1981].

The residual currents computed for varying river discharge also show freshwater influence on tides. The residual currents found in these estuaries are strong enough to push salinity toward the mouth.

The longitudinal variations of salinity (Figures 4.7 and 4.8) during the selected days during 2005–2007 indicate that in a monsoonal estuary like the Mandovi estuary, salinity is subjected to intraseasonal variations during wet season. High salinity found in the surface on 23 August 2005 was due to deficit river discharge associated with the low rainfall (see Figure 4.15). The low salinity in the surface on 13 September 2005 indicates large quantity of river discharge into estuary due to heavy rainfall. An important characteristic of the southwest monsoon is variability on sub-seasonal time-scales, with active periods of heavy rain interrupted by drier break periods [Vecchi and Harrison, 2002]. These breaks during southwest monsoon reduces river discharge into the estuaries and consequently, saline water intrudes into the estuaries. When the monsoon becomes active once again, the saline water is pushed out of the estuary as shown in Figure 4.8. Similarly in 2007 also, salinity intruded into further upstream regions in July, again in September, salinity pushed towards mouth (Figure 4.13 and 4.14). This analysis of the salinity measurements made during the selected days of 2005–2007 indicate that salinity undergoes changes due to the breaks in the southwest monsoon. The analysis of the continuous measurements of salinity on 19 September 2006 shows that salinity remains zero from surface to bottom even during a tidal cycle if there is heavy freshwater flow. Present study in the Mandovi and Zuari estuaries show that these estuaries partially mixed only in the downstream regions consisting of 10–12 km during wet season and well mixed all other seasons (see Figures 4.10 and 4.12). The measurements of salinity in the Mandovi estuary show that salinity undergoes intraseasonal variations during wet season.

Flushing time in the Mandovi is almost three times less than that of Zuari for any given river discharge. This is because of the total volume of Zuari is about  $291 Mm^3$  and that of Mandovi is about  $102 Mm^3$ . The high volume of Zuari retain the freshwater for



long time in the channel than that of Mandovi.

## **4.7 Conclusions**

The model simulated the longitudinal distribution of salinity well during dry season though the simulation of salinity at the downstream regions were not reproduced well during wet season. But the simulation of salinity distribution at upstream regions were reasonably good during this season. From the analysis of salinity measured during wet seasons, further efforts need to be brought to study variations of salinity in the downstream regions of these estuaries in detail using the 3D models in order to improve the simulation of salinity during wet season.

# Chapter 5

## Summary and Conclusions

The results obtained from this study are summarised in this chapter. The significant findings, the limitations of the present studies and the future studies to be undertaken etc. are discussed in this chapter. The objectives of the thesis were to determine the characteristics of tidal propagation and salinity distribution in the Mandovi and Zuari estuaries using a hybrid network numerical model. One of the main objective was to study the longitudinal variation of tides during dry and wet seasons and freshwater influence on tides. The study of tidal asymmetry was another objective. This is the first time an effort was made to study tidal asymmetry caused by overtides and compound tides in the estuaries on the west coast of India. Another important aim was to study the longitudinal variation of salinity distribution and freshwater influence on salinity. The study of intraseasonal variations of salinity during wet season was another important objective. The residual currents and flushing time were also computed using the model.

A hybrid network model, consisting of a vertically averaged 2D model and an area averaged 1D model was used to simulate tides and salinity distribution in the Mandovi and Zuari estuaries. The vertically averaged 2D model was used for the downstream regions of these channels. An area averaged 1D model was for the upstream regions in these estuaries and Cumbarjua canal. A finite difference numerical scheme was used for

solving partial differential equations of momentum, continuity and advection-diffusion equation of salinity.

## 5.1 Tidal propagation

Hybrid network model used for the present study was successful in simulating tidal circulation reasonably well in both dry and wet seasons in the Mandovi and Zuari estuaries. Both the observation and simulation of tide show that tidal amplitudes slightly increase toward the upstream regions. The Mandovi and Zuari estuaries are strongly converging channels and this leads to the amplification of tides in the upstream direction. The momentum balance in this type of estuary is primarily between pressure gradient and friction and the decay in amplitude due to friction gets cancelled by geometric amplification, which leaves the amplitude, unchanged over 40 *km* in these estuaries from the mouth. Tidal amplitude gets decayed in the remaining 10 *km* in these estuaries because of river discharge. The tidal oscillations are negligible at upstream stations in the Mandovi and Zuari estuaries due to small river discharge. The freshwater inflow through these narrow channel is sufficient to prevent tides entering at this stations. But the decay in tidal oscillation at the upstream station in the Zuari is less than that of the Mandovi. The channel's elevation from the sea level is also a factor preventing the tidal propagation further toward upstream regions. During wet season, the tidal oscillations are minimum at these two stations because of heavy river discharge.

Tidal currents in these estuaries are strong enough to mix the water column vertically during the dry season. The downstream velocities associated with river discharge prevent upstream propagation of tides during wet season.

Harmonic analysis of tides was carried out using observations and simulations at several station in these estuaries and the results show that the major tidal constituents increase toward the upstream regions in these estuaries. The Mandovi and Zuari estuaries are not

frictionally dominated estuaries. The amplitude and phase variations of the tidal constituents toward the upstream regions in the Mandovi and Zuari estuaries are not linear, which is a strong indication of the presence of a reflected wave in these estuaries.

Amplitude and phase of both overtides and compound tides increase toward the upstream regions in these estuaries. This rapid increase in amplitude and phase of the first and second harmonics of  $M_2$  and the nonlinear increase of compound tides show the nonlinear nature of the Mandovi and Zuari estuarine systems to the tidal forcing. The increase of  $M_4$  and decrease of relative surface phase in both the Mandovi and Zuari show that these estuaries are flood-dominated. But there are some mudflats in the Zuari estuary, that can increase the duration of ebb, which indicates that the Zuari estuary is less flood-dominant than the Mandovi estuary.

The complex difference of both observations and simulations of tidal constituents (major diurnal and semi-diurnal constituents, overtides and compound tides) increases slightly from the downstream regions to the upstream regions. One of the possible reasons for this increase is due to the use of a 2D square grid, which was not well adapted to the irregular configuration of coastline. The meandering effects of the channels influence the amplitude and phase of tide entering into the estuary.

## 5.2 Salinity distribution

The numerical model used for the present study could simulate salinity distribution well in the Mandovi and Zuari estuaries during dry season and the simulation of salinity during wet season at upstream regions was also reasonably good. Only at the down stream regions consisting of about 10–12 *km*, the simulated values of salinity were found to be underestimated.

The numerical experiment carried out for the simulation of longitudinal distribution of salinity for varying discharges in the Mandovi shows that salinity distribution undergoes

large changes with varying river discharge. River discharge in July and August in the Mandovi and Zuari estuaries is about  $400 \text{ m}^3 \text{ s}^{-1}$ , which can push saline water completely from the upstream regions to the downstream regions. The upstream regions of about 35 *km* become freshwater dominated during wet season. The computed residual currents found in the estuaries are strong enough to push saline water toward the mouth during wet season.

The longitudinal variations of salinity indicates that in a monsoonal estuary like the Mandovi estuary, salinity is subjected to intraseasonal variations during wet season. The present study in the Mandovi and Zuari estuaries show that these estuaries are partially mixed only in the downstream regions extending 10–12 *km* from the mouth during wet season. These channels become well mixed during other seasons. The estimated flushing time in the Mandovi is almost three times less than that of Zuari at any given river discharge. This is mainly because the total volume of the Zuari is much higher than that of the Mandovi.

### 5.3 Future studies

The present model could simulate tides both in the dry and wet seasons in the Mandovi and Zuari estuaries. The simulations of tidal constituents were also reasonably well both in these estuaries. However, more observations of currents are needed for better validation of computed tidal currents.

The results from Chapter 4 show that the simulations of salinity distribution is good during dry season in the Mandovi and Zuari estuaries. So this numerical model can be used in other estuaries in the tropical regions where the water column is vertically well mixed. Mandovi and Zuari estuaries are well mixed for almost 7 to 8 months in a year. The present approach is suitable for this kind of estuarine systems. From the analysis of salinity measured during wet seasons, we think that further efforts need to be brought to

study salinity distribution during wet season. Moreover, diffusion coefficient for salinity has to be estimated more accurately from field studies. The effect of wind stress on the tidal circulation, especially during southwest monsoon, needs to be examined. Using 3D models will be more appropriate for the simulation of salinity during wet season in this type of estuaries.

# Appendix A

## Notation

- $U = u(h + \eta)$  is the transport along the x-axis
- $V = v(h + \eta)$  is the transport along the y-axis
- $u$  and  $v$  are the vertically averaged velocity over the water column of height  $(h + \eta)$
- $h$ : depth
- $\eta$ : free surface
- $t$ : time
- $g$ : acceleration due to gravity
- $f$ : Coriolis parameter
- $A_H$ : coefficient of horizontal diffusion of momentum
- $C_D$ : bottom drag coefficient
- $S$ : water salinity

- 
- $K_x$ : diffusion coefficient along x-axis
  - $K_y$ : diffusion coefficient along y-axis
  - $b$ : width of the channel
  - $q$ : river discharge per unit channel length
  - $A = b(h + \eta)$  is the total cross-sectional area of the channel
  - $R = A/P_r$ : hydraulic radius, where  $P_r$  is the wetted perimeter
  - $C$ : Chezy coefficient
  - $n$ : Manning coefficient
  - $z_0$ : the distance between the bottom of the channel and an arbitrary level surface well below the bottom
  - $Q$ : along channel transport



# Bibliography

- A. Arakawa and V. R. Lamb. Computational design of the basic dynamical processes of the UCLA general circulation model. *Methods in Computational physics*, 17:174–264, 1977.
- D. G. Aubrey and P. E. Speer. A study of non-linear tidal propagation in shallow inlet/estuarine systems part I: Observations. *Estuarine Coastal and Shelf Science*, 21: 185–205, 1985.
- C. Bell, J. M. Vassie, and P. L. Woodworth. POL/PSMSL Tidal Analysis Software Kit 2000. Permanent Service for Mean Sea Level, CCMS Proudman Oceanographic Laboratory, Bidston Observatory, Birkenhead, Merseyside L43 7RA, U.K, 2000.
- D. A. Bella and W. Dobbins. Difference modelling of stream pollution. *J. Sanit. Eng. Div., Amer. Soc. Civil Eng.*, 94:995–1016, 1968.
- J. Blanton, G. Lin, and S. Elston. Tidal current asymmetry in shallow estuaries and tidal creeks. *Continental Shelf Research*, 22:1731–1743, 2002.
- A. F. Blumberg. Numerical model of estuarine circulation. *J. Hyd. Div. Proc. ASCE*, 103:295–310, 1977.
- A. F. Blumberg. The influence of density variations on estuarine tides and circulation. *Estuarine Coastal and Shelf Science*, 6:209–215, 1978.

- C. F. Bowden. Circulation and diffusion. In G. H. Lauff, editor, *Estuaries*, pages 15–36. American Association for the Advancement of Science, Washington, D. C, 1967.
- M. J. Bowman and S. M. Chiswell. Numerical tidal simulations within Hauraki Gulf, New Zealand. *Hydrodynamics of semi-enclosed seas*, Elsevier, Amsterdam, pages 349–384, 1982.
- W. M. Cameron and D. W. Pritchard. Estuaries. In M. N. Hill, editor, *The Sea*, volume 2, pages 306–324. John Wiley, New York, 1963.
- X. Chen. Modelling Transport Processes in Surface Waters Using the Tracer Method (I): Theories and Model Development. Technical Report, Institute for Fluid Mechanics and Electronic Computation in Civil Engineering, University of Hannover, Germany (in German)., 1989.
- X. Chen. Modelling Transport Processes in Surface Waters Using the Tracer Method (II): Model Applications. Technical Report, Institute for Fluid Mechanics and Electronic Computation in Civil Engineering, University of Hannover, F.R. Germany (in German)., 1990.
- X. Chen. An efficient finite difference scheme for simulating hydrodynamics in narrow rivers and estuaries. *International Journal for Numerical Methods in Fluids*, 42:233–247, 2003.
- X. Chen. Using a piecewise linear bottom to fit the bed variation in a laterally averaged, z-coordinate hydrodynamic model. *International Journal for Numerical Methods in Fluids*, 44:1185–1205, 2004a.
- X. Chen. Modelling hydrodynamics and salt transport in the Alafia River estuary, Florida during May 1999–December 2001. *Estuarine Coastal and Shelf Science*, 61:477–490, 2004b.

- X. Chen. A laterally averaged two-dimensional trajectory model for estimating transport time scales in an Alafia River Estuary, Florida. *Estuarine Coastal and Shelf Science*, 75: 358–370, 2007.
- X. Chen, M. S. Flannery, and D. L. Moore. Salinity response to the change of the upstream freshwater flow in the lower Hillsborough River, Florida. *Estuaries*, 23:735–742, 2000.
- P. K. Das, C. S. Murty, and V. V. R. Varadachari. Flow characteristics of Cumbarjua canal connecting Mandovi and Zuari estuaries. *Indian Journal of Marine Sciences*, 1: 95–102, 1972.
- P. V. Dehadrai. Changes in the environmental features of the Zuari and Mandovi estuaries in relation to tides. *Proceedings of the Indian Academy of Sciences*, 72:68–80, 1970.
- P. V. Dehadrai and R. M. S. Bhargava. Seasonal organic production in relation to environmental features in Mandovi and Zuari estuaries, Goa. *Indian Journal of Marine Sciences*, 1:52–56, 1972.
- S. N. DeSousa. Monitoring of some environmental parameter at the mouth of Zuari River, Goa. *Indian Journal of Marine Sciences*, 6:114–117, 1977.
- S. N. DeSousa. Consultancy services for disposal of treated sewage effluents in the estuary of River Mandovi at Campal, Panaji. Sponsored by Public Works Department (PWD), Government of Goa. TR-8633, NIO/SP-16/99 1999, National Inst. of Oceanography, India., 1999a.
- S. N. DeSousa. Effect of mining rejects on the nutrient chemistry of Mandovi Estuary, Goa. *Indian Journal of Marine Sciences*, 28:355–359, 1999b.
- S. N. DeSousa. Consultancy services for disposal of treated sewage effluents in the estuary of River Mandovi at Campal, Panaji. Sponsored by Public Works Depart-

- ment (PWD), Government of Goa. TR-8658, NIO/SP-21/2000 2000; National Inst. of Oceanography, India., 2000.
- S. N. DeSousa, R. Sengupta, S. Sanzgiri, and M. D. Rajagopal. Studies on nutrients of Mandovi and Zuari river systems. *Indian Journal of Marine Sciences*, 10:314–321, 1981.
- J. J. Dronkers. Tidal computation for rivers, Coastal areas and Seas. *I. Hyd. Div. Proc., ASCE*, 95:29–77, 1969.
- K. R. Dyer. *Estuaries: a physical introduction*. John Wilkey and Sons, London., 1973.
- K. R. Dyer. *Estuaries: a physical introduction, Second Edition*. John Wilkey and Sons Ltd, Chichester., 1997.
- K. R. Dyer, M. C. Christie, and E. W. Wright. The classification of intertidal mudflats. *Continental Shelf Research*, 20:1039–1060, 2000.
- R. A. Falconer, E. Wolanski, and H. L. Hardapitta. Modelling of tidal circulation in an island's wake. *Journal of Waterway, Port, Coastal, and Ocean Engineering*, 112: 234–254, 1986.
- H. B. Fischer. Mass transport mechanisms in partially stratified estuaries. *Journal of Fluid Mechanics*, 53:671–687, 1972.
- H. B. Fischer, E. J. M. List, R. C. Y. Koh, J. Imberger, and N. H. Brook. Mixing in Inland and Coastal waters. *Academic press, London*, 1979.
- C. T. Friedrichs and D. G. Aubrey. Non-linear tidal distortion in shallow well-mixed estuaries: A synthesis. *Estuarine Coastal and Shelf Science*, 27:521–545, 1988.
- C. T. Friedrichs and D. G. Aubrey. Tidal propagation in strongly converging channels. *Journal of Geophysical Research*, 99:3321–3336, 1994.

- B. S. Giese and D. A. Jay. Modelling Tidal Energetics of the Columbia River Estuary. *Estuarine Coastal and Shelf Science*, 29:549–571, 1989.
- P. A. Gillibrand and P. W. Balls. Modelling Salt Intrusion and Nitrate Concentrations in the Ythan Estuary. *Estuarine Coastal and Shelf Science*, 47:695–706, 1998.
- G. Godin. *Tides*. ANADYOMENE Edition, Ottawa, Ontario, Canada, 1988.
- M. G. Gross. *Oceanography: A view of the earth*. Prentice Hall., USA., 1972.
- M. P. Grzechnik. Three-Dimensional Tide and Surge Modelling and Layered Particle Tracking Techniques Applied to Southern Australian Coastal Seas. Ph.D. thesis, Department of Applied Mathematics, The University of Adelaide, Australia., 2000.
- P. Hamilton. A numerical model of the vertical circulation of tidal estuaries and its application to Rotterdam Waterway. *Geophy. J. Roy. Astro. Soc*, 40:1–21, 1975.
- P. Hamilton. Modelling salinity and circulation for Colombia river estuary. *Progress in Oceanography*, 25:113–156, 1990.
- D. V. Hansen and M. Rattray. Gravitational circulation in straits and estuaries. *Journal of Marine Research*, 23:104–122, 1965.
- D. V. Hansen and M. Rattray. New dimensions in estuary classification. *Limnol. Oceanography*, 11:319–326, 1966.
- W. Hansen. Theory of the calculation of water levels and storm surges at Randmeeran (in German). *Tellus*, 8:288–300, 1956.
- D. R. F. Harleman and C. H. Lee. The computation of tides and currents in estuaries and canals. Massachusetts Institute of technology, Cambridge., 1969.
- D. R. F. Harleman, C. H. Lee, and L. C. Hall. Numerical studies of unsteady dispersion in estuaries. *J. Sanitary. Engg. Div., ASCE*, 94:897–911, 1968.

- N. S. Heaps. A two dimensional numerical sea model. *Phil. Trans. Roy Soc.*, 265: 93–137, 1969.
- P. E. Holloway. Longitudinal Mixing in the Upper Reaches of the Bay of Fundy. *Estuarine Coastal and Shelf Science*, 13:495–515, 1981.
- A. T. Ippen and D. R. F. Harleman. One dimensional analysis of salinity intrusion in estuaries. Tech. Bull. No.5, WES, Vicksberg., 1961.
- Z. G. Ji, G. Hu, J. Shen, and Y. Wan. Three-dimensional modelling of hydrodynamic processes in the St. Lucie Estuary. *Estuarine Coastal and Shelf Science*, 73:188–200, 2007.
- B. Johns. The modelling of tidal flow in an channel using a turbulent energy closure scheme. *Journal of Physical Oceanography*, 8:1042–1049, 1978.
- J. W. Kang and K. S. Jun. Flood and ebb dominance in estuaries in Korea. *Continental Shelf Research*, 56:187–196, 2003.
- B. H. Ketchum. Hydro-graphic factors involved in the dispersion of pollutants introduced into tidal waters. *J. Boston Soc. Civil Eng*, 37:296–314, 1950.
- B. H. Ketchum. The exchanges of fresh and salt water in a tidal estuary. *J. Mar. Res*, 10: 18–38, 1951a.
- B. H. Ketchum. The flushing of tidal estuaries. *Sewage and Industr. Wastes*, 23:198–208, 1951b.
- B. H. Ketchum. Relation Between Circulation and Planktonic Populations in Estuaries. *Ecology*, 35:191–200, 1954.
- B. H. Ketchum. Distribution of coliform bacteria and other pollutant in tidal estuaries. *Sewage and Industrial Wastes*, 27:1288–1296, 1955.

- J. Lamoen. Tides and Current Velocities in a Sea-level Canal. *Engineering*, pages 97–99, 1949.
- M. O. Lee, R. A. Falconer, and K. H. Jin. The effect of wind stress on the pollutant dispersion in a semi enclosed Bay. *Proc. XXV Congress of Int. Ass. Hydraul. Res, Tokyo*, pages 85–92, 1993.
- J. J. Leendertse. Aspects of a computational model for long-period water-wave propagation. *United States Air Force Project Rand, The Rand Corporation, Santa Monica, CA.*, 1967.
- J. J. Leendertse. A water-quality simulation model for well mixed estuaries and coastal seas: principles of computation. *Rand Corporation Report RM-6230-rc.*, 1, 1970.
- J. J. Leendertse and E. C. Gritton. A water-quality simulation model for well mixed estuaries and coastal seas: Computational procedures. *Memo. R-708-NYC. The Rand Corp, Santa Monica, California*, 2, 1971a.
- J. J. Leendertse and E. C. Gritton. A water-quality simulation model for well mixed estuaries and coastal seas: Jamaica Bay simulation. *Memo. R-709-NYC. The Rand Corp, Santa Monica, California*, 3, 1971b.
- J. J. Leendertse, R. C. Alexander, and S. K. Liu. Three-dimensional model for estuaries and coastal seas—Principles of computation. *The RAND Corporation (California), R-1417-OWPR.*, 1:55 pp, 1973.
- R. Lewis. *Dispersion in Estuaries and Coastal Waters.* John Wilkey and Sons Ltd, Chichester., West Sussex PO19 1UD, England, 1997.
- Z. Li and A. J. Elliot. Modelling the vertical structure of tidal currents and temperature of the North sea. *Estuarine Coastal and Shelf Science*, 36:549–564, 1993.

- A. Mantovanelli, E. Marone, E. T. da Silva, L. F. Lautert, M. S. Klingenfuss, J. V. P. Prata, M. A. Noernberg, B. A. Knoppers, and R. J. Angulo. Combined tidal velocity and duration asymmetries as a determinant of water transport and residual flow in Paranagu Bay estuary. *Estuarine Coastal and Shelf Science*, 59:1325–1334, 2004.
- J. L. Martin and S. C. McCutcheon. *Hydrodynamics and transport for water quality modelling*. Lewis Publishers, Boca Raton, USA, 1999.
- S. B. McCann. Classification of tidal environments. In S. B. McCann, editor, *Sedimentary Processes and Animal-Sediment Relationships in Tidal Environments, Short Course Notes.*, volume 1, pages 1–24. Geological Association Canada, St. Johns, Newfoundland, 1980.
- J. W. McLaughlin, A. Bilgili, and D. R. Lynch. Numerical modelling of tides in the Great Bay Estuarine System: dynamical balance and spring-neap residual modulation. *Estuarine Coastal and Shelf Science*, 57:283–296, 2003.
- G. L. Mellor and Yamada. A hierarchy of turbulence closure models for planetary boundary layers. *Journal of Atmospheric Sciences*, 31:1791–1806, 1974.
- C. S. Murty and P. K. Das. Pre-monsoon tidal flow characteristics of Mandovi estuary. *Indian Journal of Marine Sciences*, 1:148–151, 1972.
- L. Y. Oey, G. L. Mellor, and R. I. Hires. A Three-Dimensional Simulation of the Hudson Raritan Estuary. Part II: Comparison with Observation. *Journal of Physical Oceanography*, 15:1693–1709, 1985.
- C. B. Officer. *Physical Oceanography of Estuaries (and Associated Coastal Waters)*. Jhon Wiley and Sons, New York, U.S.A., 1976.
- E. S. Posmentier and J. M. Rayment. Variations of Longitudinal Diffusivity in the Hudson Estuary. *Estuarine and Coastal Marine Science*, 8:555–564, 1979.



- D. Prandle. Residual flows and elevation in the Southern North Sea. *Proc. R. Soc. London*, 359:189–228, 1978.
- D. Prandle and N. Crookshank. Numerical model of St. Lawrence river estuary. *J. Hyd. Div, ASCE.*, 100:517–529, 1974.
- D. W. Pritchard. Estuarine hydrography. *Advances in Geophysics*, 1:243–280, 1952.
- D. W. Pritchard. Estuarine circulation patters. *Proceedings of the American Society of Civil Engineers*, 81(717):1–11, 1955.
- D. W. Pritchard. What is an estuary: Physical viewpoint. In G. H. Lauff, editor, *Estuaries*, pages 3–5. American Association for the Advancement of Science, Washington, D. C, 1967.
- D. W. Pritchard. Dispersion and flushing of pollutants in estuaries. *J. Hyd. Div. Proc. ASCE*, 95:114–124, 1969.
- S. Z. Qasim. *Indian Estuaries*. Allied Publishers Pvt. Limited, New Delhi, 2003.
- S. Z. Qasim and R. Sengupta. Environmental characteristics of mandovi-zuari estuarine systems in goa. *Estuarine Coastal and Shelf Science*, 13:557–578, 1981.
- M. A. Rady, M. I. El-Sabh, T. S. Murty, and J. O. Backhaus. Numerical modelling of tides in Suez, Egypt. *Marine Geodesy*, 17:11–36, 1994.
- R. O. Reid and B. R. Bodin. Numerical model for storm surges in Galveston Bay. *J. Waterways, Harbors and Coastal Div, ASCE.*, 94:33–57, 1968.
- B. E. Ross, M. W. Anderson, and P. Jerkins. Coordinated mathematical models for the coastal zone. *Hydraulic of the coastal zone, ASCE*, pages 11–18, 1977.
- R. J. Russell. Origin of estuaries. In G. H. Lauff, editor, *Estuaries*, pages 93–99. American Association for the Advancement of Science, Washington, D. C, 1967.

- H. H. Savenije. Predictive model for salt intrusion in estuaries. *Journal of Hydrology*, 148:203–218, 1993.
- D. Shankar and S. R. Shetye. Are interdecadal sea level changes along the Indian coast influenced by variability of monsoon rainfall?. *Journal of Geophysical Research*, 104:26031–26042, 1999.
- D. Shankar and S. R. Shetye. Why is mean sea level along the Indian coast higher in the Bay of Bengal than the Arabian Sea?. *Geophysical Research Letters*, 28:563–565, 2001.
- D. Shankar, V. Kotamraju, and S. R. Shetye. A quantitative framework for estimating water resources in India. *Current Science*, 86:543–552, 2004.
- D. Shankar, S. Shenoi, R. K. Nayak, P. N. Vinayachandran, G. Nampoothiri, A. M. Almeida, G. S. Michael, M. R. Rameshkumar, D. Sundar, and O. P. Sreejith. Hydrography of the eastern Arabian Sea during summer monsoon 2002. *Journal of Earth System Sciences*, 114:459–474, 2005.
- S. S. C. Shenoi, D. Shankar, and S. R. Shetye. Differences in heat budgets of the near-surface Arabian Sea and Bay of Bengal: Implications for the summer monsoon. *Journal of Geophysical Research*, 107:10.1029/2000JC000679, 2002.
- S. R. Shetye. Tides in the Gulf of Kutch, India. *Continental Shelf Research*, 19:1771–1782, 1999.
- S. R. Shetye and C. S. Murty. Seasonal variation of the salinity in Zuari estuary. *Proceedings of the Indian Academy of Sciences (Earth and Planetary Sciences)*, 96:249–257, 1987.
- S. R. Shetye, A. D. Gouveia, S. Y. Singbal, C. G. Naik, D. Sundar, G. S. Michael, and G. Namboothiri. Propagation of tides in Mandovi-Zuari estuarine network. *Proceedings of the Indian Academy of Sciences (Earth and Planetary Sciences)*, 104:667–682, 1995.

- S. Y. S. Singbal. Diurnal variations of some physico-chemical factors in the Zuari estuary of Goa. *Indian Journal of Marine Sciences*, 2:90–93, 1973.
- P. E. Speer and D. G. Aubrey. A study of non-linear tidal propagation in shallow inlet/estuarine systems part II: Theory. *Estuarine Coastal and Shelf Science*, 21:207–224, 1985.
- D. Sundar and S. R. Shetye. Tides in Mandovi and Zuari estuaries, Goa, West coast of India. *Journal of Earth System Sciences*, 144:493–503, 2005.
- K. Suprit and Shankar. Resolving Orographic Rainfall On The Indian West Coast. *International Journal of Climatology*, 28(5):643–657, 2008.
- M. L. Thatcher and D. R. F. Harleman. Prediction of unsteady salinity intrusion in estuaries: Mathematical model and user's Manual. Massachusetts Institute of technology, Cambridge., 1972.
- M. L. Thatcher and D. R. F. Harleman. Long term salinity calculation in Delaware estuary. *J. Env. Engg. Proc., ASCE*, 107:11–28, 1981.
- C. Thomas, L. V. G. Rao, and K. K. Varma. Variation in physical characteristics of the waters of Zuari estuary. *Indian Journal of Marine Sciences*, 4:5–10, 1975.
- J. Thubum. Rossby wave dispersion on the C-grid. *Atmospheric Science Letters*, 8: 37–42, 2007.
- R. J. Uncles and M. B. Jordan. A One-Dimensional Representation of Residual Currents in the Severn Estuary and Associated Observations. *Estuarine and Coastal Marine Science*, 10:39–60, 1980.
- A. S. Unnikrishnan and J. L. Luick. A finite element simulation of tidal circulation in the Gulf of Kutch, India. *Estuarine Coastal and Shelf Science*, 56:131–138, 2003.

A. S. Unnikrishnan, S. R. Shetye, and A. D. Gouveia. Tidal propagation in Mandovi-Zuari Estuarine network, West coast of India: Impact of Freshwater influx. *Estuarine Coastal and Shelf Science*, 45:737–744, 1997.

A. S. Unnikrishnan, A. D. Gouveia, and P. Vethamony. Tidal regime in the Gulf of Kutch, west coast of India by 2D model. *Journal of Waterway, Port, Coastal, and Ocean Engineering*, 125:276–284, 1999a.

A. S. Unnikrishnan, S. R. Shetye, and G. S. Michael. Tidal propagation in the Gulf of Khambhat, Bombay High and surrounding areas. *Proceedings of the Indian Academy of Sciences (Earth and Planetary Sciences)*, 108:155–177, 1999b.

K. K. Varma, L. V. Rao, and C. Thomas. Temporal and spatial variations in hydrographic conditions of Mandovi estuary. *Indian Journal of Marine Sciences*, 4:11–17, 1975.

G. A. Vecchi and D. E. Harrison. Monsoon breaks and sub seasonal sea surface temperature variability in the Bay of Bengal. *Journal of Climate*, 15:1485–1493, 2002.

C. F. Wang, M. H. Hsu, and A. Y. Kuo. Residence time of the Danshuei River estuary, Taiwan. *Estuarine Coastal and Shelf Science*, 60:381–393, 2004.

W. Zhou. An Alternative Leapfrog Scheme for Surface Gravity Wave Equations. *Journal of Atmospheric and Oceanic Technology*, 19:1415–1423, 2002.

